

*Citation for published version:*

Cautis, S, Craw, A & Logvinenko, T 2017, 'Derived Reid's recipe for abelian subgroups of  $SL_3()$ ', Journal Fur Die Reine Und Angewandte Mathematik, vol. 727, pp. 1-48. <https://doi.org/10.1515/crelle-2014-0086>

*DOI:*

[10.1515/crelle-2014-0086](https://doi.org/10.1515/crelle-2014-0086)

*Publication date:*

2017

*Document Version*

Peer reviewed version

[Link to publication](#)

This is the author's accepted version of Cautis, S, Craw, A & Logvinenko, T 2014, 'Derived Reid's recipe for abelian subgroups of  $SL_3()$ ' Journal Fur Die Reine Und Angewandte Mathematik., available online via: <http://dx.doi.org/10.1515/crelle-2014-0086>.

## University of Bath

### General rights

Copyright and moral rights for the publications made accessible in the public portal are retained by the authors and/or other copyright owners and it is a condition of accessing publications that users recognise and abide by the legal requirements associated with these rights.

### Take down policy

If you believe that this document breaches copyright please contact us providing details, and we will remove access to the work immediately and investigate your claim.

# DERIVED REID’S RECIPE FOR ABELIAN SUBGROUPS OF $\mathrm{SL}_3(\mathbb{C})$

SABIN CAUTIS, ALASTAIR CRAW AND TIMOTHY LOGVINENKO

ABSTRACT. For any finite subgroup  $G \subset \mathrm{SL}_3(\mathbb{C})$ , work of Bridgeland-King-Reid constructs an equivalence between the  $G$ -equivariant derived category of  $\mathbb{C}^3$  and the derived category of the crepant resolution  $Y = G\text{-Hilb } \mathbb{C}^3$  of  $\mathbb{C}^3/G$ . When  $G$  is abelian we show that this equivalence gives a natural correspondence between irreducible representations of  $G$  and exceptional subvarieties of  $Y$ , thereby extending the McKay correspondence from two to three dimensions. This categorifies Reid’s recipe and extends earlier work from [CL09] and [Log10] which dealt only with the case when  $\mathbb{C}^3/G$  has one isolated singularity.

## CONTENTS

1. Introduction	1
2. Preliminaries	4
3. Sink-source graphs and non-compact exceptional divisors	9
4. CT-subdivisions	14
5. Derived Reid’s recipe	25
6. Worked example	34
References	44

## 1. INTRODUCTION

Originating in observations by John McKay [McK80], the classical McKay correspondence for a finite subgroup  $G \subset \mathrm{SL}_2(\mathbb{C})$  is a bijection between the nontrivial irreducible representations of  $G$  and the irreducible exceptional divisors on the minimal resolution  $Y$  of  $\mathbb{C}^2/G$ .

The representation ring of  $G$  is naturally isomorphic to  $K^G(\mathbb{C}^2)$ , the Grothendieck group of  $G$ -equivariant coherent sheaves on  $\mathbb{C}^2$ . Subsequently, the McKay correspondence was realized geometrically in [GSV83] as an isomorphism  $K^G(\mathbb{C}^2) \xrightarrow{\sim} K(Y)$ . In [KV00] this isomorphism was lifted to an equivalence  $D^G(\mathbb{C}^2) \xrightarrow{\sim} D(Y)$  of derived categories of coherent sheaves. For each non-trivial irreducible  $G$ -representation  $\rho$  it sends the sheaf  $\mathcal{O}_0 \otimes \rho$  to the structure sheaf of the corresponding exceptional divisor (twisted by  $\mathcal{O}(-1)$ ).

In dimension three, for a finite subgroup  $G \subset \mathrm{SL}_3(\mathbb{C})$ , the  $G$ -Hilbert scheme  $Y = G\text{-Hilb } \mathbb{C}^3$  is a crepant resolution of  $\mathbb{C}^3/G$ . This is a consequence of the derived equivalence  $\Psi: D^G(\mathbb{C}^3) \xrightarrow{\sim} D(Y)$  constructed by Bridgeland–King–Reid [BKR01]. Such an equivalence was conjectured by Reid [Rei97] while building on Nakamura’s description of  $G\text{-Hilb}(\mathbb{C}^3)$  [Nak00]. For  $G$  abelian, Reid also defined in *loc.cit.* a basis of  $H^*(Y, \mathbb{Z})$  using an ad-hoc combinatorial construction that was dubbed “Reid’s recipe” by Craw [Cra05].

In [CL09] the first and third authors conjectured that  $\Psi: D^G(\mathbb{C}^3) \xrightarrow{\sim} D(Y)$  sends  $\mathcal{O}_0 \otimes \rho$  to a sheaf supported on the exceptional subvariety of  $Y$  which is either a single divisor, a single curve or a chain of divisors, depending on the role of  $\rho$  in Reid’s recipe. The conjectured correspondence between irreducible representations of  $G$  and sheaves on exceptional subvarieties of  $Y$  generalises naturally the classical McKay correspondence for  $\mathrm{SL}_2(\mathbb{C})$  and was subsequently called the *derived Reid’s recipe*.

The fact that the image of each  $\mathcal{O}_0 \otimes \rho$  is a single sheaf was proved in [CL09] when  $G$  is abelian and  $\mathbb{C}^3/G$  has a single isolated singularity. Under these same conditions, the third author proved in [Log10] that the support of this sheaf is indeed determined by the role of  $\rho$  in Reid’s recipe.

When the singularities of  $\mathbb{C}^3/G$  are not isolated, the geometry of the exceptional locus of  $Y$  is more complicated and the methods of [CL09] and [Log10] do not apply. Moreover, these methods only compute the support of  $\Psi(\mathcal{O}_0 \otimes \rho)$  rather than the sheaf itself. In dimension two this extra data encoded very little, being just the line bundle  $\mathcal{O}(-1)$  for each exceptional  $\mathbb{P}^1$ . In dimension three, the situation is more subtle and the extra data provided by the sheaf forms a meaningful part of the correspondence.

In this paper, we compute the whole of derived Reid’s recipe for any finite abelian subgroup of  $\mathrm{SL}_3(\mathbb{C})$ . We can do this due to a new approach via *CT-subdivisions* (see Section 4). This technique may make it possible to generalise the derived Reid’s recipe to dimer models [?].

**1.1. Summary of results.** Let  $G \subset \mathrm{SL}_3(\mathbb{C})$  be a finite subgroup. The *G-Hilbert scheme*  $Y = G\text{-Hilb } \mathbb{C}^3$  is the fine moduli space parametrizing subschemes  $Z \subset \mathbb{C}^3$  for which  $H^0(\mathcal{O}_Z)$  is isomorphic to  $\mathbb{C}[G]$  as a  $\mathbb{C}[G]$ -module. Let  $\mathcal{Z} \subset Y \times \mathbb{C}^3$  denote the universal subscheme. As a Fourier-Mukai kernel,  $\mathcal{O}_{\mathcal{Z}}$  induces a functor  $\Psi: D^G(\mathbb{C}^3) \rightarrow D(Y)$  between the bounded derived categories of coherent sheaves on  $Y$  and  $G$ -equivariant coherent sheaves on  $\mathbb{C}^3$ . Bridgeland–King–Reid [BKR01] showed that  $\Psi$  is an exact equivalence of triangulated categories and that the Hilbert–Chow morphism  $\pi: Y \rightarrow \mathbb{C}^3/G$  is a projective, crepant resolution.

An irreducible representation  $\rho$  of  $G$  defines two natural  $G$ -equivariant sheaves on  $\mathbb{C}^3$ , namely  $\mathcal{O}_{\mathbb{C}^3} \otimes \rho$  and  $\mathcal{O}_0 \otimes \rho$ , where  $\mathcal{O}_0$  is the structure sheaf of the origin in  $\mathbb{C}^3$ .

The image  $\Psi(\mathcal{O}_{\mathbb{C}^3} \otimes \rho)$  is isomorphic to  $\mathcal{L}_\rho^\vee$ , where  $\mathcal{L}_\rho$  is one of the *tautological vector bundles*. These are vector bundles on  $Y$  defined via  $\pi_{Y*}\mathcal{O}_{\mathcal{Z}} = \bigoplus \mathcal{L}_\rho \otimes \rho$  where  $\pi_Y: Y \times \mathbb{C}^3 \rightarrow Y$  is the natural projection and the decomposition is with respect to the trivial  $G$ -action on  $Y$ .

On the other hand,  $\Psi(\mathcal{O}_0 \otimes \rho)$  is more complicated to describe. We do this for abelian  $G$ , so the irreducible representations of  $G$  are the characters  $\chi \in G^\vee$ . A priori, each  $\Psi(\mathcal{O}_0 \otimes \chi)$  is an abstract complex in  $D(Y)$ , but our first main result is:

**Theorem 1.1.** *Let  $G \subset \mathrm{SL}_3(\mathbb{C})$  be a finite abelian subgroup and let  $\chi \in G^\vee$  be nontrivial. Then  $\Psi(\mathcal{O}_0 \otimes \chi)$  is the pushforward of a (shift of a) coherent sheaf  $\mathcal{F}_\chi$  from the exceptional subvariety  $Z_\chi = \mathrm{Supp } \Psi(\mathcal{O}_0 \otimes \chi)$  of  $Y$ .*

Our second result describes explicitly  $\Psi(\mathcal{O}_0 \otimes \chi)$  in terms of Reid’s recipe. The variety  $Y$  is a toric variety and its toric fan defines a triangulation  $\Sigma$  of the junior simplex  $\Delta$ , cf. Section 2.2. Reid’s recipe marks each interior vertex and each interior edge of  $\Sigma$  with one or two non-trivial characters of  $G$ , cf. Section 2.3.

Craw [Cra05] proves that every non-trivial  $\chi$  marks in  $\Sigma$  either a unique vertex, a unique edge, a single chain of edges or three chains of edges meeting in a vertex. We give a worked example illustrating the results of this paper for  $G = \frac{1}{15}(1, 5, 9)$  in Section 6. In particular, there is a picture of Reid's recipe in Fig. 19(b). There are further examples in [Rei97, §6], [Cra05, §3] and [CL09, §1].

The vertices and edges of  $\Sigma$  correspond to the exceptional toric divisors and curves of  $Y$ . A chain of edges of  $\Sigma$  corresponds to a chain of divisors on  $Y$ : the edges correspond to the curves in which the divisors intersect. We say that  $\chi$  marks a divisor, a curve or a chain of divisors, if it marks the corresponding vertex, edge or chain of edges.

Finally, to deal with the trivial character  $\chi_0$  which did not appear in Reid's recipe, we need to consider the fibre  $\text{ZF}$  of  $Y$  over  $0 \in \mathbb{C}^3/G$ . In general,  $\text{ZF}$  is not equidimensional and we split it up into  $\text{ZF}_1$  and  $\text{ZF}_2$ , scheme-theoretic unions of its 1- and 2-dimensional components.

**Theorem 1.2** (Derived Reid's recipe). *Let  $G \subset \text{SL}_3(\mathbb{C})$  be a finite abelian subgroup and let  $\chi \in G^\vee$ . Then  $\mathcal{H}^i(\Psi(\mathcal{O}_0 \otimes \chi)) = 0$  unless  $i = 0, -1, -2$ . Moreover, one of the following holds:*

Reid's recipe	$\mathcal{H}^{-2}$	$\mathcal{H}^{-1}$	$\mathcal{H}^0$
$\chi$ marks a single divisor $E$	0	0	$\mathcal{L}_\chi^{-1} \otimes \mathcal{O}_E$
$\chi$ marks a single curve $C$	0	0	$\mathcal{L}_\chi^{-1} \otimes \mathcal{O}_C$
$\chi$ marks a chain of divisors which starts at a divisor $E$ and terminates at a divisor $F$	0	$\mathcal{L}_\chi^{-1}(-E - F) \otimes \mathcal{O}_Z$ , where $Z$ is the reduced union of the internal divisors of the chain	0
$\chi$ marks three chains of divisors, which start at $E_x, E_y$ and $E_z$ and meet at a divisor $P$	0	$\mathcal{L}_\chi^{-1}(-E_x - E_y - E_z) \otimes \mathcal{V}_Z^\dagger$	0
$\chi$ marks nothing ( $\chi = \chi_0$ )	$\omega_{\text{ZF}_2}^\dagger$	$\omega_{\text{ZF}_1}(\text{ZF}_2)^\dagger$	0

†: Here  $\omega_{\text{ZF}_i}$  is the dualizing sheaf of  $\text{ZF}_i$ . In fact,  $\Psi(\mathcal{O}_0 \otimes \chi_0)$  is the dualizing complex  $\omega_{\text{ZF}}$  of  $\text{ZF}$ , cf. §5.6.

‡: The support of  $\mathcal{V}_Z$  is the reduced union  $Z$  of the internal divisors of the chains. Away from where the three chains meet  $\mathcal{V}_Z \simeq \mathcal{O}_Z$ , but on that locus it is locally free of rank 2. To be precise,  $\mathcal{V}_Z$  is the cokernel of  $\mathcal{O}_Y \xrightarrow{E_x \oplus E_y \oplus E_z} \mathcal{O}_{Z_x}(E_x) \oplus \mathcal{O}_{Z_y}(E_y) \oplus \mathcal{O}_{Z_z}(E_z)$  where  $Z_x = E_y P \cup E_z P$  and similarly for  $Z_y$  and  $Z_z$ , cf. §5.4

Thus, roughly, the *derived Reid's recipe* assigns to each non-trivial  $\chi$  one of the following:

- An exceptional divisor or an exceptional curve.
- A chain of exceptional divisors with two marked curves on the two endpoint divisors.
- A tree of exceptional divisors with one fork and three branches, together with three marked curves on the three endpoint divisors.

We close with two remarks. First, the sheaf data is necessary. For instance, when  $G = \frac{1}{6}(1, 2, 3)$  there exist two representations which correspond to the same divisor but with different marked curves. Secondly, the representations that correspond to a single divisor or a curve are called *essential*. They possess an independent characterisation in terms of moduli of quiver representations [Tak11].

**Acknowledgements.** S.C. is supported by NSF grant DMS-1101439 and the Alfred P. Sloan foundation, A.C. is supported by EPSRC grant EP/G004048 and T.L. is supported by EPSRC grant EP/H023267/1. We would like to thank Miles Reid, Michael Wemyss, Yukari Ito, Keisuke Takahashi and Yuih Sekiya for useful discussions while writing this paper.

## 2. PRELIMINARIES

**2.1. Action of  $G$  on  $\mathbb{C}^3$ .** Let  $G$  be a finite subgroup of  $\mathrm{SL}_3(\mathbb{C})$ . It acts naturally on  $\mathbb{C}^3$  on the left. Let  $V$  be the corresponding representation. We identify  $V^\vee$  with the space of linear functions on  $\mathbb{C}^3$ . Let  $x_1, x_2$  and  $x_3$  be the basis of  $V^\vee$  dual to the canonical basis of  $\mathbb{C}^3$ . Sometimes, we use  $x, y$  and  $z$  for  $x_1, x_2$  and  $x_3$ . The (left) action of  $G$  on  $V$  defines a *right* action of  $G$  on  $V^\vee$ , which we make into a left action by setting

$$g \cdot m(v) = m(g^{-1} \cdot v) \quad \text{for all } g \in G, m \in V^\vee \text{ and } v \in V. \quad (2.1)$$

This action extends naturally to an action on the symmetric algebra  $R = S(V^\vee) = \mathbb{C}[x, y, z]$ . We give  $\mathbb{C}^3$  the structure of a  $G$ -scheme by identifying it with the closed points of  $\mathrm{Spec} R$ .

Denote by  $G^\vee$  the character group  $\mathrm{Hom}_{\mathbb{Z}}(G, \mathbb{C}^*)$  of  $G$ . A rational function  $f \in K(\mathbb{C}^3)$  is said to be a *semi-invariant of  $G$* , or a  *$G$ -eigenvector*, if there is  $\chi \in G^\vee$  such that  $g \cdot f = \chi(g)f$ . We denote the weight  $\chi$  of  $f$  by  $\kappa(f)$ . Suppose  $G$  is abelian, then  $\mathbb{C}^3$  has a basis of  $G$ -eigenvectors. Replacing  $G$  by a conjugate subgroup of  $\mathrm{SL}_3(\mathbb{C})$  if necessary, we assume that the canonical basis of  $\mathbb{C}^3$  is one such, i.e. every Laurent monomial is a  $G$ -eigenvector.

**2.2.  $G$ -Hilb  $\mathbb{C}^3$  and its toric geometry.** A  $G$ -cluster is a  $G$ -invariant subscheme of  $\mathbb{C}^3$  whose global sections are  $G$ -equivariantly isomorphic to the regular representation  $V_{\mathrm{reg}}$ . The support of any  $G$ -cluster is a set-theoretic  $G$ -orbit, and we think of  $G$ -clusters as scheme-theoretic orbits of  $G$  in  $\mathbb{C}^3$ . By [BKR01] the fine moduli space  $G\text{-Hilb } \mathbb{C}^3$  of  $G$ -clusters together with its *Hilbert-Chow map*  $G\text{-Hilb } \mathbb{C}^3 \rightarrow \mathbb{C}^3/G$ , which sends each  $G$ -cluster to the corresponding  $G$ -orbit, is a crepant resolution. For abelian  $G$  this resolution is well understood in terms of toric geometry. Below we summarize the main points, for more detail cf. [Nak00], [CR02] or [Log03, §3.1].

Let  $\mathbb{Z}^3$  be the lattice of Laurent monomials, where we identify  $m = (m_1, m_2, m_3)$  with the monomial  $x_1^{m_1} x_2^{m_2} x_3^{m_3}$ . Let  $M \subset \mathbb{Z}^3$  be the sublattice of  $G$ -invariant monomials. The dual lattice of  $G$ -weights  $L = \mathrm{Hom}_{\mathbb{Z}}(M, \mathbb{Z})$  contains  $\mathrm{Hom}_{\mathbb{Z}}(\mathbb{Z}^3, \mathbb{Z})$  as a sublattice. As  $G$  is finite we have  $L \subset \mathbb{Q}^3$  and write each  $l \in L$  as a triplet  $(l_1, l_2, l_3) \in \mathbb{Q}^3$ . Let  $\sigma_+$  denote the cone  $\{(e_1, e_2, e_3) \mid e_i \geq 0\}$  in  $\mathbb{R}^3 \simeq L \otimes \mathbb{R}$ . Then:

- $\mathbb{C}^3$  is defined as a toric variety by the lattice  $\mathbb{Z}^3$  and the cone  $\sigma_+$ .
- $\mathbb{C}^3/G$  is defined by the lattice  $L$  and the cone  $\sigma_+$ .
- A toric resolution of  $\mathbb{C}^3/G$  is defined by the lattice  $L$  and a fan that subdivides the cone  $\sigma_+$  into regular subcones.

Let the *junior simplex*  $\Delta$  be the triangle formed by cutting  $\sigma_+$  by the hyperplane  $\sum e_i = 1$ . A fan  $\mathfrak{F}$  which subdivides  $\sigma_+$  into regular subcones is determined by how it triangulates  $\Delta$ . Let  $\mathfrak{E}$  be the set of the generators of the rays of  $\mathfrak{F}$ . For any crepant resolution,  $\mathfrak{E} = L \cap \Delta$  and moreover:

- The vertices of  $\Sigma$  are the elements of  $\mathfrak{E}$ . For any vertex  $e$  of  $\Sigma$  we write  $E_e$  for the toric divisor which corresponds to the ray  $\langle e \rangle$ .
- The edges of  $\Sigma$  correspond to the two-dimensional cones of  $\mathfrak{F}$ . Two vertices  $e, f \in \mathfrak{E}$  are joined by an edge if and only if divisors  $E_e$  and  $E_f$  intersect. The intersection is then the torus-invariant  $\mathbb{P}^1$  which corresponds to the cone  $\langle e, f \rangle$ .
- The triangles of  $\Sigma$  correspond to three-dimensional cones of  $\mathfrak{F}$ . A triangle  $(e, f, g)$  corresponds to  $E_e, E_f$  and  $E_g$  intersecting at the torus fixed point  $\langle e, f, g \rangle$ .

- Each three-dimensional cone  $\sigma$  in  $\mathfrak{F}$  defines a toric affine chart  $A_\sigma$  isomorphic to  $\mathbb{C}^3$ . In terms of toric geometry,  $A_\sigma$  is the union of the torus orbits defined by subcones of  $\sigma$ .

[CR02] describes how to construct the triangulation  $\Sigma$  of  $\Delta$  corresponding to  $Y = G\text{-Hilb } \mathbb{C}^3$ . The toric divisors of  $Y$  defined by vertices of  $\Sigma$  divide into three groups:

- The corner vertices of  $\Delta$  give the strict transforms of coordinate hyperplanes of  $\mathbb{C}^3/G$ .
- The vertices on the sides of  $\Delta$  give the non-compact exceptional divisors. Each of these is a  $\mathbb{P}^1$ -fibration over one of the coordinate lines of  $\mathbb{C}^3/G$ , possibly degenerating over the origin to a pair of  $\mathbb{P}^1$ s intersecting transversally.
- The vertices in the interior of  $\Delta$  give the compact exceptional divisors. These lie over the origin of  $\mathbb{C}^3/G$  and are either a  $\mathbb{P}^2$ , a rational scroll blown up in 0, 1 or 2 points, or a del Pezzo surface of degree six [CR02, Cor. 1.4].

Let  $ZF$  denote the fiber of  $Y$  over the origin of  $\mathbb{C}^3/G$ . In general,  $ZF$  is just a section of the exceptional set  $\text{Exc}(Y)$ . It is a reducible variety with a two-dimensional and a one-dimensional stratum which we denote by  $ZF_2$  and  $ZF_1$ . The irreducible components of  $ZF_2$  are the compact exceptional divisors of  $Y$  defined by the internal vertices of  $\Delta$ . The non-compact exceptional divisors of  $Y$  each meet  $ZF$  in a  $\mathbb{P}^1$  or a pair of  $\mathbb{P}^1$ s. The irreducible components of  $ZF_1$  are those of these  $\mathbb{P}^1$ s which do not lie on any of the divisors in  $ZF_2$ . These are the curves defined by the edges of  $\Sigma$  which cross the interior of  $\Delta$  but whose endpoints lie on the sides of  $\Delta$ .

**2.3. Reid's recipe.** Reid's recipe [Rei97], [Cra05] is an algorithm to construct the cohomological version of the McKay correspondence for abelian  $G \subset \text{SL}_3(\mathbb{C})$ . It begins with a toric geometry computation which marks internal edges and vertices of the  $G$ -Hilb triangulation  $\Sigma$  with characters of  $G$ . This marking is a key to stating our main result, Theorem 1.2, so below we give a brief summary of its construction.

First we mark each edge  $(e, f)$  in  $\Sigma$  according to the following rule. The one-dimensional ray in  $M$  perpendicular to the hyperplane  $\langle e, f \rangle$  in  $L$  has two primitive generators:  $\frac{m_1}{m_2}$  and  $\frac{m_2}{m_1}$ , where  $m_1, m_2$  are co-prime regular monomials in  $R$ . As  $M$  is the lattice of  $G$ -invariant Laurent monomials,  $m_1$  and  $m_2$  have to be of the same character  $\chi$  for some  $\chi \in G^\vee$ . We say that  $(e, f)$  is *carved out* by the ratio  $m_1 : m_2$  (or  $m_2 : m_1$ ) and *mark it* by  $\chi$ .

Then we mark each internal vertex  $e$  of  $\Sigma$  according to whether the corresponding exceptional divisor is a  $\mathbb{P}^2$ , a rational scroll blown-up in 0, 1 or 2 points or a del Pezzo surface  $dP_6$ :

- (1) If  $E_e$  is a  $\mathbb{P}^2$ , then there are three edges incident to  $e$  in  $\Sigma$ . By [Cra05, Lemma 3.1] they lie on three lines joining  $e$  to the three corner vertices of  $\Delta$  and are marked with same character  $\chi \in G^\vee$ . Reid's recipe prescribes for  $E_e$  to be marked with character  $\chi \cdot \chi$ .
- (2) If  $E_e$  is a rational scroll blown-up in 0, 1 or 2 points then there are 4, 5 or 6 edges incident to  $e$  in  $\Sigma$ , respectively. By [Cra05, Lemma 3.2-3.3] two of these lie on a straight line joining  $e$  to a corner vertex of  $\Delta$  and are marked by same character  $\chi \in G^\vee$ . Of the remaining ones exactly two are marked by the same character. Denote this character by  $\chi' \in G^\vee$ , then Reid's recipe prescribes for  $E_e$  to be marked with character  $\chi \cdot \chi'$ .
- (3) If  $E_e$  is a del Pezzo surface  $dP_6$ , then there are 6 edges incident to  $e$  in  $\Sigma$ . These lie on three straight lines which intersect at  $e$ . By [Cra05, Lemma 3.4] the two toric projections  $E_e \rightarrow \mathbb{P}^2$  are given by monomial maps  $(m_0 : m_1 : m_2)$  and  $(m'_0 : m'_1 : m'_2)$  with  $m_i \in R$

being all of same character  $\chi$  and  $m'_i \in R$  being all of same character  $\chi'$ . Reid's recipe prescribes  $E_e$  to be marked with two characters:  $\chi$  and  $\chi'$ .

**2.4. Universal family  $\mathcal{M}$  and its dual  $\tilde{\mathcal{M}}$ .** The fine moduli space  $Y = G\text{-Hilb } \mathbb{C}^3$  comes equipped with the universal family  $Z \subset Y \times \mathbb{C}^3$  of  $G$ -clusters. Let  $G$  act trivially on  $Y$ , then we can speak of  $G$ -equivariant sheaves on  $Y \times \mathbb{C}^3$ . Let  $\mathcal{M} \in \text{Coh}^G(Y \times \mathbb{C}^3)$  denote the structure sheaf of  $Z$ . It is a coherent  $G$ -sheaf flat over  $Y$  whose fiber over any point of  $Y$  is a finite-length  $G$ -sheaf on  $\mathbb{C}^3$ . Therefore  $\pi_{Y*}\mathcal{M} \in \text{Coh}^G(Y)$  is a locally free  $G$ -sheaf of finite rank on  $Y$ . Since  $G$  acts trivially on  $Y$ , we can decompose  $\pi_{Y*}\mathcal{M}$  into  $G$ -eigsheaves as  $\bigoplus_{\rho \in \text{Irr } G} \mathcal{L}_\rho \otimes \rho$  where  $\mathcal{L}_\rho$  are locally-free sheaves of rank  $\dim(\rho)$ . In the literature  $\mathcal{L}_\rho$  are known as *tautological* or *Gonzales-Sprinberg and Verdier* ( $GSp$ - $V$ ) sheaves.

The equivalence  $\Phi: D(Y) \rightarrow D^G(\mathbb{C}^3)$  of [BKR01] is a Fourier-Mukai transform whose Fourier-Mukai kernel is  $\mathcal{M}$ . To compute derived Reid's recipe we need its inverse  $\Psi: D^G(\mathbb{C}^3) \rightarrow D(Y)$ . In [CL09] we've shown that  $\Psi$  is also a Fourier-Mukai transform and that its Fourier-Mukai kernel  $\tilde{\mathcal{M}}$  is also a flat family of finite-length sheaves on  $\mathbb{C}^3$  which can be understood as follows.

A  $G$ -constellation is a coherent  $G$ -sheaf on  $\mathbb{C}^3$  whose space of global sections is isomorphic to  $V_{\text{reg}}$  as a representation of  $G$ . We view  $G$ -clusters as a subclass of  $G$ -constellations by looking at their structure sheaves. From the point of view of the McKay correspondence we are only interested in  $G$ -constellations which still make sense as generalized  $G$ -orbits, i.e. whose support in  $\mathbb{C}^3$  is a single  $G$ -orbit. Flat families of such  $G$ -constellations over  $Y = G\text{-Hilb } \mathbb{C}^3$  whose Hilbert-Chow map  $Y \rightarrow \mathbb{C}^3/G$  coincides with the resolution morphism are called *gnat-families*. Tautologically, the universal family  $\mathcal{M}$  of  $G$ -clusters is a *gnat-family*. Given a *gnat-family*  $\mathcal{F}$  over  $Y$  we denote by  $\mathcal{F}_p$  the  $G$ -constellation parametrised in  $\mathcal{F}$  by a point  $p \in Y$ .

Since  $\mathbb{C}^3$  is affine, any  $G$ -constellation  $\mathcal{W}$  is determined by its space of global sections  $\Gamma(\mathcal{W})$  with the natural action of  $R \rtimes G$  on it. Since  $V_{\text{reg}}^* \simeq V_{\text{reg}}$ , the complex vector space dual  $\Gamma(\mathcal{W})^*$  with the dual  $R \rtimes G$ -action defines a new  $G$ -constellation  $\tilde{\mathcal{W}}$  called *the dual of  $\mathcal{F}$* . Given a *gnat-family*  $\mathcal{F}$  we define similarly *the dual gnat-family  $\tilde{\mathcal{F}}$*  which is a fibre-wise dual of  $\mathcal{F}$ . In [CL09, §2] we prove an alternative description of dualizing a  $G$ -constellation:  $\tilde{\mathcal{W}} = \mathcal{W}^\vee[n]$ , where  $\mathcal{W}^\vee$  is the derived dual  $\mathbf{R}\text{Hom}_Y(\mathcal{W}, \mathcal{O}_Y)$ . In other words,  $\tilde{\mathcal{W}}$  is the unique non-zero cohomology sheaf of  $\mathcal{W}^\vee$ , located in degree  $n$ . Similarly,  $\tilde{\mathcal{F}} = \mathcal{F}^\vee[n]$  [CL09, Prop. 2.1]. It follows naturally [Log08a, Lemma 4] that on  $Y = G\text{-Hilb } \mathbb{C}^3$  the inverse  $\Psi$  of the equivalence  $\Phi$  of [BKR01] is the Fourier-Mukai transform defined by the dual family  $\tilde{\mathcal{M}}$ .

**2.5. The McKay quiver of  $G$  and its representations.** To any finite subgroup  $G$  of  $\text{GL}_n(\mathbb{C})$  we associate a quiver  $Q(G)$  called *the McKay quiver of  $G$* . For an abelian  $G \subset \text{SL}_3(\mathbb{C})$  quiver  $Q(G)$  has as its vertices the characters  $\chi \in G^\vee$  of  $G$  and from every vertex  $\chi$  there are three arrows going to vertices  $\kappa(x_i)\chi$  for  $i = 1, 2, 3$ . For each arrow  $(\chi, x_i): \chi \xrightarrow{x_i} \kappa(x_i)\chi$  we fix a choice of basis for (one-dimensional) space  $G\text{-Hom}_{\mathbb{C}}(\chi \otimes \mathbb{C}x_i, \chi\kappa(x_i))$ . This can be thought of as fixing a choice of all the Schur's lemma isomorphisms we need.

There is a standard planar embedding of  $Q(G)$  into a real two dimensional torus  $T_G$ . It was first constructed by Craw and Ishii in [CI04, §10.2]. This embedding tessellates  $T_G$  into  $2|G|$  regular triangles. Locally near each vertex  $\chi$  it looks as on Figure 1. We denote by  $\text{Hex}(\chi)$  the subquiver of  $Q(G)$  which consists of the six triangles which meet at  $\chi$ .



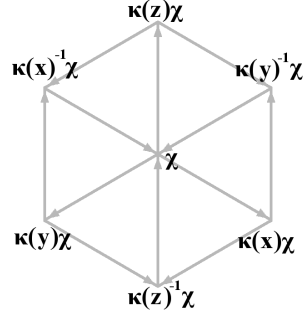
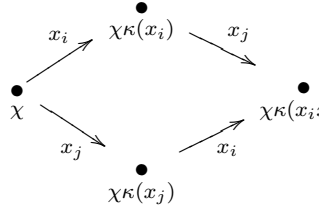


FIGURE 1. Subquiver  $\text{Hex}(\chi)$  of  $Q(G)$

A representation of  $Q(G)$  consists of a vector space  $V_\chi$  for each vertex  $\chi$  and a linear map  $\alpha_{\chi,i} : V_\chi \rightarrow V_{\chi\kappa(x_i)}$  for each arrow  $(\chi, i)$ . The category of the representations of  $Q(G)$  in which

the linear maps representing each square



commute is equivalent to

the category of quasi-coherent  $G$ -sheaves on  $\mathbb{C}^n$ . Given any quasi-coherent  $G$ -sheaf  $\mathcal{M}$  on  $\mathbb{C}^n$  we define its *associated representation*  $Q(G)_\mathcal{M}$  as follows. The space of global sections  $\Gamma(\mathcal{M})$  of  $\mathcal{M}$  is a  $\mathbb{R} \rtimes G$ -module and the evaluation map

$$\bigoplus_{\chi \in G^\vee} G\text{-Hom}_{\mathbb{C}}(\chi, \Gamma(\mathcal{M})) \otimes \chi \xrightarrow{\sim} \Gamma(\mathcal{M}) \quad (2.2)$$

is an isomorphism which decomposes  $\Gamma(\mathcal{M})$  into  $G$ -eigenspaces. We define  $Q(G)_\mathcal{M}$  by setting  $V_\chi = G\text{-Hom}_{\mathbb{C}}(\chi, \Gamma(\mathcal{M}))$ , then under (2.2) the actions of  $x_i$  on  $\Gamma(\mathcal{M})$  become maps

$$\left( \bigoplus_{\chi \in G^\vee} V_\chi \otimes \chi \right) \otimes \mathbb{C}x_i \xrightarrow{\text{action of } x_i} \bigoplus_{\chi \in G^\vee} V_\chi \otimes \chi$$

and the choice of Schur's lemma isomorphisms we've fixed above makes these into the requisite linear maps  $\alpha_{\chi,x_i} : V_\chi \rightarrow V_{\chi\kappa(x_i)}$ .

Similarly, given a *gnat*-family  $\mathcal{F} \in \text{Coh}^G(Y \times \mathbb{C}^n)$  the direct image  $\pi_{Y*}\mathcal{F}$  is a sheaf of  $\mathcal{O}_Y \otimes_{\mathbb{C}} (\mathbb{R} \rtimes G)$ -modules on  $Y$  which is locally-free as an  $\mathcal{O}_Y$ -module. Since the action of  $G$  on  $Y$  is trivial, we can decompose  $\pi_{Y*}\mathcal{F}$  into  $G$ -eigensheaves as  $\bigoplus \mathcal{L}_\chi \otimes \chi$ , where each  $\mathcal{L}_\chi$  is a line bundle on  $Y$ . We then define the *associated representation*  $Q(G)_\mathcal{F}$  by representing each vertex  $\chi$  of  $Q(G)$  by  $\mathcal{L}_\chi$  and representing each arrow  $(\chi, x_i)$  of  $Q(G)$  by the map  $\alpha_{\chi,i} : \mathcal{L}_\chi \rightarrow \mathcal{L}_{\chi\kappa(x_i)}$ , which is obtained as above: taking the action of  $x_i$  on  $\pi_{Y*}\mathcal{F}$  and restricting it to  $\mathcal{L}_\chi$  via our choice of Schur's lemma isomorphisms.

We say that in  $\mathcal{F}$  an arrow  $(\chi, x_i)$  vanishes at a point  $p \in Y$  if so does map  $\alpha_{\chi,x_i}$  of  $Q(G)_\mathcal{F}$ . The locus of all such points is a divisor called the *vanishing divisor*  $B_{\chi,x_i}$  of  $(\chi, x_i)$  in  $\mathcal{F}$ . Note that divisors  $B_{\chi,x_i}$  are independent of our choice of Schur's lemma isomorphisms, since a different choice would amount to multiplying each  $\alpha_{\chi,x_i}$  by a non-zero scalar.



For any abelian  $G \subset \mathrm{SL}_3(\mathbb{C})$  any *gnat*-family  $\mathcal{F}$  on  $Y$  can be written down numerically using the classification of *gnat*-families introduced in [Log08b]. The vanishing divisors  $B_{\chi, x_i}$  of  $Q(G)_{\mathcal{F}}$  can then be explicitly computed in terms of the numerical data defining  $\mathcal{F}$  [Log08a, §4.6]. A detailed example of such computation for the dual family  $\tilde{M}$  of the universal family of  $G$ -clusters is given in [CL09, §6].

**2.6. Transforms  $\Psi(\mathcal{O}_0 \otimes \chi)$  and skew-commutative cubes of line bundles.** Derived Reid's recipe assigns to each character  $\chi \in G^\vee$  the object  $\Psi(\mathcal{O}_0 \times \chi)$  of  $D(Y)$ . It was shown in [CL09, §2] that  $\Psi(\mathcal{O}_0 \otimes \chi)$  is isomorphic to the total complex of the skew-commutative cube of line bundles obtained from the subrepresentation  $\mathrm{Hex}(\chi^{-1})_{\tilde{\mathcal{M}}}$  of  $Q(G)_{\tilde{\mathcal{M}}}$  in the following way.

The generalities on cubes of line bundles are laid out in [CL09], §3. For our purposes, a cube of line bundles on  $Y$  is the following collection of line bundles and maps between them:

$$\begin{array}{ccccc}
 & & \mathcal{L}_{23} & & \alpha_1^3 \nearrow \mathcal{L}_1 \\
 & \alpha_{23}^1 \nearrow & & \alpha_3^2 \nearrow & \\
 \mathcal{L}_{123} & \xrightarrow{\alpha_{13}^2} & \mathcal{L}_{13} & \xrightarrow{\alpha_1^2} & \mathcal{L}_2 \\
 & \alpha_{12}^3 \searrow & & \alpha_2^1 \searrow & \\
 & & \mathcal{L}_{12} & & \alpha_3^1 \searrow \mathcal{L}_3
 \end{array}
 \quad (2.3)$$

If the cube in (2.3) is skew-commutative, we define its *total complex*  $T^\bullet$  to be

$$0 \rightarrow \mathcal{L}_{123} \rightarrow \mathcal{L}_{23} \oplus \mathcal{L}_{13} \oplus \mathcal{L}_{12} \rightarrow \mathcal{L}_1 \oplus \mathcal{L}_2 \oplus \mathcal{L}_3 \rightarrow \underline{\mathcal{L}} \rightarrow 0$$

The differential maps of  $T^\bullet$  are defined by summing up all the appropriate maps of the cube.

On Fig. 2(a) we draw the subquiver  $\mathrm{Hex}(\chi^{-1})$  of the McKay quiver  $Q(G)$ . We arrange the subrepresentation  $\mathrm{Hex}(\chi^{-1})_{\tilde{\mathcal{M}}}$  into a commutative cube of line bundles as depicted on Fig. 2(b). We make this commutative cube skew-commutative by setting  $\alpha_{(\dots)}^i = (-1)^i \alpha_{(\dots)}^i$ . The total

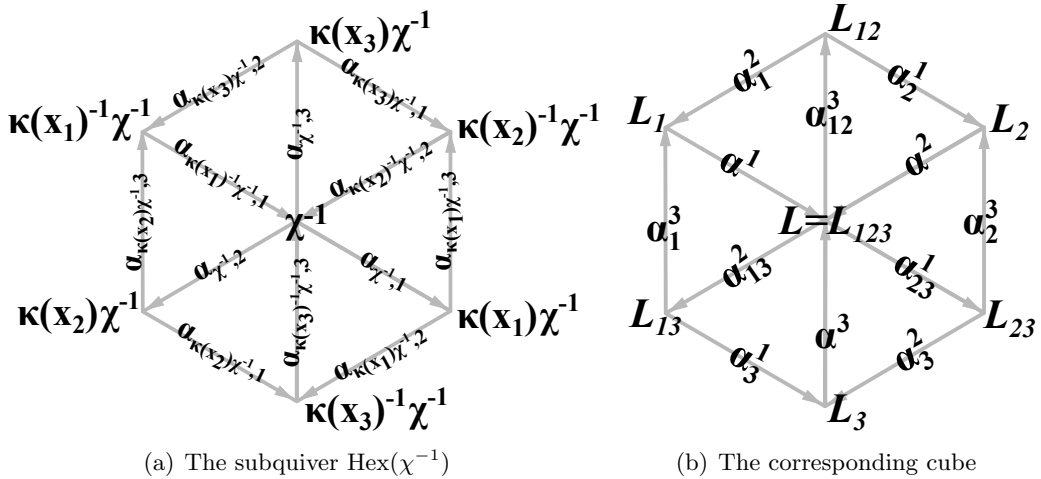


FIGURE 2. The cube of line bundles defined by  $\mathrm{Hex}(\chi^{-1})_{\tilde{\mathcal{M}}}$

complex  $T^\bullet$  of the resulting cube is isomorphic to  $\Psi(\mathcal{O}_0 \times \chi)$  in  $D(Y)$  [CL09, Prop. 4.6].

Write  $D_{23}^1$  for the vanishing divisor of map  $\alpha_{23}^1$  of the cube in (2.3) and similarly for its other maps. The cohomology sheaves of  $T^\bullet$  can be computed in terms of these vanishing divisors:

**Lemma 2.1.** *Let  $T^\bullet$  be the total complex of the skew-commutative cube in (2.3). Then:*

- (1)  $H^0(T^\bullet) \cong \mathcal{L} \otimes \mathcal{O}_Z$  where  $Z$  is the scheme theoretic intersection  $D^1 \cap D^2 \cap D^3$ .
- (2) For any permutation  $\{I, J, K\}$  of  $\{12, 13, 23\}$  there is a three-step filtration of  $H^{-1}(T^\bullet)$  with successive quotients  $\mathcal{F}_I'', \mathcal{F}_J'$  and  $\mathcal{F}_K$ . Here:
  - $\mathcal{F}_{12} = \mathcal{O}_Z \otimes \mathcal{L}_{12}(\gcd(D_1^2, D_2^1))$  where  $Z$  is the scheme theoretic intersection of  $\gcd(D_1^2, D_2^1)$  and the effective part of  $D^3 + \text{lcm}(D_3^1, D_3^2) - \tilde{D}_1^2 - D^1$
  - $\mathcal{F}_{13} = \mathcal{O}_Z \otimes \mathcal{L}_{13}(\gcd(D_1^3, D_3^1))$  where  $Z$  is the scheme theoretic intersection of  $\gcd(D_1^3, D_3^1)$  and the effective part of  $D^2 + \text{lcm}(D_2^1, D_2^3) - \tilde{D}_3^1 - D^3$
  - $\mathcal{F}_{23} = \mathcal{O}_Z \otimes \mathcal{L}_{23}(\gcd(D_2^3, D_3^2))$  where  $Z$  is the scheme theoretic intersection of  $\gcd(D_2^3, D_3^2)$  and the effective part of  $D^1 + \text{lcm}(D_1^2, D_1^3) - \tilde{D}_2^3 - D^2$ .
and  $\tilde{D}_j^i = D_j^i - \gcd(D_j^i, D_i^j)$ . To define  $\mathcal{F}_J'$  we replace  $\text{lcm}(D_k^i, D_k^j)$  in its definition with  $\text{lcm}(D_k^i, \tilde{D}_k^j)$  where  $j$  is chosen so that  $K = \{jk\}$ . To define  $\mathcal{F}_I''$  we replace  $\text{lcm}(D_k^i, D_k^j)$  with  $\text{lcm}(\tilde{D}_k^i, \tilde{D}_k^j)$ .
- (3)  $H^{-2}(T^\bullet) \cong \mathcal{L}_{123}(D) \otimes \mathcal{O}_D$  where  $D = \gcd(D_{23}^1, D_{13}^2, D_{12}^3)$
- (4)  $H^{-i}(T^\bullet) \cong 0$  for all  $i \neq 0, -1$  and  $-2$ .

*Proof.* Same as the proof of [CL09, Lemma 3.1]. □

### 3. SINK-SOURCE GRAPHS AND NON-COMPACT EXCEPTIONAL DIVISORS

Let  $Y$  be  $G\text{-Hilb}(\mathbb{C}^3)$ ,  $\tilde{\mathcal{M}}$  be the universal family of  $G$ -clusters and  $E$  be a toric divisor on  $Y$ . In [CL09, Prop. 4.7] we've classified the vertices of  $Q(G)$  according to which of the arrows in the subquiver  $\text{Hex}(\chi)$  on Fig. 1 vanish along  $E$  in  $\tilde{\mathcal{M}}$ . On Fig. 3 - 6 we list all possible cases, drawing in black the arrows which vanish and in grey the arrows which don't. There are four vertex types: the *charges*, the *sources*, the *sinks* and the *tiles*. The charge vertices always occur in  $Q(G)$  in straight lines propagating from a source vertex to a sink vertex. An  $x_i$ -oriented charge propagates along  $x_i$ -arrows of  $Q(G)$ . A type  $(1, 0)$ -charge propagates in the direction of the arrows, while a type  $(0, 1)$ -charge propagates against it. A type  $(a, b)$ -source (resp. sink) emits (resp. receives)  $a$  charges of type  $(1, 0)$  and  $b$  charges of type  $(0, 1)$ .

The *sink-source graph*  $SS_{\tilde{\mathcal{M}}, E}$  is a graph drawn on top of  $Q(G)$  whose vertices are the sinks and the sources and whose edges are the charge lines. This graph subdivides the torus  $T_H$  into several connected regions which are each  $x$ -,  $y$ - or  $z$ -tiled. In particular, if  $SS_{\tilde{\mathcal{M}}, E}$  is empty then the whole of  $T_H$  is either  $x$ -,  $y$ - or  $z$ -tiled. Here we say that a region is, for example,  $x$ -tiled if all its internal vertices are  $x$ -tiles.

The sink-source graph  $SS_{\tilde{\mathcal{M}}, E}$  completely determines the divisor  $E$ , because we can read off from  $SS_{\tilde{\mathcal{M}}, E}$  which arrows of  $Q(G)$  do and do not vanish along  $E$ , and then apply the following:

**Lemma 3.1** ([Log10], Lemma 2.5). *Let  $E$  be a torus-invariant divisor of  $Y$ . Suppose the total numbers of  $x$ -,  $y$ - and  $z$ -oriented arrows of  $Q(G)$  which vanish along  $E$  in  $\tilde{\mathcal{M}}$  are  $a$ ,  $b$  and  $c$ , respectively. Then  $E$  is the divisor defined by  $e = \frac{1}{|G|}(a, b, c) \in \mathfrak{E} \subset \mathbb{Q}^3$ .*

If  $E$  is a compact exceptional divisor of  $Y$ , then it was shown in [Log10, Prop. 3.1-3.3] that there are only three possible shapes that  $SS_{\tilde{\mathcal{M}}, E}$  can have and these correspond precisely to  $E$

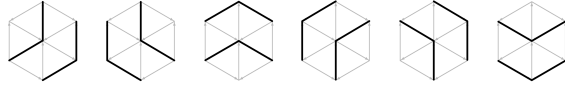


FIGURE 3. The  $x$ -,  $y$ -,  $z$ -(1,0)-charges and the  $x$ -,  $y$ -,  $z$ -(0,1)-charges

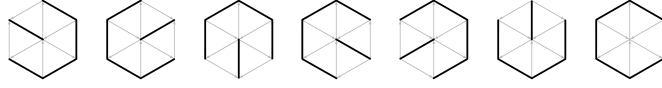


FIGURE 4. The  $x$ -,  $y$ -,  $z$ -(1,2)-sources, the  $x$ -,  $y$ -,  $z$ -(2,1)-sources and the (3,3)-source.

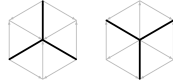


FIGURE 5. The (3,0)-sink and the (0,3)-sink.

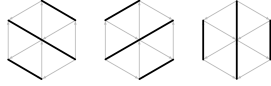


FIGURE 6. The  $x$ -tile, the  $y$ -tile and the  $z$ -tile.

being a  $\mathbb{P}^2$ , a rational scroll blown-up in 0, 1 or 2 points or a del Pezzo surface  $dP_6$ . Moreover, as demonstrated on Figures 7-9, the precise dimensions of  $SS_{\tilde{\mathcal{M}},E}$  determine completely the triangulation  $\Sigma$  locally around the corresponding point  $e \in \mathfrak{E}$ . In particular, they determine monomial ratios which carve out the edges incident to  $e$  in  $\Sigma$ . This provides a crucial link with Reid's recipe marking described in §2.3. E.g. the characters with which Reid's recipe prescribes to mark  $E$  are precisely the (0,3)-sink vertices of  $SS_{\tilde{\mathcal{M}},E}$ .

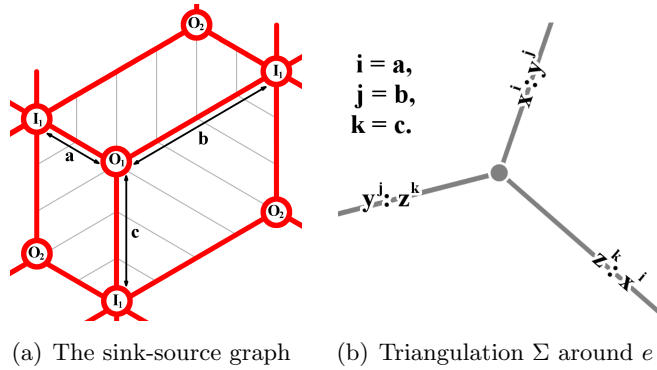


FIGURE 7. One (3,3)-source

In this section, we extend the above results on sink-source graphs to cover the non-compact exceptional divisors, which appear when the singularities of  $\mathbb{C}^3/G$  are not isolated:

**Lemma 3.2.** *Let  $E$  be an irreducible toric divisor on  $Y$ . The sink-source graph  $SS_{\tilde{\mathcal{M}},E}$*

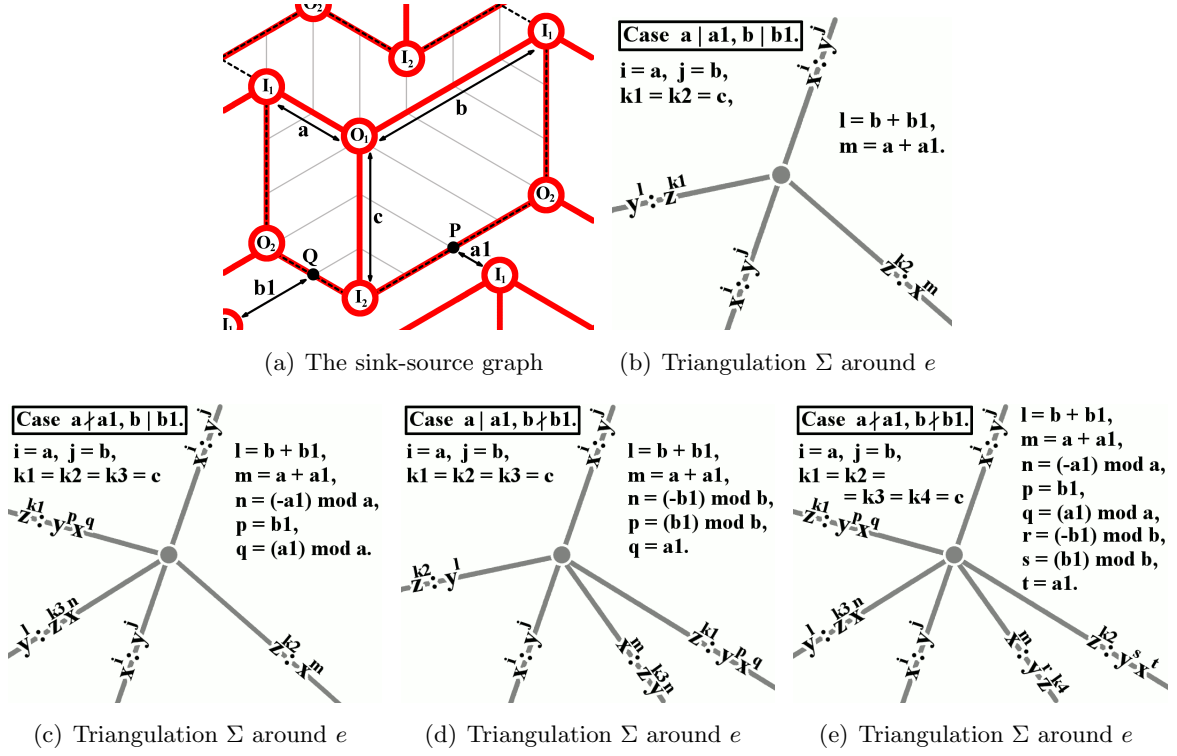


FIGURE 8. One  $(1, 2)$ -source and one  $(2, 1)$ -source

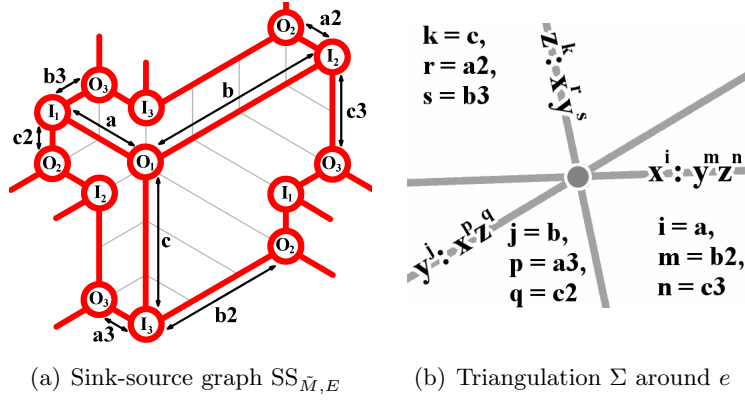


FIGURE 9. Three  $(2, 1)$ -sources

- (1) is empty if and only if  $E$  is the strict transform of one of the coordinate hyperplanes in  $\mathbb{C}^3/G$ . Moreover,  $T_H$  is  $x$ -tiled (resp.  $y$ -tiled,  $z$ -tiled) if and only if  $E$  is the strict transform of the  $yz$ -plane (resp.  $xz$ -plane,  $xy$ -plane).
- (2) consists of one looping  $(1, 0)$ -charge line (passing through vertex  $\chi_0$ ) and one looping  $(0, 1)$ -charge line if  $E$  is a non-compact exceptional divisor.
- (3) contains exactly one  $(3, 0)$ -sink (given by vertex  $\chi_0$ ) if  $E$  is a compact exceptional divisor.

*Proof.* By definition  $SS_{\mathcal{M}, E}$  is empty and  $T_H$  is, for example,  $x$ -tiled if and only if every  $x$ -oriented arrow vanishes along  $E$  in the associated representation  $Q(G)_{\tilde{\mathcal{M}}}$ , while none of  $y$ - or

$z$ -oriented ones do. On the other hand, we know that  $\pi(E)$  is a closed torus-invariant subset of  $\mathbb{C}^3/G$ . This makes it either the origin, one of the three coordinate lines, one of the three coordinate hyperplanes or the whole of  $\mathbb{C}^3/G$ . Among these, the property that  $x^{|G|}$  vanishes along the subset, while  $y^{|G|}$  and  $z^{|G|}$  do not, uniquely identifies the  $yz$ -plane. This settles the first assertion.

Suppose now  $E$  is a compact exceptional divisor. Then its image in  $\mathbb{C}^3/G$  can only be the origin. Therefore the argument in the proof of Prop. 4.14 of [CL09] demonstrates that  $SS_{\tilde{\mathcal{M}},E}$  has a single  $(3,0)$ -sink given by vertex  $\chi_0$ . This settles the third assertion.

Finally, suppose  $E$  is a non-compact exceptional divisor. Then its image in  $\mathbb{C}^3/G$  must be an irreducible toric curve. There are three of them on  $\mathbb{C}^3/G$ , corresponding to the three coordinate axes of  $\mathbb{C}^3$ . Assume without loss of generality that it's the  $z$ -axis. Let  $p$  be any point on  $E$  whose image  $\pi(p)$  in  $\mathbb{C}^3/G$  is a point on the  $z$ -axis away from the origin, i.e.  $z^{|G|}(\pi(p)) \neq 0$ . Since  $\tilde{\mathcal{M}}$  is a *gnat*-family any  $m \in R^G$  acts on  $\tilde{\mathcal{M}}_p$  by multiplication by  $m(\pi(p))$ . In particular, this is true for  $G$ -invariant monomial  $z^{|G|}$ . Since  $z^{|G|}(\pi(p)) \neq 0$  it follows that  $z \cdot s \neq 0$  for any non-zero section  $s$  of  $\tilde{\mathcal{M}}_p$ , i.e. no  $z$ -arrow vanishes along the whole of  $E$  in the associated representation  $Q(G)_{\tilde{\mathcal{M}}}$ . So every vertex  $\chi \in Q(G)$  is either an  $x$ -tile, a  $y$ -tile, a  $z$ -(1,0)-charge or a  $z$ -(0,1)-charge and thus  $SS_{\tilde{\mathcal{M}},E}$  can only consist of looping  $z$ -charge lines which do not intersect each other.

Start at any vertex in  $T_H$  and move in the direction of  $x$ -arrows until we come full circle. By inspection, crossing any  $z$ -(1,0)-charge line we move from  $y$ -tiled region to  $z$ -tiled region and vice versa for crossing any  $z$ -(0,1)-charge line. Since we end up in the same region we've started, there are as many  $z$ -(0,1)-charge lines as there are  $z$ -(1,0)-charge lines. By the first assertion of this lemma  $SS_{\tilde{\mathcal{M}},E}$  is non-empty, hence there exists at least one  $z$ -(1,0)-charge line.

On the other hand, observe that any arrow which leaves a  $z$ -(1,0)-charge line must vanish along  $E$ . Therefore, if you start at a vertex on a  $z$ -(1,0)-charge line the only vertices you can reach by following only non-vanishing arrows are the other vertices on that charge line. But by the argument in [CL09], Prop. 4.12 there must exist a path from every vertex of  $Q(G)$  to  $\chi_0$  which consists entirely of non-vanishing arrows. Therefore any  $z$ -(1,0)-charge line must contain  $\chi_0$ . Since the charge lines may not intersect we conclude that there exists at most one  $z$ -(1,0)-charge line. This settles the second assertion.  $\square$

**Proposition 3.3.** *Let  $e \in \mathfrak{E}$  and let  $E$  be the corresponding toric divisor on  $Y$ . If the sink-source graph  $SS_{\tilde{\mathcal{M}},E}$  is as depicted on Figure 10, then the coordinates of  $e$  in  $L$  are  $\frac{1}{|G|}(ac, bc, 0)$  and locally around  $e$  triangulation  $\Sigma$  looks as depicted on Figure 11. Moreover, the monomial ratios carving out the edges incident to  $e$  can be computed in terms of the indicated lengths in  $SS_{\tilde{\mathcal{M}},E}$  as shown on Figures 11(a)-11(b).*

*If the shape of  $SS_{\tilde{\mathcal{M}},E}$  is a rotation of Figure 10 by  $\frac{2\pi}{3}$  or  $\frac{4\pi}{3}$  one permutes  $x$ ,  $y$  and  $z$  accordingly in all of the above.*

To explain the notation of Figure 10: let  $P$  be the vertex where we first meet the looping (1,0)-charge line if we follow the line of  $x$ -arrows backwards from  $\chi_0$ . Let  $Q$  be same but for a line of  $y$ -arrows. Let  $a$  and  $b$  be the lengths (in arrows) of the resulting paths from  $P$  and  $Q$  to  $\chi_0$ , as indicated. Let  $c$  be the number of distinct characters which occur on the (0,1)-charge line, i.e. the length of the path of  $z$ -arrows which starts at  $\chi_0$  and ends when it first comes

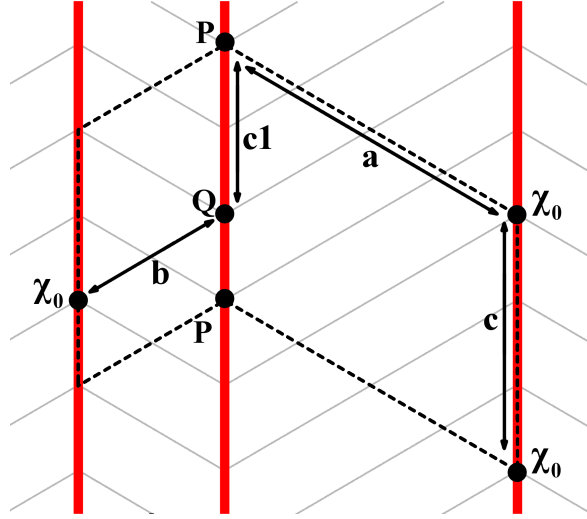


FIGURE 10. A single looping  $(0, 1)$ -charge line sink-source graph

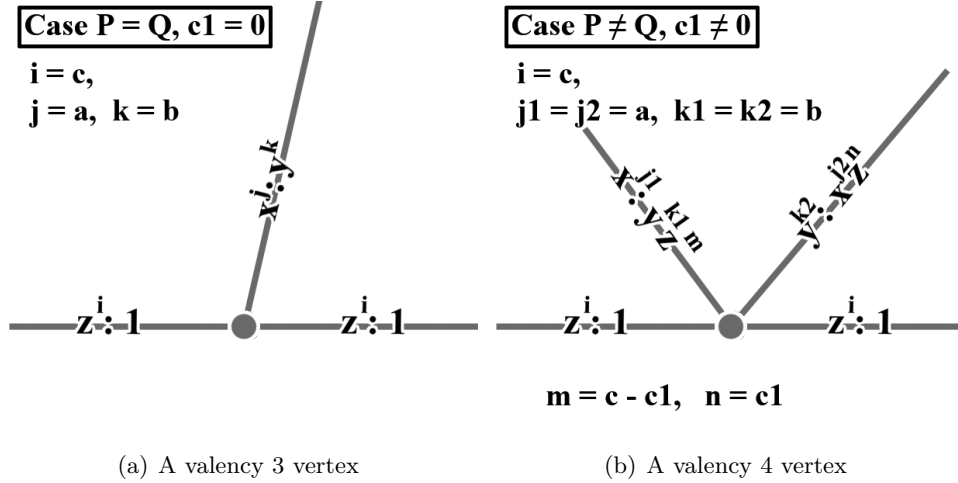


FIGURE 11. A side vertex of  $\Delta$

back to  $\chi_0$ . Then the dotted line on Figure 10 gives a choice of a fundamental domain of  $Q(G)$ . Finally,  $c_1$  is the length a path of  $z$ -arrows from  $Q$  to  $P$ . If  $P$  and  $Q$  coincide we set  $c_1 = 0$ .

*Proof.* The proof proceeds very similarly to the proofs of Props. 3.1-3.3 of [Log10], except we work with  $\text{SS}_{\tilde{\mathcal{M}}, E}$  instead of  $\text{SS}_{\mathcal{M}, E}$ . Suppose there is an edge incident to  $e$  which is carved by a ratio of form  $z^{k'} : x^{i'} y^{j'}$  for some  $i', j', k' \geq 0$ . Let  $\chi$  denote the common character of  $z^{k'}$  and  $x^{i'} y^{j'}$ . Any path which starts at  $\chi^{-1}$  and consists of  $k'$   $z$ -arrows or of  $i'$   $x$ -arrows and  $j'$   $y$ -arrows terminates at  $\chi_0$ . By the dual of the argument which begins the proof of Prop. 3.1 of [Log10] such path may not contain any arrows which vanish along  $E$ . In particular, the  $x$ -arrow which leaves  $\chi^{-1}$  can not vanish along  $E$  unless  $i' = 0$  and the  $y$ -arrow which leaves  $\chi^{-1}$  can not vanish unless  $j' = 0$ . On the other hand, observe that  $\chi^{-1}$  must lie on the same looping  $z$ -(1, 0)-charge line as  $\chi_0$  since we can reach the latter by taking a path of  $z$ -arrows from the former. Therefore

both the  $x$ -arrow and the  $y$ -arrow which leave  $\chi^{-1}$  vanish along  $E$ . We conclude that  $\chi = \chi_0$ ,  $i' = j' = 0$  and  $k' = c$ . In other words, the ratio in question can only be  $z^c : 1$ .

Suppose now there is an edge incident to  $e$  which is carved by a ratio of form  $x^{i'} : y^{j'} z^{k'}$  for some  $i', j', k' \geq 0$ . We may further assume that  $i' \neq 0$  and  $j' \neq 0$  as we've already dealt with that case. Let  $\chi$  denote the common character of  $x^{i'}$  and  $y^{j'} z^{k'}$ . Then, arguing as above, no arrow in the path of  $i'$   $x$ -arrows from  $\chi^{-1}$  to  $\chi_0$  vanishes along  $E$ . Therefore  $\chi^{-1}$  must lie somewhere on the path of  $x$ -arrows between  $P$  and  $\chi_0$  (see Figure 10). On the other hand, no arrow in any path of  $j'$   $y$ -arrows and  $k'$   $z$ -arrows vanishes along  $E$ . In particular, since  $j' \neq 0$  the  $y$ -arrow which leaves  $\chi^{-1}$  doesn't vanish. From Figure 10 we can see that the only possibility is  $\chi^{-1} = P$ ,  $i' = a$ ,  $j' = b$  and  $k' = (-c_1) \bmod c$ . So the ratio in question can only be  $x^a : y^b z^{(-c_1 \bmod c)}$ . A similar argument for a ratio of form  $y^{j'} : x^{i'} z^{k'}$  shows that the only possibility is  $\chi^{-1} = Q$  and the ratio  $y^b : x^a z^{c_1}$ .

By Lemma 3.1 we have  $e = \frac{1}{G}(a, b, c)$  where  $a, b$  and  $c$  are the numbers of  $x$ -,  $y$ - and  $z$ -oriented arrows which vanish along  $E$  in  $SS_{\tilde{\mathcal{M}}, E}$ . The choice of a fundamental domain indicated by the dotted line on Figure 10 demonstrates that  $e = \frac{1}{G}(ac, bc, 0)$ .

Now suppose  $P$  and  $Q$  coincide, i.e.  $c_1 = 0$ . Then the above shows that the only ratios which can mark an edge incident to  $e$  are  $z^c : 1$  and  $x^a : y^b$ , so the triangulation  $\Sigma$  must look locally around  $e$  as depicted on Figure 11(a). Suppose  $P$  and  $Q$  do not coincide, i.e.  $c_1 \neq 0$ . Then the only ratios which can mark an edge incident to  $e$  are  $z^c : 1$ ,  $x^a : y^b z^{c-c_1}$  and  $y^b : x^a z^{c_1}$  and so the triangulation  $\Sigma$  must look locally around  $e$  as depicted on Figure 11(b).  $\square$

With Lemma 3.2 and Prop. 3.3 we obtain immediately a refined version of Theorem 3.1 of [Log10] which takes into account every vertex in  $\mathfrak{E}$  and not just those which lie in the interior of  $\Delta$  and correspond to compact exceptional divisors:

**Theorem 3.4.** *Let  $e \in \mathfrak{E}$ . Then one of the following must hold:*

$SS_{\tilde{\mathcal{M}}, E_e}$	$e$	Triangulation $\Sigma$ locally around $e$	Reid's recipe ([Cra05], §3)	$E_e$
Empty	A corner vertex of $\Delta$	A corner of $\Delta$	–	The strict transform of a coordinate hyperplane
Fig. 10 (up to rotation <sup>†</sup> )	A side vertex of $\Delta$	Fig. 11(a)-(b) (up to rotation <sup>†</sup> )	–	$\mathbb{P}^1 \times \mathbb{C}$ , blown-up in 0 or 1 points
Fig. 7(a)	An interior vertex of $\Delta$	Fig. 7(b)	Case 1	$\mathbb{P}^2$
Fig. 8(a) (up to rotation <sup>†</sup> )	An interior vertex of $\Delta$	Fig. 8(b) - 8(e) (up to rotation <sup>†</sup> )	Cases 2-3	A surface scroll, blown-up in 0, 1 or 2 points
Fig. 9(a)	An interior vertex of $\Delta$	Fig. 9(b)	Case 4	Del Pezzo surface $dP_6$

<sup>†</sup>: The sink-source graph  $SS_{\tilde{\mathcal{M}}, E}$  may also be a rotation of the diagram by an angle of  $\frac{2\pi}{3}$  or  $\frac{4\pi}{3}$ . In this case the corresponding diagram of triangulation  $\Sigma$  locally around  $e$  should be rotated by the same angle and  $x, y$  and  $z$  should be permuted.

#### 4. CT-SUBDIVISIONS

Fix a character  $\chi \in G^\vee$ . Section 2.6 describes the transform  $\Psi(\mathcal{O}_0 \otimes \chi)$  in terms of the vanishing divisors of the skew-commutative cube of line bundles  $\text{Hex}(\chi^{-1})_{\tilde{\mathcal{M}}}$ . Each of these vanishing divisors is a reduced union of irreducible toric divisors on  $Y$  [CL09, §4.2]. For an



irreducible toric divisor  $E$ , we may ask which maps in the cube corresponding to  $\text{Hex}(\chi^{-1})_{\tilde{\mathcal{M}}}$  vanish along  $E$ . The answer is encoded in the vertex type of  $\chi^{-1}$  in  $\text{SS}_{\tilde{\mathcal{M}}, E}$ . The table that translates between the two is provided on Fig. 2. Therefore, to compute all the vanishing divisors of  $\text{Hex}(\chi^{-1})_{\tilde{\mathcal{M}}}$  it suffices to know the vertex type of  $\chi^{-1}$  for each toric divisor on  $Y$ . This turns out to be directly linked to the following notion introduced in [Cra05, §5]:

**Definition 4.1.** Given a monomial  $m \in \mathbb{C}[x, y, z]$  define  $\text{Conv}(m)$  to be the union of all the basic triangles in  $\Sigma$  whose  $G$ -graph contains  $m$ .

The union of the nonempty  $\text{Conv}(m)$  as  $m$  ranges over all the monomials of weight  $\chi$  provides a subdivision of  $\Delta$ . We need the following coarsening of it. Let  $Cz^\bullet$  be the union of the basic triangles in  $\Sigma$  in whose  $G$ -graph  $\chi$  is represented by  $z^c$  for  $c > 0$ . Similarly for  $Cx^\bullet$  and  $Cy^\bullet$ . Let  $Tx^\bullet y^\bullet$  be the union of all the basic triangles in  $\Sigma$  in whose  $G$ -graph  $\chi$  is represented by  $x^a y^b$  for  $a, b > 0$ . Similarly for  $Ty^\bullet z^\bullet$  and  $Tx^\bullet z^\bullet$ . Together these six give a subdivision of  $\Delta$  which we call the *CT-subdivision*.

It was proved in [Cra05, Lemma 5.3] that when non-empty  $\text{Conv}(m)$  is a convex region of  $\Delta$  which contains  $e_x$  (resp.  $e_y, e_z$ ) if and only if  $x$  (resp.  $y, z$ ) doesn't divide  $m$ . So if non-empty:

- $Cx^\bullet$  is a convex area containing side  $e_y e_z$  of  $\Delta$ .
- $Cy^\bullet$  is a convex area containing side  $e_x e_z$  of  $\Delta$ .
- $Cz^\bullet$  is a convex area containing side  $e_x e_y$  of  $\Delta$ .
- $Ty^\bullet z^\bullet$  is a union of convex areas each containing corner vertex  $e_x$  of  $\Delta$ .
- $Tx^\bullet z^\bullet$  is a union of convex areas each containing corner vertex  $e_y$  of  $\Delta$ .
- $Tx^\bullet y^\bullet$  is a union of convex areas each containing corner vertex  $e_z$  of  $\Delta$ .

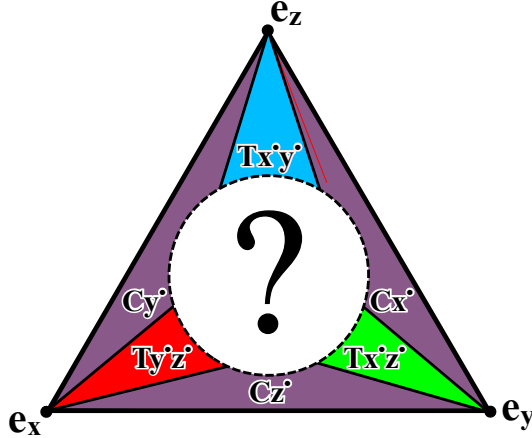


FIGURE 12. CT-subdivision of  $\Delta$

Thus a CT-subdivision looks, in general, as depicted on Figure 12. However any of the six areas can be empty. We want to think of such cases as degenerations of the general picture above. When  $Cx^\bullet$ ,  $Cy^\bullet$  or  $Cz^\bullet$  is empty we think of them as having degenerated away completely. But for  $Ty^\bullet z^\bullet$ ,  $Tx^\bullet z^\bullet$  or  $Tx^\bullet y^\bullet$  we distinguish two cases. When  $Tx^\bullet y^\bullet$  is empty, the areas  $Cx^\bullet$  and  $Cy^\bullet$  share a boundary that is necessarily a line segment  $l$  out of  $e_z$ . If  $\chi$  doesn't mark  $l$  we think of  $Tx^\bullet y^\bullet$  as having degenerated into an infinitesimally thin strip along  $l$ . In other words,

we do not consider the points of  $l$  as lying on the boundary of  $Cx^\bullet$  and  $Cy^\bullet$  but rather as lying on the degeneration of  $Tx^\bullet y^\bullet$  still wedged in between the two. If, on the other hand,  $\chi$  does mark  $l$  we think of  $Tx^\bullet y^\bullet$  as having degenerated to just the vertex  $e_z$ , allowing  $Cx^\bullet$  and  $Cy^\bullet$  to share a boundary along  $l$ .

We formalise this as follows:

**Definition 4.2.** (1) Define  $Cz^\bullet$  to be the union of all the basic triangles in  $\Sigma$  in whose  $G$ -graph  $\chi$  is represented by  $z^c$  for  $c > 0$ . Define  $Cx^\bullet$  and  $Cy^\bullet$  similarly.

(2) Define  $Tx^\bullet y^\bullet$  as follows:

- If non-empty, define  $Tx^\bullet y^\bullet$  to be the union of the basic triangles in  $\Sigma$  in whose  $G$ -graph  $\chi$  is represented by  $x^a y^b$  for  $a, b > 0$ .
- Otherwise, we consider the boundary  $l$  between  $Cx^\bullet$  (or  $e_z e_y$  if  $Cx^\bullet$  empty) and  $Cy^\bullet$  (or  $e_z e_x$  if  $Cy^\bullet$  empty).
  - ◊ If  $\chi$  doesn't mark  $l$ , define  $Tx^\bullet y^\bullet$  to be  $l$ .
  - ◊ If  $\chi$  does mark  $l$ , define  $Tx^\bullet y^\bullet$  to be  $e_z$ .

Define  $Ty^\bullet z^\bullet$  and  $Tx^\bullet z^\bullet$  similarly.

Our reason for adopting these conventions becomes clear in the course of proving the following:

**Lemma 4.1.** *Let  $e$  be a vertex of  $\Sigma$  and  $E$  be the corresponding toric divisor on  $Y$ . Then an area of the CT-subdivision for  $\chi$  contains  $e$  if and only if  $Q(G)$  has a path from  $\chi^{-1}$  to  $\chi_0$  which doesn't vanish along  $E$  in  $Q(G)_{\tilde{M}}$  and which represents monomial of the same type as this area. E.g. there is a non-vanishing  $x^i y^j$  path of arrows with  $i, j > 0$  if and only if  $e$  belongs to  $Tx^\bullet y^\bullet$ .*

*Proof. "Only If" direction:*

Suppose  $e$  belongs to a C-area or a non-degenerate T-area of the CT-subdivision for  $\chi$ . Then  $m$  represents  $\chi$  in the  $G$ -graph of some basic triangle  $\tau$  which contains  $e$ . A monomial  $m$  represents  $\chi$  in the  $G$ -graph of  $\tau$  if and only if  $m.1 \neq 0$  in the  $G$ -cluster parametrised by the toric fixed point  $p_\tau$  of  $\tau$ . Equivalently, all the paths from 0 to  $\chi$  which correspond to  $m$  must not vanishing at  $p_\tau$  in the associated representation  $Q(G)_M$ . Dually, all the paths from  $\chi^{-1}$  to 0 which correspond to  $m$  must not vanish at  $p_\tau$  in  $Q(G)_{\tilde{M}}$ . Finally, since  $E$  contains  $p_\tau$ , if a path doesn't vanish at  $p_\tau$  it certainly doesn't vanish along  $E$ .

It remains to deal with degenerate T-areas. Suppose, without loss of generality, that  $e$  belongs to a degenerate  $Tx^\bullet y^\bullet$ -area. Then either  $e = e_z$ , or one of  $Cx^\bullet$  and  $Cy^\bullet$  is empty and  $e$  lies on the corresponding side of  $\Delta$ , or  $e$  lies on the border of  $Cx^\bullet$  and  $Cy^\bullet$  and  $\chi$  doesn't mark this border. If  $e = e_z$ , then every path of  $x^\bullet y^\bullet$ -type is non-vanishing in  $\text{SS}_{\tilde{\mathcal{M}}, E}$ . If  $e$  lies on a side of  $\Delta$ , the existence of the desired non-vanishing path can be readily verified on (appropriately rotated) Fig. 10-11. Finally, let  $e$  lie on the border of  $Cx^\bullet$  and  $Cy^\bullet$ . This border is a line  $l$  carved out by  $x^a : y^b$  and  $\chi$  is represented by  $x^{ka}$  and  $y^{kb}$  in the  $G$ -graphs to  $e_y$ -side and to  $e_x$ -side of  $l$ . In particular,  $x^{ka}$  and  $y^{kb}$  define non-vanishing paths from  $\chi^{-1}$  to  $\chi_0$  in  $\text{SS}_{\tilde{\mathcal{M}}, E}$ . Since  $\chi$  doesn't mark  $l$  we have  $k > 1$ , and any one of  $x^{(k-1)a} y^b, \dots, x^a y^{(k-1)b}$  defines the desired non-vanishing path of  $x^\bullet y^\bullet$ -type.

*"If" direction:*

A non-vanishing path from  $\chi^{-1}$  to  $\chi_0$  must be contained completely within one (or more) of the tiled regions  $\text{SS}_{\tilde{\mathcal{M}}, E}$  subdivides  $T_H$  into. E.g. a non-vanishing  $x^\bullet y^\bullet$  path has to be contained

within the  $z$ -tilted region. The possible sink-source graph shapes listed in Theorem 3.4 give us a total of twelve tiled regions to consider. Five of these are contractible and we deal with them first. Within a contractible region of  $T_H$  any two paths between the same pair of vertices of  $Q(G)$  lift to the same monomial modulo  $xyz$ . Therefore within a contractible tiled region of  $T_H$  all non-vanishing paths from a given vertex to  $\chi_0$  correspond to the same monomial. It is then easy to verify that this monomial does indeed occur in the  $G$ -graph of at least one of the basic triangles containing  $e$ .

For example, if  $\text{SS}_{\tilde{\mathcal{M}},E}$  is as depicted on Figure 9(a) then the non-vanishing paths from the vertices in the  $z$ -tilted region to  $\chi_0$  yield the monomials

$$\{x^i y^j \mid 0 \leq i \leq a, 0 \leq j \leq b_3 \text{ or } 0 \leq i \leq a_2, 0 \leq j \leq b\}. \quad (4.1)$$

On the other hand, we see on Figure 9(b) that one of the six triangles containing  $e$  has  $\frac{y^{b_2} z^{c_3}}{x^a}$ ,  $\frac{x^{a_3} z^{c_2}}{y^b}$  and  $\frac{x^{a_2+1} y^{b_3+1}}{z^{c-1}}$  as the coordinates of its affine chart. Its  $G$ -graph is then readily seen to contain all the monomials in (4.1). The other contractible regions are dealt with similarly.

We now proceed to deal with non-contractible tiled regions.

Suppose, that  $\text{SS}_{\tilde{\mathcal{M}},E}$  is as depicted on Figure 8(a) with no rotations necessary. Then it has a single non-contractible region: the  $z$ -tilted one. Suppose that  $\chi^{-1}$  is some vertex within this region or on its boundary. Let  $x^\alpha y^{\bar{\beta}}$  be the monomial of the path which goes along  $x$ -arrows from  $\chi^{-1}$  until it hits  $y$ -(1,0)-charge line  $I_1 O_1$  and then follows the  $y$ -arrows of this charge line to  $\chi_0$ . Similarly let  $x^{\bar{\alpha}} y^\beta$  be the monomial of the path along the  $y$ -arrows and then  $x$ -(1,0)-charge line  $I_1 O_1$ . Note that  $0 \leq \bar{\alpha} < a$  and  $0 \leq \bar{\beta} < b$ . Next, note that the monomials of any two paths from  $\chi^{-1}$  to  $\chi_0$  must differ by a power of  $\frac{x^a}{y^b}$ . It follows that  $\alpha = ak + \bar{\alpha}$  and  $\beta = bk + \bar{\beta}$  for some  $k \geq 0$ . Hence the non-vanishing paths from  $\chi^{-1}$  to  $\chi_0$  correspond to the following monomials:

$$x^\alpha y^{\bar{\beta}}, x^{\alpha-a} y^{\bar{\beta}+b}, \dots, x^{\bar{\alpha}+a} y^{\bar{\beta}-b}, x^{\bar{\alpha}} y^{\bar{\beta}}. \quad (4.2)$$

Now note that in all the triangles to the  $e_y$  side of line  $x^a: y^b$  the ratio  $\frac{y^b}{x^a}$  is a regular function. Every monomial in (4.2) is a product of  $x^\alpha y^{\bar{\beta}}$  and a power of  $\frac{y^b}{x^a}$ , so only  $x^\alpha y^{\bar{\beta}}$  can appear in the  $G$ -graphs of the triangles to the  $e_y$  side of line  $x^a: y^b$ . Similarly, only  $x^{\bar{\alpha}} y^\beta$  can appear in the  $G$ -graphs of the triangles to the  $e_x$  side of line  $x^a: y^b$ . On the other hand, observe that one of the triangles around  $e$  has  $\frac{y^b}{x^a}$  and  $\frac{z^c}{x^{a_1} y^{b_1} \bmod b}$  as two of its coordinates. Hence  $x^{a_1} y^{b-1}$  is in its  $G$ -graph. Since  $0 \leq \alpha \leq a_1$  and  $0 \leq \bar{\beta} \leq b-1$  (see Figure 8(a)) it follows that  $x^\alpha y^{\bar{\beta}}$  must also be in its  $G$ -graph. Similarly, the basic triangle with  $\frac{x^a}{y^b}$  and  $\frac{z^c}{x^{a_1} \bmod a y^{b_1}}$  as coordinates has  $x^{\bar{\alpha}} y^\beta$  in its  $G$ -graph. Thus, of the monomials in (4.2) only  $x^\alpha y^{\bar{\beta}}$  and  $x^{\bar{\alpha}} y^\beta$  do appear the  $G$ -graphs around  $e$ . The remaining ones are the “ghost” monomials, the ones which appear as non-vanishing paths in  $\text{SS}_{\tilde{\mathcal{M}},E}$ , but not in the  $G$ -graphs around  $e$ .


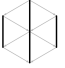
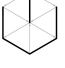



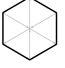
Observe, however, that all the “ghost” monomials in (4.2) are of  $x^\bullet y^\bullet$  type. So a problem arises only when neither  $x^\alpha y^{\bar{\beta}}$  nor  $x^{\bar{\alpha}} y^\beta$  are of  $x^\bullet y^\bullet$  type, i.e. when  $\bar{\alpha} = \bar{\beta} = 0$ . It is here that our peculiar choice of conventions for degeneration of  $Ty^\bullet z^\bullet$ ,  $Tx^\bullet z^\bullet$  and  $Tx^\bullet y^\bullet$  comes into play. Suppose  $\bar{\alpha} = \bar{\beta} = 0$ . The monomials of the non-vanishing paths from  $\chi^{-1}$  to  $\chi_0$  are then

$$x^{ka}, x^{(k-1)a} y, \dots, x y^{(k-1)b}, y^{kb}$$

for some  $k \geq 1$ . By above, in the  $G$ -graphs on  $e_x$  side of line  $x^a: y^b$  character  $\chi$  is represented by  $y^{ka}$  and in the  $G$ -graphs on  $e_y$  side – by  $x^{kb}$ . So line  $x^a: y^b$  is the border between  $Cx^\bullet$  and  $Cy^\bullet$  in the CT-subdivision for  $\chi$ , and  $Tx^\bullet y^\bullet$ , which is usually wedged in between the two, is empty. If  $k > 1$  then  $\chi$  doesn't actually mark line  $x^a: y^b$ . By our conventions this means that  $Tx^\bullet y^\bullet$  degenerates to an infinitesimally thin strip still wedged in between  $Cx^\bullet$  and  $Cy^\bullet$ . Vertex  $e$  lies on  $x^a: y^b$ , and therefore belongs to this degeneration of  $Tx^\bullet y^\bullet$ . This accounts for the “ghost” monomials  $x^{(k-1)a}y, \dots, xy^{(k-1)b}$ . On the other hand, when  $k = 1$  the non-vanishing paths from  $\chi^{-1}$  are given by  $x^a$  and  $y^b$ , both of which appear in  $G$ -graphs around  $e$ , i.e. there are no “ghost” monomials. This matches the fact that  $\chi$  does mark the line  $x^a: y^b$  through  $e$ , which by our conventions means that  $Tx^\bullet y^\bullet$  degenerates away from  $e$  to just  $e_z$ .

The non-contractible regions which occur when  $\text{SS}_{\tilde{\mathcal{M}}, E}$  is as depicted on Fig. 7(a), as depicted on Fig. 10 or empty are dealt with similarly.  $\square$

**Proposition 4.2.** *Let  $\chi$  be a non-trivial character of  $G$ . Let  $E$  be a toric divisor on  $Y$  and  $e$  be the corresponding vertex of  $\Sigma$ . The vertex type of  $\chi^{-1}$  in  $\text{SS}_{\tilde{\mathcal{M}}, E}$  and the role of  $e$  in the CT-subdivision for  $\chi$  are related in the following way:*

Vertex type of $\chi^{-1}$ in $\text{SS}_{\tilde{\mathcal{M}}, E}$	The role of $e$ in the CT-subdivision of $\Delta$ : ( $e$ belongs to the following areas and none other)
 $z\text{-(1,0)-charge}$	An internal vertex of $Cz^\bullet$
 $z\text{-tile}$	<ul style="list-style-type: none"> <li>• An internal vertex of <math>Tx^\bullet y^\bullet</math></li> <li>• A vertex on the border of <math>Tx^\bullet y^\bullet</math> with <math>Cx^\bullet</math> or <math>Cy^\bullet</math></li> </ul>
 $z\text{-(2,1)-source}$	A vertex on the border of $Cx^\bullet$ and $Cy^\bullet$
 $z\text{-(1,2)-source}$	A vertex on the border of $Cz^\bullet$ and $Tx^\bullet y^\bullet$ (plus, possibly, $Cx^\bullet$ or $Cy^\bullet$ or both)
 $z\text{-(0,1)-charge}$	A vertex on the border of $Tx^\bullet z^\bullet$ and $Ty^\bullet z^\bullet$ (plus, possibly, one or two of $Cx^\bullet$ , $Cy^\bullet$ or $Cz^\bullet$ )
(similarly for the $x$ - and $y$ - vertex types)	
 $(0,3)\text{-sink}$	A vertex on the border of $Ty^\bullet z^\bullet$ , $Tx^\bullet z^\bullet$ and $Tx^\bullet y^\bullet$ (plus, possibly, one, two or three of $Cx^\bullet$ , $Cy^\bullet$ or $Cz^\bullet$ )
 $(3,3)\text{-source}$	A vertex on the border of $Cx^\bullet$ , $Cy^\bullet$ and $Cz^\bullet$

(4.3)

*Proof.* The proof works by directly verifying the data of Table (4.3) for every possible shape of the sink-source graph  $\text{SS}_{\tilde{\mathcal{M}}, E}$  as listed in Theorem 3.4.  $\text{SS}_{\tilde{\mathcal{M}}, E}$  subdivides  $T_H$  into three tiled regions. Within each region we locate all non-vanishing paths from  $\chi^{-1}$  to  $\chi_0$ . By Lemma 4.1 these determine all the areas of the CT-subdivision for  $\chi$  which  $e$  belongs to.

Suppose, for example,  $\chi^{-1}$  is a  $z\text{-(1,0)-charge}$ . Then it lies on the border of the  $x$ -tiled and the  $y$ -tiled regions. So we look in each region for non-vanishing paths from  $\chi^{-1}$  to  $\chi_0$ . Inspecting the possible sink-source graph shapes listed in Theorem 3.4 we see in each of the two regions a unique non-vanishing path: the same path which follows the  $z\text{-(1,0)-charge}$  line from  $\chi^{-1}$  to

the  $(3,0)$ -sink at  $\chi_0$ . Hence both the regions contribute the same monomial of type  $z^\bullet$  and so  $e$  has to be an internal vertex of  $Cz^\bullet$ . Suppose, on the other hand, that  $\chi^{-1}$  is  $z$ -tile. Then it lies in the interior of the  $z$ -tiled region. Inspecting all the possible sink-source graph shapes we see that from any  $z$ -tile there is always a non-vanishing path to  $\chi_0$  of  $x^\bullet y^\bullet$  type, and sometimes there is also a path of  $x^\bullet$ -type, or of  $y^\bullet$ -type, or both. We conclude that  $\chi^{-1}$  is either an internal vertex of  $Tx^\bullet y^\bullet$  or it lies on the border of  $Tx^\bullet y^\bullet$  with  $Cx^\bullet$ , or  $Cy^\bullet$  or both. Now suppose  $\chi^{-1}$  is a  $z$ -(0,1)-charge. Then it lies on the border of  $x$ -tiled and  $y$ -tiled regions. Inspecting the four possible sink-source graph shapes we see the  $x$ -tiled region will always contain a non-vanishing path of type  $y^\bullet z^\bullet$ : take the path which goes along  $y$ -arrows until it hits  $z$ -(1,0)-charge line, and then follows that charge line back to  $\chi_0$ , possibly doing a single loop along it if  $\text{SS}_{\tilde{\mathcal{M}},E}$  is as depicted on Fig. 10. The  $x$ -tiled region can also contain non-vanishing paths of type  $y^\bullet$  and  $z^\bullet$ , but we note that it can only contain both if  $\text{SS}_{\tilde{\mathcal{M}},E}$  is as depicted on Fig. 10 or the rotation of Fig. 8 by  $\frac{2\pi}{3}$  clockwise. We further note that in both these cases there doesn't also exist a non-vanishing path of type  $x^\bullet$  from  $\chi^{-1}$  to  $\chi_0$ . Repeating the same argument for the  $y$ -tiled region, we conclude that  $\chi^{-1}$  lies on the border of  $Ty^\bullet z^\bullet$ ,  $Tx^\bullet z^\bullet$  and, possibly, one or two of the  $C$ -areas. The remaining vertex types are dealt with similarly.  $\square$

We now prove several corollaries of Prop. 4.2 which relate the geometry of  $CT$ -subdivisions to the calculation of the cohomology sheaves of the total complex  $T^\bullet$  of the skew-commutative cube of line bundles  $\text{Hex}(\chi^{-1})_{\tilde{\mathcal{M}}}$ . Denote by  $D^i$ ,  $D_j^i$  and  $D_{jk}^i$  the vanishing divisors of the maps in the cube, as per §2.6. By Lemma 2.1 we have  $\mathcal{H}^0(T^\bullet) = \mathcal{L}_\chi^{-1} \otimes \mathcal{O}_{D^1 \cap D^2 \cap D^3}$  and correspondingly:

**Corollary 4.3.** *Let  $\chi \in G^\vee$  be non-trivial, let  $E$  be a toric divisor on  $Y$  and let  $e$  be the corresponding vertex of  $\mathfrak{E}$ . Then:*

- $E \in D^1$  if and only if  $e \in Ty^\bullet z^\bullet$ .
- $E \in D^2$  if and only if  $e \in Tx^\bullet z^\bullet$ .
- $E \in D^3$  if and only if  $e \in Tx^\bullet y^\bullet$ .

*In particular,  $\mathcal{H}^0(T^\bullet) \neq 0$  if and only if there exists a basic triangle in  $\Sigma$  which touches each of  $Ty^\bullet z^\bullet$ ,  $Tx^\bullet z^\bullet$  and  $Tx^\bullet y^\bullet$ .*

*Proof.* By inspection of Table (4.3) and Fig. 2.  $\square$

On the other hand, by Lemma 2.1 sheaf  $\mathcal{H}^{-1}(T^\bullet)$  admits a three-step filtration whose successive quotients are supported on:

- intersection of  $\gcd(D_2^3, D_3^2)$  and the effective part of  $D^1 + \text{lcm}(D_1^2, D_1^3) - \tilde{D}_2^3 - D^2$ .
- intersection of  $\gcd(D_1^3, D_3^1)$  and the effective part of  $D^2 + \text{lcm}(D_2^1, D_2^3) - \tilde{D}_3^1 - D^3$
- intersection of  $\gcd(D_1^2, D_2^1)$  and the effective part of  $D^3 + \text{lcm}(D_3^1, D_3^2) - \tilde{D}_1^2 - D^1$ .

Correspondingly:

**Corollary 4.4.** *Let  $\chi \in G^\vee$  be non-trivial, let  $E$  be a toric divisor on  $Y$  and let  $e$  be the corresponding vertex of  $\mathfrak{E}$ . Then:*

- $E \in \gcd(D_2^3, D_3^2)$  if and only if  $e \in Cx^\bullet \setminus (Tx^\bullet z^\bullet \cup Tx^\bullet y^\bullet)$ .
- $E \in \gcd(D_1^3, D_3^1)$  if and only if  $e \in Cy^\bullet \setminus (Ty^\bullet z^\bullet \cup Tx^\bullet y^\bullet)$ .
- $E \in \gcd(D_1^2, D_2^1)$  if and only if  $e \in Cz^\bullet \setminus (Ty^\bullet z^\bullet \cup Tx^\bullet z^\bullet)$ .

*Proof.* By inspection of Table (4.3) and Fig. 2.  $\square$

**Corollary 4.5.** *Let  $\chi \in G^\vee$  be non-trivial, let  $E$  be a toric divisor on  $Y$  and let  $e$  be the corresponding vertex of  $\mathfrak{E}$ . Then*

- *$E$  lies in the effective part of  $D^1 + \text{lcm}(D_1^2, D_1^3) - \tilde{D}_2^3 - D^2$  if and only if*

$$e \in (Cy^\bullet \cup Ty^\bullet z^\bullet \cup Cz^\bullet) \setminus (Tx^\bullet z^\bullet \cup Tx^\bullet y^\bullet).$$

- *$E$  lies in the effective part of  $D^2 + \text{lcm}(D_2^1, D_2^3) - \tilde{D}_3^1 - D^3$  if and only if*

$$e \in (Cx^\bullet \cup Tx^\bullet z^\bullet \cup Cz^\bullet) \setminus (Ty^\bullet z^\bullet \cup Tx^\bullet y^\bullet).$$

- *$E$  lies in the effective part of  $D^3 + \text{lcm}(D_3^1, D_3^2) - \tilde{D}_1^2 - D^1$  if and only if*

$$e \in (Cx^\bullet \cup Tx^\bullet y^\bullet \cup Cy^\bullet) \setminus (Ty^\bullet z^\bullet \cup Tx^\bullet z^\bullet).$$

*Proof.* By inspection of Table (4.3) and Fig. 2. □

*Remark 4.6.* It follows that for  $\mathcal{H}^{-1}(T^\bullet)$  to be non-zero a  $C$ -area must have a direct border with either the  $T$ -area opposite it or the two other  $C$ -areas. Moreover, this border must have internal vertices: those which don't also belong to one of the two remaining  $T$ -areas. In other words, one of  $C$ -areas must contain within its boundary a tip of a “wedge” and/or squashed legs of  $T$  and these must be more than one edge long in total.

Let now  $T$  be the union of  $Ty^\bullet z^\bullet$ ,  $Tx^\bullet z^\bullet$  and  $Ty^\bullet z^\bullet$ . It is a concave triangle with vertices  $e_x$ ,  $e_y$  and  $e_z$  and three sides which are the boundaries of the three  $C$ -areas and hence concave piecewise linear curves from one vertex of  $\Delta$  to another. If a  $C$ -area is empty we take the corresponding side of  $\Delta$  as the side of  $T$ .

The three  $T$ -areas are each connected. Each of them contains precisely one of the vertices of  $T$  and is a union of convex pieces all containing that vertex. If all three  $T$ -areas are non-degenerate we have a dichotomy depicted on Figure 13:

- “Meeting point”: The three  $T$ -areas meet in a unique point  $P \in T$ .

or

- “Wedge”: One of the  $T$ -areas wedges in between the other two and disconnects them by touching the opposite side of  $T$  in more than a point.

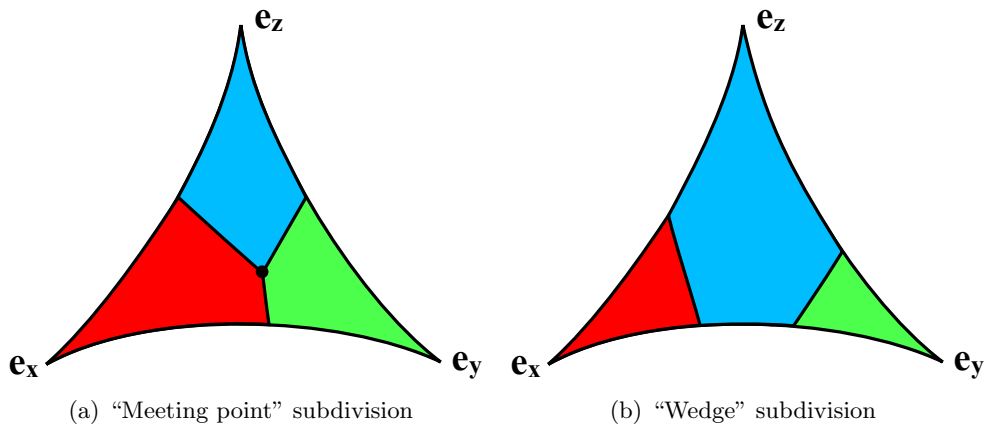


FIGURE 13. Concave triangle  $T$  (non-degenerate case)

When a  $T$ -area degenerates, the neighboring pair of  $C$ -areas squash the leg of  $T$  between them into a straight line. The  $T$ -area then either stretches out into an infinitesimally thin strip along the squashed leg or degenerates to just the vertex at the tip of the leg, snapped off from the rest of  $T$ .

On Figures 14 and 15 we depict all the degenerations which are possible in the view of Prop. 4.2. All of them can be seen to actually occur in examples. On Figure 14 we list those degenerations where there is a meeting point and on Figure 15 those where there isn't. Note that in all the latter cases either one or both of the following must occur:

- “Wedge”: one  $T$ -area touches the opposite side of  $T$  in more than a point.
- “Snap”: a pair of  $C$ -areas squash a leg of  $T$  and snap a  $T$ -area off.

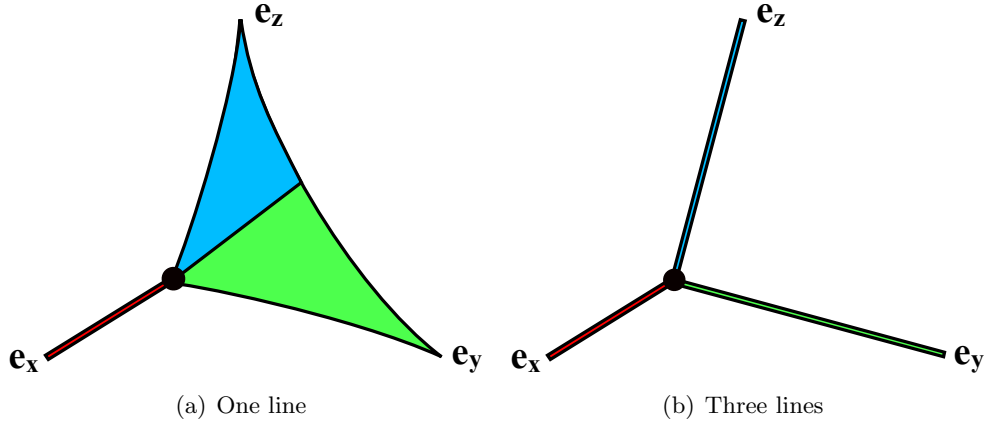


FIGURE 14. “Meeting point” degenerations

We can now see the reason only one of  $\mathcal{H}^0(T^\bullet)$  and  $\mathcal{H}^{-1}(T^\bullet)$  can be non-zero. In light of the dichotomy above, Cor. 4.3 implies that if  $\mathcal{H}^0(T^\bullet) \neq 0$  then the CT-subdivision either contains a “meeting point” or at least the three  $T$ -areas are close enough for there to be a basic triangle which touches all three. While Remark 4.6 implies that  $\mathcal{H}^{-1}(T^\bullet) \neq 0$  only when two  $T$ -areas become disconnected and the gap is at least two edges along the side of  $T$  they share.

To make the argument above into a proof of Theorem 1.1 it remains to deal with the following issue. Suppose two  $T$ -areas were disconnected by a “wedge” whose tip is more than two edges long. Then a basic triangle certainly couldn't connect them along this tip. But, a priori, there could be a basic triangle somewhere else in the “wedge” which spans it border-to-border and thus touches all three  $T$ -areas. However, it turns out that any basic triangle which connects up the  $T$ -areas can only do so along the tip of the “wedge”. To prove this assertion, we first observe the following:

**Corollary 4.7.** *Let  $\chi \in^\vee$  be non-trivial. An edge  $ef$  of  $\Sigma$  is marked by  $\chi$  if and only if it belongs to either the tip of a “wedge” or to a squashed leg with a snapped-off  $T$ -area at the tip.*

*Proof.* Consider the monomial ratio  $m : m'$  which carved out  $ef$ . By [Log10, Cor. 2.3]  $m$  and  $m'$  represent  $\chi$  in the  $G$ -graphs of the two basic triangles which contain  $ef$ . Therefore edge  $ef$  either lies on the border of  $Cx^\bullet$  and  $Ty^\bullet z^\bullet$ , or on the border of  $Cy^\bullet$  and  $Tx^\bullet z^\bullet$ , or on the border of  $Cz^\bullet$  and  $Tx^\bullet y^\bullet$ , which places it on the tip of a “wedge” or it lies on the border of  $Cx^\bullet$



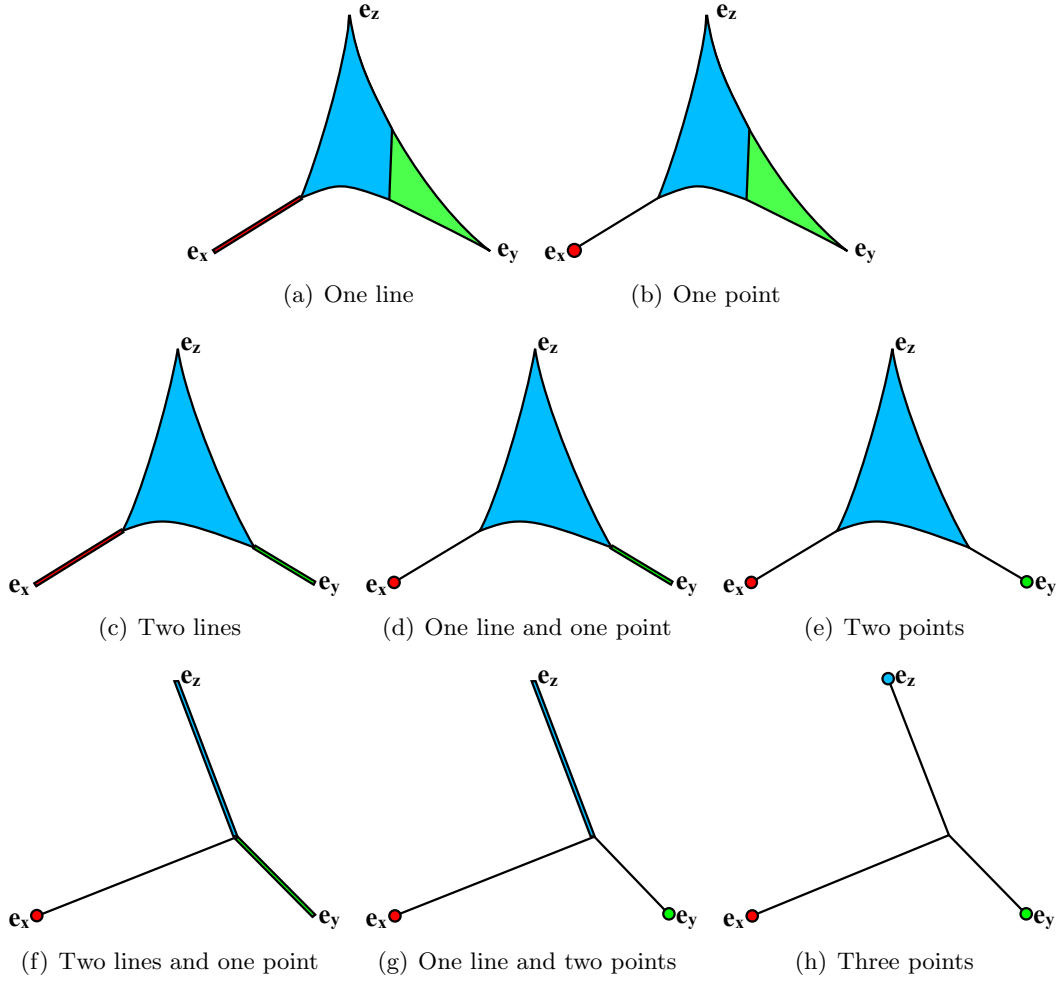


FIGURE 15. “Wedge” and “Snap” degenerations

and  $Cy^\bullet$ , or on the border of  $Cy^\bullet$  and  $Cz^\bullet$ , or on the border of  $Cz^\bullet$  and  $Cx^\bullet$ , which places it along a squashed leg of  $T$ . And since  $\chi$  marks  $ef$  it is the type of degeneration where a  $T$ -area is reduced to just the vertex at the tip of leg.  $\square$

Recall that  $D^1$ ,  $D^2$  and  $D^3$  are the vanishing divisors of the maps which in the dual family  $\tilde{\mathcal{M}}$  represent the  $x$ -,  $y$ - and  $z$ -arrows entering  $\chi^{-1}$ . Hence they are also the vanishing divisors of the maps which in the  $G$ -cluster  $\mathcal{M}$  represent the  $x$ -,  $y$ - and  $z$ -arrows leaving  $\chi$ . So a point  $p \in Y$  lies in  $D^1 \cap D^2 \cap D^3$  if and only if the whole of  $\mathbb{C}[x, y, z]$  acts by zero on the  $\chi$ -eigenspace of the corresponding  $G$ -cluster. It is then said that  $\chi$  *lies in the socle* of  $\mathcal{Z}_p$ . It was shown in [Cra05, §6] and [CI04, Lemma 9.1] that  $\chi$  marks a vertex of  $\Sigma$  if and only if  $\chi$  is in the socle of every  $G$ -cluster in the corresponding divisor. We now improve upon that observation:

**Proposition 4.8.** *Let  $\tau$  be a basic triangle of  $\Sigma$ . If  $\chi$  lies in the socle of the torus-invariant  $G$ -cluster defined by  $\tau$ , then  $\chi$  marks either a vertex or an edge of  $\tau$ . Moreover  $\chi$  lies in the socle of every  $G$ -cluster in the corresponding divisor or curve of  $Y$ .*

*Proof.* Assume that  $\tau$  lies in a regular corner triangle  $\Lambda$  of side  $r$ , the case of a meeting of champions triangle (cf. [CR02, §3.1]) is similar. Assume that  $\tau$  is an ‘up’ triangle, the ‘down’ case is similar. Up to permutation of  $x, y, z$ , the edges of  $\tau$  are cut out by  $x^{d-i} : y^{b+i} z^i$ ,  $y^{e-j} : x^{a+j} z^j$  and  $z^{f-k} : x^k y^{c+k}$  for some  $0 \leq i, j, k \leq r-1$  with  $i+j+k = r-1$ , where  $d-a = e-b = c = f = r$ . The shape of the  $G$ -graph of  $\tau$  and the position of  $\tau$  within  $\Lambda$  are determined by which of  $i, j, k$  are zero, and we distinguish several cases:

CASE 1: If  $i, j, k > 0$  then each vertex of  $\tau$  lies in the interior of  $\Lambda$ , the  $G$ -graph is shown in [Cra05, Figure 9], and the socle of the torus-invariant  $G$ -cluster has basis

$$x^{d-i-1} y^{c+k}, \quad x^{d-i-1} z^j, \quad x^k y^{e-j-1}, \quad y^{e-j-1} z^i, \quad x^{a+j} z^{f-k-1}, \quad y^{b+i} z^{f-k-1}. \quad (4.4)$$

The proof of [CI04, Lemma 9.1] shows that Reid’s recipe labels the vertices of  $\tau$  by the characters  $\chi$  of these 6 monomials, so the first statement holds in Case 1.

CASE 2: If precisely one of  $i, j, k$  is zero, say  $k = 0$ , then the edge of  $\tau$  cut out by  $z^f : y^c$  lies on an edge of  $\Lambda$ . Since  $k = 0$  we have  $x^k y^{e-j-1} | y^{e-j-1} z^i$  and  $x^{d-i-1} z^j | x^{a+j} z^{f-1}$ , so the second and third monomials from (4.4) are not in the socle. If  $c > 0$  then the remaining four monomials from (4.4) are a basis of the socle. Moreover, by [Cra05, (4,6)] the characters of  $x^{a+j} z^{f-1}$  and  $y^{b+i} z^{f-1}$  mark the vertex of  $\tau$  in the interior of  $\Lambda$ , while the characters of  $x^{d-i-1} y^c$  and  $y^{e-j-1} z^i$  mark the vertices of  $\tau$  on the edge of  $\Lambda$  as required. If  $c = 0$  then the edge of  $\tau$  cut out by  $z^f : y^c$  lies in an edge of  $\Delta$  and the socle has basis  $x^{a+j} z^{f-1}$  and  $y^{b+i} z^{f-1}$  because  $x^{d-i-1} y^c | x^{a+j} z^{f-1}$  and  $y^{e-j-1} z^i | y^{b+i} z^{f-1}$ . The corresponding pair of characters marks the vertex of  $\tau$  in the interior of  $\Lambda$ . Thus the first statement holds in Case 2.

CASE 3: If precisely two of  $i, j, k$  are zero, then we distinguish three subcases:

(i) If  $j = k = 0$ , then the edges of  $\tau$  cut out by  $x^a : y^e$  and  $z^f : y^c$  lie in edges of  $\Lambda$ . Since  $i = f-1$  we have  $y^{b+i} z^{f-k-1} | y^{e-j-1} z^i$ , so the sixth monomial from (4.4) does not lie in the socle, and neither do the second and third monomials because  $k = 0$ . If  $a, c > 0$  then the first, fourth and fifth monomials from (4.4) are a basis of the socle and the corresponding characters mark the three vertices of  $\tau$ . If  $a = 0$  and  $c \neq 0$  then the edge cut out by  $x^a : y^e$  lies in an edge of  $\Delta$ , the socle has basis  $y^{e-1} z^i$  and the corresponding character marks the unique vertex of  $\tau$  that lies inside  $\Delta$ . The case  $c = 0$  and  $a \neq 0$  is similar. If  $a = c = 0$ , then the unique monomial in the socle  $y^{e-1} z^{f-1}$  is equal to  $y^{b+r-1} z^{r-1}$ , and the corresponding character marks the unique edge of  $\tau$  which lies inside  $\Delta$ .

(ii) If  $i = k = 0$ , then the edges of  $\tau$  cut out by  $x^d : y^b$  and  $z^f : y^c$  lie in edges of  $\Lambda$ . If  $b, c > 0$  then the socle has basis  $x^{d-1} y^c$ ,  $x^{d-1} z^{f-1}$ ,  $y^{e-r}$  and  $y^b z^{f-1}$ . The characters of three of these monomials mark the vertices of  $\tau$ , while  $x^{d-1} z^{f-1} = x^{a+j} z^j$  and so its character marks the unique edge of  $\tau$  that does not lie in an edge of  $\Lambda$ . The degenerate cases where  $b = 0$  or  $c = 0$ , or both, are similar to those in Case (i) above.

(iii) If  $i = j = 0$ , then the edges of  $\tau$  cut out by  $x^d : y^b$  and  $x^a : y^e$  lie in edges of  $\Lambda$  and one vertex of  $\tau$  is  $e_z$ . If  $a, b > 0$  then the socle has basis  $x^{r-1} y^{e-1}$  and  $x^{d-1} y^{c+r-1}$  and the corresponding characters mark the two vertices of  $\tau$  that are not  $e_z$ . The degenerate cases with  $a = 0$  or  $b = 0$ , or both, are similar to those in Case (i) above. When  $a = b = 0$  the character of the unique monomial  $x^{d-1} y^{c+r-1}$  in the socle marks an edge of  $\tau$ . This completes the proof of the first statement in Case 3.

CASE 4: If  $i = j = k = 0$ , then  $\Lambda$  is a corner triangle with vertex  $e_z$  and side  $r = 1$ , i.e.  $\tau$  is the whole of  $\Lambda$ . Assume that  $a, b > 0$ , otherwise edges of  $\tau$  lie in edges of  $\Delta$  and the calculation simplifies further. The socle has basis  $x^a y^c$  and  $y^{b+c}$  and the corresponding monomials mark the two of vertices of  $\tau$  which are not  $e_z$ . This proves the first statement in Case 4.

This completes the proof of the first statement. The second statement follows immediately from [CI04, Lemma 9.1] whenever  $\chi$  marks a vertex of  $\tau$ . It remains to prove it when  $\chi$  marks an edge of  $\tau$ . The only nondegenerate case where this happens is Case 3(ii) in which the relevant edge of  $\tau$  is cut out by  $y^{e-r+1} : x^{d-1} z^{f-1}$ . The degenerate cases are similar. So let  $\tau'$  denote the basic triangle adjacent to  $\tau$  that shares this edge. The  $G$ -graph of  $\tau'$  is obtained from that of  $\tau$  by performing the  $G$ -igsaw transform in the sense of [Nak00] using  $y^{e-r+1}/x^{d-1} z^{f-1}$ . This removes the monomial  $x^{d-1} z^{f-1}$  from the  $G$ -graph of  $\tau$  and replaces it by the monomial  $y^{e-r+1}$ . Since  $y^{e-r}$  lies in the socle of the  $G$ -graph of  $\tau$ , it is immediate that  $y^{e-r+1}$  lies in the socle of the  $G$ -graph of  $\tau'$ . Therefore  $\chi$  lies in the socle of both torus-invariant  $G$ -clusters in the curve in  $Y$  defined by the edge it marks. This proves the second statement.  $\square$

In the language of CT-subdivisions Prop. 4.8 states that any basic triangle of  $\Sigma$  which touches all three  $T$ -areas must contain a vertex or an edge marked by  $\chi$  which also touches all three  $T$ -areas. In light of Cor. 4.7, it proves our prior assertion that a basic triangle connecting up two  $T$ -areas disconnected by a “wedge” must lie along the tip of the “wedge”. In fact, it proves:

*Proof of Theorem 1.1.* The transform  $\Psi(\mathcal{O}_0 \otimes \chi)$  is isomorphic to the total complex  $T^\bullet$  of the skew-commutative cube of line bundles  $\text{Hex}(\chi^{-1})_{\tilde{\mathcal{M}}}$ . By Lemma 2.1(4) we have  $\mathcal{H}^i(T^\bullet) = 0$  unless  $i = 0, -1, -2$ . Since by Lemma 3.2 a non-trivial  $\chi$  could never be a  $(3, 0)$ -sink, we also have  $\mathcal{H}^{-2}(T^\bullet) = 0$  by Lemma 2.1(3). To prove the theorem it therefore suffices to prove that for any non-trivial  $\chi$  only one of  $\mathcal{H}^0(T^\bullet)$  and  $\mathcal{H}^{-1}(T^\bullet)$  is non-zero. The assertion about being a pushforward from its support follows from the formulas for  $\mathcal{H}^0$  and  $\mathcal{H}^{-1}$  in Lemma 2.1.

Suppose that  $\mathcal{H}^0(T^\bullet) \neq 0$ . Then by Lemma 2.1(1) and Cor. 4.3 there exists a basic triangle in  $\Sigma$  whose vertices touch all three  $T$ -areas. By Prop. 4.8 such triangle must contain a vertex or an edge marked by  $\chi$  which also touches all three  $T$ -areas.

Suppose there is a vertex  $e$  which touches all three  $T$ -areas. Then the CT-subdivision for  $\chi$  is of the “meeting point” type and looks as depicted on Figure 13(a) or Figure 14. In particular, it is clear that there can be no “wedges” or squashed legs of  $T$  snapping off a  $T$ -area. We conclude that  $\mathcal{H}^{-1}(T^\bullet) = 0$  since by Lemma 2.1(2), Cor. 4.4 and Cor. 4.5 the support of  $\mathcal{H}^{-1}(T^\bullet)$  consists of all the vertices which are interior to the tip of a “wedge”, interior to a squashed leg snapping off a  $T$ -area, or are a meeting point of the two.

Suppose there is a  $\chi$ -marked edge  $ef$  which touches all three  $T$ -areas. Any edge marked by  $\chi$  belongs by Cor. 4.7 to the tip of a “wedge” or a squashed leg of  $T$  which snaps off a  $T$ -area. So the CT-subdivision for  $\chi$  looks as depicted on Figure 13(b) or on Figure 15. In particular, it is clear that if a “wedge” contains  $ef$  in its tip, then  $ef$  must be the whole of the tip and there are no snapped off  $T$ -areas. Similarly, if a  $T$ -area is snapped off by a squashed leg of  $T$  which contains  $ef$ , then  $ef$  is the whole of this leg and there are no “wedges” or other snapped off  $T$ -areas. In either case we have  $\mathcal{H}^{-1}(T^\bullet) = 0$  for the same reason as above.  $\square$

## 5. DERIVED REID'S RECIPE

In this section we compute the transform  $\Psi(\mathcal{O}_0 \otimes \chi)$  for each  $\chi \in G^\vee$  based on the role that  $\chi$  plays in Reid's recipe. The results in this section give a proof of Theorem 1.2. Throughout we use the notation from §2.6.

**5.1. Refined list of the roles  $\chi$  can play in Reid's recipe.** First, we need a refinement of the list given in [Cra05, §4] of the roles  $\chi$  can play in Reid's recipe:

**Proposition 5.1.** *For any character  $\chi \in G^\vee$  precisely one of the following holds:*

- (1)  $\chi$  marks a single vertex  $e$  of  $\Sigma$ .
- (2)  $\chi$  marks a single concave chain of edges of  $\Sigma$  contained within the boundary of a unique  $C$ -area. If this area is, for example,  $Cz^\bullet$ , then as illustrated on Fig. 16(a) and 16(b) the chain consists of one or more straight-line segments  $P_1P_2, \dots, P_mP_{m+1}$  such that:
  - $e_xP_1$  is the boundary of  $Cz^\bullet$  with  $Ty^\bullet z^\bullet$ .
  - $P_{m+1}e_y$  is the boundary of  $Cz^\bullet$  with  $Tx^\bullet z^\bullet$ .
  - $P_2, \dots, P_m$  lie on a succession of lines out of  $e_z$
  - each  $P_iP_{i+1}$  is carved out by ratio  $z^c: x^{a_i}y^{b_i}$  for some  $a_i, b_i, c \in \mathbb{Z}$  with

$$0 \leq a_1 \leq \dots \leq a_m \quad \text{and} \quad b_1 \geq \dots \geq b_m \geq 0. \quad (5.1)$$

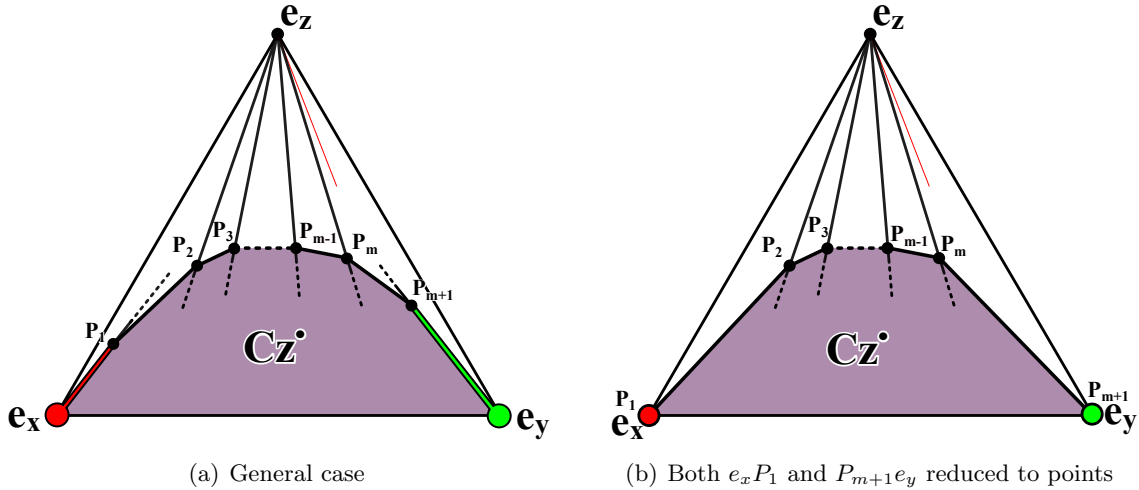


FIGURE 16. A single  $Cz^\bullet$ -concave chain

- (3) “Meeting of champions”:  $\chi$  marks three lines in  $\Sigma$  which start at the three corners of  $\Delta$  and meet at some internal vertex  $P$ . The monomial ratios which carve out these lines are  $x^a: y^b$ ,  $y^b: z^c$  and  $z^c: x^a$  for some  $a, b, c > 0$  and the CT-subdivision for  $\chi$  is as depicted on Fig. 17(a).
- (4) “Long side”:  $\chi$  marks a line out of  $e_x$ ,  $e_y$  or  $e_z$  which runs all the way to a vertex  $P$  on the opposite side of  $\Delta$ . The CT-subdivision for  $\chi$  is as depicted on Figure 17(b).
- (5)  $\chi$  is the trivial character and marks nothing in Reid's recipe.

*Proof.* In light of [Cra05], we need only show that if  $\chi$  marks an edge in  $\Sigma$  then precisely one of (2), (3) or (4) holds. Permuting  $x, y, z$  if necessary, the edge is cut out by  $z^f: x^d y^e$  for  $d \geq 0$

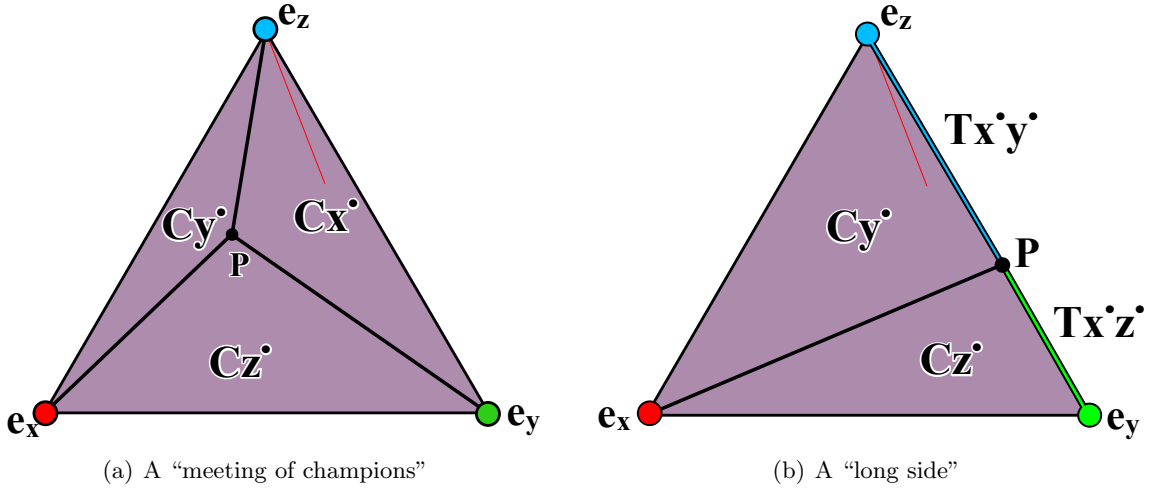


FIGURE 17. A “meeting of champions” and a “long side”

and  $e, f > 0$ . Now, [Cra05, Lemma 5.3] shows that the edge forms part of the piecewise-linear boundary of the convex region  $Cz^\bullet$ . If  $\chi$  marks an edge that touches a vertex of valency 3, then the local picture of  $\Sigma$  shown in Figure 7(b) forces the CT-subdivision to be as in Figure 17(a) and we are in case (3). Otherwise,  $\chi$  marks a piecewise-linear curve in the boundary of  $Cz^\bullet$  where, following [Cra05, Section 3], a chain of edges marked  $\chi$  changes direction in  $\Sigma$  only if the chain crosses a line emanating from  $e_z$ . Label by  $P_1$  the end of the chain which is closer to  $e_x$ , then label by  $P_2, \dots, P_m$  all the points in succession where the chain crosses a line out of  $e_z$ , and finally label the other end by  $P_{m+1}$ . We now analyze the boundary of  $Cz^\bullet$ . If it is a straight line from  $e_x$  or  $e_y$ , then every edge in the boundary is cut out by  $z^f : y^e$ . Then by [Cra05, Lemma 5.3] the CT-subdivision comprises two convex regions as shown in Figure 17(b) and we are in case (4). Otherwise, if  $P_1 \neq e_x$ , then the boundary of  $Cz^\bullet$  that joins  $e_x$  to  $P_1$  is with  $Ty^\bullet z^\bullet$  and by convexity it must be a straight line. We argue similarly for  $P_{m+1}$  and conclude that the boundary of  $Cz^\bullet$  consists of two straight lines  $e_x P_1$  and  $P_{m+1} e_y$  (either may have length zero) joined by the  $\chi$ -marked chain  $P_1 \dots P_{m+1}$ . Since the chain lies on the boundary of  $Cz^\bullet$ , each edge in the chain is carved out by ratios of type  $z^\bullet : x^\bullet, z^\bullet : x^\bullet y^\bullet, z^\bullet : y^\bullet$ . By inspecting every possible local picture of  $\Sigma$  around a vertex, we see that if the chain crosses a line  $l$  out of  $e_z$ , then the edge adjacent to  $l$  on the same side as  $e_x$  is cut out by  $z^c : x^a y^b$  for some  $b, c > 0$  and  $a \geq 0$ , while on the other side of  $l$  the adjacent edge is cut out by  $z^c : x^{a'} y^{b'}$  for some  $a' > 0, b' \geq 0$ . Moreover, we have  $a \leq a'$  and  $b \geq b'$ , and both inequalities are strict if and only if the chain changes direction after crossing  $l$ . Thus, each segment  $P_i P_{i+1}$  is carved out by a ratio  $z^c : x^{a_i} y^{b_i}$  with  $c, a_i, b_i \in \mathbb{Z}$  satisfying the inequalities (5.1) and we are in case (2).  $\square$

**5.2. The case of  $\chi$  marking a single vertex.** Let  $\chi \in G^\vee$  marks a single vertex  $e$  of  $\Sigma$  and let  $E$  be the corresponding toric divisor on  $Y$ .

**Proposition 5.2.** *We have  $\Psi(\mathcal{O}_0 \otimes \chi) = \mathcal{L}_\chi^{-1} \otimes \mathcal{O}_E$ .*

*Proof.* This was proved in [CI04, Prop. 9.3], but a direct proof is short enough to include it here. Recall that a point  $p \in Y$  lies in  $D^1 \cap D^2 \cap D^3$  if and only if  $\chi$  is in the socle of the  $G$ -cluster  $\mathcal{Z}_p$ . By Prop. 4.8 a  $G$ -cluster  $\mathcal{Z}_p$  has  $\chi$  in the socle only when the point  $p$  lies on a

divisor or curve marked by  $\chi$ . Since  $\chi$  marks only  $E$ , we must have  $D^1 \cap D^2 \cap D^3 \subseteq E$ . On the other hand, by Theorem 3.4 (or, in fact, [CI04, Prop. 9.1]), character  $\chi$  marks  $e$  if and only if  $E \subseteq D^1 \cap D^2 \cap D^3$ . We conclude that  $D^1 \cap D^2 \cap D^3 = E$ , so Lemma 2.1 gives

$$\mathcal{H}^0(\Psi(\mathcal{O}_0 \otimes \chi)) = \mathcal{L}_\chi^{-1} \otimes \mathcal{O}_E.$$

Finally, Theorem 1.1 implies that all the other cohomology sheaves of  $\Psi(\mathcal{O}_0 \otimes \chi)$  vanish.  $\square$

**5.3. The case of  $\chi$  marking a single concave chain of edges.** Let  $\chi \in G^\vee$  be such that  $\chi$  marks a single concave chain of edges of  $\Sigma$  contained within the boundary of a unique  $C$ -area. Permuting  $x, y$  or  $z$  if necessary, we may assume that the chain is contained within the boundary of  $Cz^\bullet$ , as described in Prop. 5.1(2) and illustrated on Fig. 16.

**Proposition 5.3.** (1) *If the chain consists of a single edge  $P_1P_2$ , then*

$$\Psi(\mathcal{O}_0 \otimes \chi) = \mathcal{L}_\chi^{-1} \otimes \mathcal{O}_C$$

*where  $C$  is the toric curve  $P_1 \cap P_2$  corresponding to that edge.*

(2) *If the chain consists of more than one edge, then*

$$\Psi(\mathcal{O}_0 \otimes \chi) = \mathcal{L}_\chi^{-1}(-P_1 - P_{m+1}) \otimes \mathcal{O}_Z[1]$$

*where  $Z$  is the union of the divisors which correspond to the internal vertices of chain  $P_1 \dots P_{m+1}$ .*

*Proof.* Suppose first, that the chain consist of a single edge  $P_1P_2$ . Consider the CT-subdivision for  $\chi$ . By Cor. 4.7 the edges marked by  $\chi$  are those in the tip of a “wedge” or in a squashed leg of  $T$  snapping off a  $T$ -area. So either there is a single wedge with tip  $P_1P_2$  and no “snaps” (Fig. 13(b), 15(a), 15(c)) or a single “snap”  $P_1P_2$  and no “wedge” (Fig. 15(f)). In both cases  $P_1P_2$  touches all three  $T$ -areas and hence by Cor. 4.3 we have  $P_1 \cap P_2 \subseteq D^1 \cap D^2 \cap D^3$ . Then we argue as in Prop. 5.2: by Prop. 4.8  $P_1 \cap P_2$  is the whole of  $D^1 \cap D^2 \cap D^3$ , by Lemma 2.1

$$\mathcal{H}^0(\Psi(\mathcal{O}_0 \otimes \chi)) = \mathcal{L}_\chi^{-1} \otimes \mathcal{O}_{P_1 \cap P_2}$$

and by Theorem 1.1 all the other cohomology sheaves of  $\Psi(\mathcal{O}_0 \otimes \chi)$  vanish.

Suppose now the chain consists of more than one edge. Taking  $I = \{23\}$ ,  $J = \{13\}$  and  $K = \{12\}$  in Lemma 2.1(2) it follows that there is a three-step filtration of  $\mathcal{H}^{-1}(\Psi(\mathcal{O}_0 \otimes \chi))$  with successive quotients

- $\mathcal{F}_{23}'' = \mathcal{O}_{Z_{23}} \otimes \mathcal{L}_{23}(\gcd(D_2^3, D_3^2))$  with  $Z_{23}$  being the scheme theoretic intersection of  $\gcd(D_2^3, D_3^2)$  and the effective part of  $D^1 + \text{lcm}(\tilde{D}_1^2, \tilde{D}_1^3) - \tilde{D}_2^3 - D^2$ .
- $\mathcal{F}_{13} = \mathcal{O}_{Z_{13}} \otimes \mathcal{L}_{13}(\gcd(D_1^3, D_3^1))$  with  $Z_{13}$  being the scheme theoretic intersection of  $\gcd(D_1^3, D_3^1)$  and the effective part of  $D^2 + \text{lcm}(\tilde{D}_2^1, \tilde{D}_2^3) - \tilde{D}_3^1 - D^3$
- $\mathcal{F}_{12} = \mathcal{O}_{Z_{12}} \otimes \mathcal{L}_{12}(\gcd(D_1^2, D_2^1))$  with  $Z_{12}$  is the scheme theoretic intersection of  $\gcd(D_1^2, D_2^1)$  and the effective part of  $D^3 + \text{lcm}(D_3^1, D_3^2) - \tilde{D}_1^2 - D^1$

where  $\tilde{D}_j^i = D_j^i - \gcd(D_j^i, D_i^j)$ .

Corollaries 4.4 and 4.5 imply that

$$Z_{12} = (Cz^\bullet \cap (Cx^\bullet \cup Tx^\bullet y^\bullet \cup Cy^\bullet)) \setminus (Ty^\bullet z^\bullet \cup Tx^\bullet z^\bullet).$$

The chain  $P_1 \dots P_{m+1}$  is the boundary of  $Cz^\bullet$  with  $Cx^\bullet \cup Tx^\bullet y^\bullet \cup Cy^\bullet$ , while  $e_x P_1$  and  $P_{m+1} e_y$  are its boundaries with  $Ty^\bullet z^\bullet$  and with  $Tx^\bullet z^\bullet$ . Therefore  $Z_{12}$  is the union of the toric divisors corresponding to the internal vertices of the chain  $P_1 \dots P_{m+1}$ .

On the other, we claim that  $Z_{13} = \emptyset = Z_{23}$ . To verify the claim for  $Z_{13}$ , note that

$$Z_{13} = (Cy^\bullet \cap (Cx^\bullet \cup Tx^\bullet z^\bullet)) \setminus (Ty^\bullet z^\bullet \cup Tx^\bullet y^\bullet).$$

Suppose  $Z_{13}$  is non-empty. Since  $Cy^\bullet$  and  $Cx^\bullet \cup Tx^\bullet z^\bullet$  are disconnected by  $Cz^\bullet \cup Tx^\bullet y^\bullet$ , there has to be a basic triangle  $\tau$  in  $Cz^\bullet$  with one vertex on the border with  $Cy^\bullet$  and another on the border with  $Cx^\bullet \cup Tx^\bullet z^\bullet$ . The border between  $Cz^\bullet$  and  $Cy^\bullet$  exists only when  $P_1 = e_x$  and is  $P_1 P_2$ . Therefore  $P_1 = e_x$  and one vertex of  $\tau$  must be an internal vertex of  $P_1 P_2$ . Since  $\chi$  doesn't mark a "long side", line  $P_1 P_2$  terminates at an internal line  $e_z P_2$  out of  $e_z$ , see Fig. 16. The Craw-Reid algorithm dictates then that  $\tau$  must lie on the same side of  $e_z P_2$  as  $P_1 P_2$ . On the other hand, the border of  $Cz^\bullet$  with  $Tx^\bullet z^\bullet$  is  $P_{m+1} e_y$  and the border of  $Cz^\bullet$  with  $Cx^\bullet$  exists only when  $P_{m+1} = e_y$  and is  $P_m P_{m+1}$ . Both of these lie on the other side of line  $e_z P_2$  from  $P_1 P_2$ , and can't therefore contain a vertex of  $\tau$ . This is a contradiction, and we conclude that  $Z_{13} = \emptyset$ . A similar argument for

$$Z_{23} = (Cx^\bullet \cap Ty^\bullet z^\bullet) \setminus (Tx^\bullet z^\bullet \cup Tx^\bullet y^\bullet).$$

shows that  $Z_{23} = \emptyset$ .

Thus far, we've shown that

$$\mathcal{H}^{-1}(\Psi(\mathcal{O}_0 \otimes \chi)) = \mathcal{L}_{12}(\gcd(D_1^2, D_2^1)) \otimes \mathcal{O}_Z$$

where  $Z$  is the union of all the divisors corresponding to the internal vertices of  $P_1 \dots P_{m+1}$ . In Fig. 2(b) we have  $\mathcal{L} = \mathcal{L}_{123} = \mathcal{L}_\chi^{-1}$ . Since  $D_{12}^3$  was defined to be the vanishing divisor of the regular map  $\mathcal{L}_{123} \xrightarrow{\alpha_{12}^3} \mathcal{L}_{12}$  we have  $\mathcal{L}_{12} = \mathcal{L}_{123}(D_{12}^3)$ . Therefore

$$\mathcal{L}_{12}(\gcd(D_1^2, D_2^1)) = \mathcal{L}_\chi^{-1}(D_{12}^3 + \gcd(D_1^2, D_2^1)).$$

The sum of vanishing divisors along any path from  $\mathcal{L}_{123}$  to  $\mathcal{L}$  is the principal divisor  $(xyz)$ , so  $D_{12}^3 + \gcd(D_1^2, D_2^1) = (xyz) - \text{lcm}(D^1, D^2)$ . By Cor. 4.3  $\text{lcm}(D^1, D^2) = Ty^\bullet z^\bullet \cup Tx^\bullet z^\bullet$ , so

$$\mathcal{H}^{-1}(\Psi(\mathcal{O}_0 \otimes \chi)) = \mathcal{L}_\chi^{-1}(-Ty^\bullet z^\bullet \cup Tx^\bullet z^\bullet) \otimes \mathcal{O}_Z.$$

Two toric divisors intersect if and only if the corresponding vertices of  $\Sigma$  are adjacent. So when we restrict  $\mathcal{O}_Y(-Ty^\bullet z^\bullet \cup Tx^\bullet z^\bullet)$  to  $Z$  only those vertices in  $Ty^\bullet z^\bullet$  and  $Tx^\bullet z^\bullet$  which are adjacent to the internal vertices of  $P_1 \dots P_{m+1}$  make a non-zero contribution. But  $P_1 \dots P_{m+1}$  is the border of  $Cz^\bullet$  and  $Cx^\bullet \cup Tx^\bullet y^\bullet \cup Cy^\bullet$  and it is clear from Figure 16 that the only vertices of  $Ty^\bullet z^\bullet \cup Tx^\bullet z^\bullet$  which are adjacent to the internal vertices of  $P_1 \dots P_{m+1}$  are  $P_1$  and  $P_{m+1}$ . Hence  $\mathcal{O}_Y(-Ty^\bullet z^\bullet \cup Tx^\bullet z^\bullet)$  and  $\mathcal{O}_Y(-P_1 - P_{m+1})$  restrict to the same line-bundle on  $Z$ . We conclude that

$$\mathcal{H}^{-1}(\Psi(\mathcal{O}_0 \otimes \chi)) = \mathcal{L}_\chi^{-1}(-P_1 - P_{m+1}) \otimes \mathcal{O}_Z.$$

Since  $Z$  is non-empty,  $\mathcal{L}_\chi^{-1}(-P_1 - P_{m+1}) \otimes \mathcal{O}_Z$  is non-zero and by Theorem 1.1 all the other cohomology sheaves of  $\Psi(\mathcal{O}_0 \otimes \chi)$  vanish.  $\square$



**5.4. The case of a “meeting of champions”.** Throughout this section let  $\chi \in G^\vee$  be such that  $\chi$  marks a “meeting of champions” as depicted on Figure 17(a). The configuration of edges of  $\Sigma$  can be viewed as three concave chains  $e_yPe_z$ ,  $e_xPe_z$  and  $e_xPe_y$ . We show below that  $\mathcal{H}^{-1}(\Psi(\mathcal{O}_0 \otimes \chi))$  consists of the three answers Section 5.3 would give for each of these chains individually, glued together in a certain natural way. It is important to understand the geometry of the support of these three chains. In the next three paragraphs we establish some needed notation and translate into concrete geometrical terms the toric data on Figure 17(a).

Denote by  $Z_x$ ,  $Z_y$  and  $Z_z$  the chains of reduced divisors corresponding to the interior vertices of  $e_yPe_z$ ,  $e_xPe_z$  and  $e_xPe_y$ . The total support of  $Z_x$ ,  $Z_y$  and  $Z_z$  consists of  $P \simeq \mathbb{P}^2$  and the three chains of (possibly blowup) rational scrolls which link coordinate hyperplanes  $E_x$ ,  $E_y$  and  $E_z$  to  $P$ . Each of  $Z_x$ ,  $Z_y$  and  $Z_z$  consists of two of these chains of rational scrolls joined together by  $P$  (see Fig. 18). Note that some of these chains of rational scrolls may be empty, i.e.  $E_x$ ,  $E_y$  or  $E_z$  may intersect  $P$  directly with no rational scrolls in between.

Let  $Q_x$ ,  $Q_y$  and  $Q_z$  denote the divisors on  $e_xP$ ,  $e_yP$  and  $e_zP$  which are adjacent to  $P$ . In other words,  $Q_x$  is either the last scroll in the chain of rational scrolls joining  $E_x$  to  $P$  or  $E_x$  itself if the chain is empty. Then each of  $Q_x$ ,  $Q_y$  and  $Q_z$  intersect  $P \simeq \mathbb{P}^2$  in a  $\mathbb{P}^1$  passing through two out of the three toric fixed points of  $P$ . They also intersect each other in three  $\mathbb{P}^1$ s which are attached to  $P$  at its toric fixed points. We’ve depicted this configuration on Fig. 18(a) in general case and on Fig. 18(b) when one of the rational scroll chains is empty.

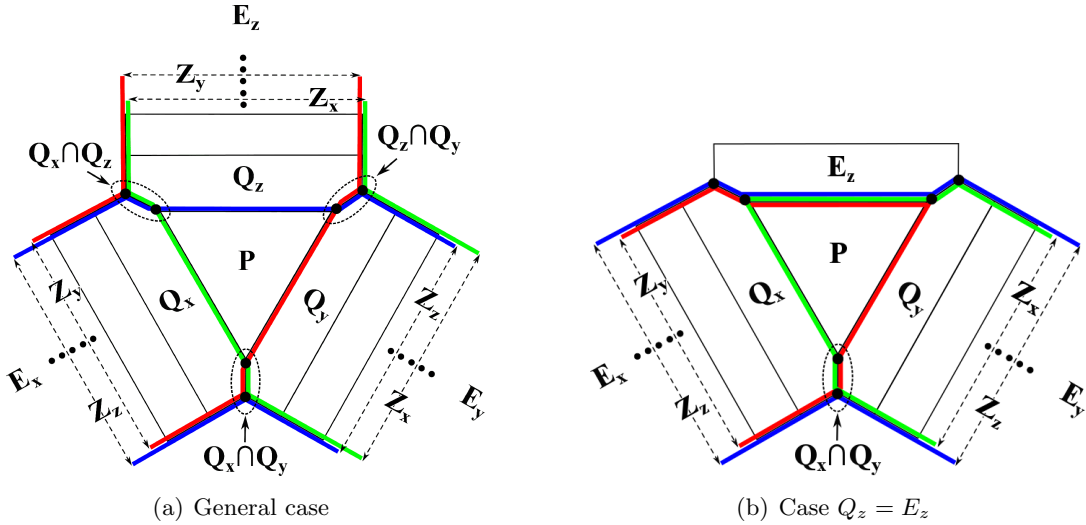


FIGURE 18. Divisor chains  $Z_x$ ,  $Z_y$  and  $Z_z$  around divisor  $P$

Thus  $S = Z_x \cup Z_y \cup Z_z$  has the following stratification:

- $S_2$ : Points which lie on precisely two out of  $Z_x$ ,  $Z_y$  and  $Z_z$ . This is a disjoint union of the three rational scroll chains joining  $E_x$ ,  $E_y$  and  $E_z$  to  $P$  minus their pairwise intersections.
- $S_3$ : Points which lie on all three of  $Z_x$ ,  $Z_y$  and  $Z_z$ . This is a union of  $P \simeq \mathbb{P}^2$  and  $\mathbb{P}^1$ s formed by pairwise intersections of those of  $Q_x$ ,  $Q_y$  and  $Q_z$  which are rational scrolls.

**Proposition 5.4.** (1) We have

$$\mathcal{H}^{-1}(\Psi(\mathcal{O}_0 \otimes \chi)) = \mathcal{L}_\chi^{-1}(-E_x - E_y - E_z) \otimes \mathcal{F}$$

where  $\mathcal{F}$  is the cokernel of

$$\mathcal{O}_Y \xrightarrow{E_x \oplus E_y \oplus E_z} \mathcal{O}_{Z_x}(E_x) \oplus \mathcal{O}_{Z_y}(E_y) \oplus \mathcal{O}_{Z_z}(E_z).$$

(2) The support of  $\mathcal{F}$  is  $S = Z_x \cup Z_y \cup Z_z$ . Moreover:

- $\mathcal{F}|_{S_2}$  is a free sheaf of rank 1.
- If  $P$  doesn't intersect any of  $E_x$ ,  $E_y$  or  $E_z$ , then  $\mathcal{F}|_{S_3}$  is a free sheaf of rank 2.
- Otherwise, up to permuting  $x$ ,  $y$  and  $z$ :
  - ◊ If  $P$  intersects  $E_x$ , but not  $E_y$  or  $E_z$ , then  $\mathcal{F}|_{S_3} = \mathcal{O}(E_x) \oplus \mathcal{O}$ .
  - ◊ If  $P$  intersects  $E_x$  and  $E_y$ , but not  $E_z$ , then  $\mathcal{F}|_{S_3} = \mathcal{O}(E_x) \oplus \mathcal{O}(E_y)$ .
  - ◊ If  $P$  intersects  $E_x$ ,  $E_y$  and  $E_z$ , then  $S_3 = P$  and  $\mathcal{F}|_P = T_{\mathbb{P}^2}$ .

*Proof.* We compute the sheaf  $\mathcal{L}_\chi \otimes \mathcal{H}^{-1}(\Psi(\mathcal{O}_0 \otimes \chi))$ . Prop. 4.2 and Figure 17(a) together tell us the vertex type of  $\chi^{-1}$  for every toric divisor of  $Y$ . We can therefore write down explicitly the skew-commutative cube of line bundles corresponding to  $\mathcal{L}_\chi \otimes \text{Hex}(\chi^{-1})_{\tilde{\mathcal{M}}}$ :

$$\begin{array}{ccccc}
& \mathcal{O}_Y(-Cx^\bullet) & \xrightarrow{\alpha_2^3} & \mathcal{O}_Y(-E_x) & \\
\alpha_{23}^1 \nearrow & & \alpha_3^2 \searrow & & \alpha^1 \searrow \\
\mathcal{O}_Y(-\Delta) & \xrightarrow{\alpha_{13}^2} & \mathcal{O}_Y(-Cy^\bullet) & \xrightarrow{\alpha^2} & \mathcal{O}_Y \\
\alpha_{12}^3 \searrow & & \alpha_1^2 \nearrow & & \alpha^3 \nearrow \\
& \mathcal{O}_Y(-Cz^\bullet) & \xrightarrow{\alpha_2^1} & \mathcal{O}_Y(-E_z) &
\end{array} \quad (5.2)$$

where maps  $\alpha^\bullet$  are given by natural inclusions. Denote by  $T^\bullet$  the total complex of this cube.

The maps  $\alpha^1$ ,  $\alpha^2$  and  $\alpha^3$  are defined by pairwise co-prime divisors  $E_x$ ,  $E_y$  and  $E_z$ . Arguing as in [CL09, Lemma 3.1(2)] we see that  $\text{Ker}(T^{-1} \rightarrow T^0)$  is isomorphic to the cokernel of

$$\mathcal{O}_Y(-E_x - E_y - E_z) \xrightarrow{E_x \oplus E_y \oplus E_z} \mathcal{O}_Y(-E_y - E_z) \oplus \mathcal{O}_Y(-E_x - E_z) \oplus \mathcal{O}_Y(-E_x - E_y) \quad (5.3)$$

and that  $\text{Im}(T^{-2} \rightarrow T^{-1})$  is then the image in  $\text{Ker}(T^{-1} \rightarrow T^0)$  of the subsheaf

$$\mathcal{O}_Y(-Cx^\bullet) \oplus \mathcal{O}_Y(-Cy^\bullet) \oplus \mathcal{O}_Y(-Cz^\bullet) \quad (5.4)$$

of

$$\mathcal{O}_Y(-E_y - E_z) \oplus \mathcal{O}_Y(-E_x - E_z) \oplus \mathcal{O}_Y(-E_x - E_y). \quad (5.5)$$

So  $\mathcal{H}^{-1}(T^\bullet)$  is the quotient of the cokernel of (5.3) by the image of (5.4). On the other hand, claim (1) is equivalent to  $\mathcal{H}^{-1}(T^\bullet)$  being the quotient of the cokernel of (5.3) by the image of

$$\mathcal{O}_Y(-e_y P e_z) \oplus \mathcal{O}_Y(-e_x P e_z) \oplus \mathcal{O}_Y(-e_x P e_y). \quad (5.6)$$

This is because  $e_y P e_z = E_y + E_z + Z_x$  as Weil divisors, and similarly for  $-e_x P e_z$  and  $-e_x P e_y$ .

To establish claim (1) it now suffices to show that the natural inclusion of (5.4) into (5.6) becomes an isomorphism in the cokernel of (5.3). This is a local problem, so take any basic triangle  $\sigma$  in  $\Sigma$  and let  $A_\sigma$  be the corresponding affine chart. Since  $Cx^\bullet$ ,  $Cy^\bullet$  and  $Cz^\bullet$  subdivide

$\Delta$  triangle  $\sigma$  must lie in precisely one of the three. Suppose, without loss of generality, it lies in  $Cx^\bullet$ . But then  $E_x$  and  $A_\sigma$  do not intersect, so (5.3) restricts to  $A_\sigma$  as

$$\mathcal{O}(-E_y - E_z) \xrightarrow{\text{Id} \oplus E_y \oplus E_z} \mathcal{O}(-E_y - E_z) \oplus \mathcal{O}(-E_z) \oplus \mathcal{O}(-E_y)$$

and its cokernel can therefore be identified with  $\mathcal{O}(-E_z) \oplus \mathcal{O}(-E_y)$ . Under this identification the images of (5.4) and (5.6) become subsheaves of  $\mathcal{O}(-E_z) \oplus \mathcal{O}(-E_y)$  generated by

$$\text{Im}(\mathcal{O}(-Cx^\bullet) \hookrightarrow \mathcal{O}(-E_z) \oplus \mathcal{O}(-E_y)), \quad \mathcal{O}(-Cy^\bullet) \oplus \mathcal{O}(-Cz^\bullet) \quad (5.7)$$

$$\text{Im}(\mathcal{O}(-e_yPe_z) \hookrightarrow \mathcal{O}(-E_z) \oplus \mathcal{O}(-E_y)), \quad \mathcal{O}(-e_xPe_z) \oplus \mathcal{O}(-e_xPe_y) \quad (5.8)$$

respectively. On the other hand, since  $\sigma \in Cx^\bullet$  we have on  $A_\sigma$

$$\begin{aligned} \mathcal{O}(-Cy^\bullet) &= \mathcal{O}(-e_xPe_z) = \mathcal{O}(-e_zP) \\ \mathcal{O}(-Cz^\bullet) &= \mathcal{O}(-e_xPe_y) = \mathcal{O}(-e_yP) \end{aligned}$$

and therefore

$$\mathcal{O}(-Cy^\bullet) \oplus \mathcal{O}(-Cz^\bullet) = \mathcal{O}(-e_xPe_z) \oplus \mathcal{O}(-e_xPe_y) = \mathcal{O}(-E_z) \oplus \mathcal{O}(-E_y).$$

Lines  $e_yP$  and  $e_zP$  are both contained in  $e_yPe_z$  and therefore in  $Cx^\bullet$ . Hence images of  $\mathcal{O}(-Cx^\bullet)$  and  $\mathcal{O}(-e_yPe_z)$  in  $\mathcal{O}(-E_z) \oplus \mathcal{O}(-E_y)$  are both contained in its subsheaf  $\mathcal{O}(-e_zP) \oplus \mathcal{O}(-e_yP)$ . They are therefore redundant in (5.7) and (5.8). Thus after identifying the cokernel of (5.3) with  $\mathcal{O}(-E_z) \oplus \mathcal{O}(-E_y)$  the image of the natural inclusion of (5.4) into (5.6) becomes

$$\mathcal{O}(-e_zP) \oplus \mathcal{O}(-e_yP) \xrightarrow{\text{Id}} \mathcal{O}(-e_zP) \oplus \mathcal{O}(-e_yP).$$

This establishes claim (1).

For claim (2) first note that  $S_2$  is a union of three disjoint pieces  $S \setminus Z_x$ ,  $S \setminus Z_y$  and  $S \setminus Z_z$ . Piece  $S \setminus Z_z$  is the rational scroll chain joining  $E_z$  to  $P$ , so it is contained within  $Z_x$  and  $Z_y$  and it is disjoint from  $E_x$  and  $E_y$ . Therefore  $\mathcal{F}_{S \setminus Z_z}$  is the cokernel of

$$\mathcal{O} \xrightarrow{\text{Id} \oplus \text{Id} \oplus 0} \mathcal{O} \oplus \mathcal{O} \oplus 0,$$

which is isomorphic to  $\mathcal{O}$ , as required.  $\mathcal{F}|_{S \setminus Z_x}$  and  $\mathcal{F}|_{S \setminus Z_y}$  are computed similarly.

Next we note that  $S_3$  intersects  $E_x$ ,  $E_y$  and  $E_z$  if and only if  $P$  does. To compute the restriction of  $\mathcal{F}$  to  $S_3$ , suppose first that  $P$  doesn't intersect one of  $E_x$ ,  $E_y$  or  $E_z$ . Let it be  $E_z$ , then  $\mathcal{F}|_{S_3}$  is the cokernel of

$$\mathcal{O} \xrightarrow{E_x \oplus E_y \oplus \text{Id}} \mathcal{O}(E_x) \oplus \mathcal{O}(E_y) \oplus \mathcal{O},$$

which is isomorphic to  $\mathcal{O}(-E_x) \oplus \mathcal{O}(-E_y)$ , as required.

Finally, suppose  $S_3$  intersects  $E_x$ ,  $E_y$  and  $E_z$ . This means that all the rational scroll chains are empty and  $S_3$  is just  $P \simeq \mathbb{P}^2$ . We then have a short exact sequence

$$0 \longrightarrow \mathcal{O} \longrightarrow \mathcal{O}(1)^{\oplus 3} \longrightarrow \mathcal{F} \longrightarrow 0.$$

Dualizing Euler exact sequence

$$0 \longrightarrow \Omega_{\mathbb{P}^2} \longrightarrow \mathcal{O}(-1)^{\oplus 3} \longrightarrow \mathcal{O} \longrightarrow 0$$

we see that  $\mathcal{F}$  is isomorphic to  $\Omega_{\mathbb{P}^2}^*$ , i.e. to  $T_{\mathbb{P}^2}$ . □

**5.5. The case of a “long side”.** Suppose that in Reid’s recipe  $\chi$  marks a single straight chain of edges running from one of the vertices of  $\Delta$  to the opposite side. We may assume, without loss of generality, that it is as depicted on Figure 17(b).

The expression for  $\Psi(\mathcal{O}_0 \otimes \chi)$  we obtain below is the same as in Section 5.3, but the proof is quite different. In the setup of Section 5.3 it was always to choose the filtration in Lemma 2.1 so that all the quotients vanish but one. Lemma 2.1 then implied that the remaining quotient is isomorphic to  $\Psi(\mathcal{O}_0 \otimes \chi)$ . Here, for any choice of filtration Lemma 2.1 only gives us two non-zero quotients and says that  $\Psi(\mathcal{O}_0 \otimes \chi)$  is some extension of them. We therefore have to analyze the skew-commutative cube of line bundles  $\mathcal{L}_\chi \otimes \text{Hex}(\chi^{-1})_{\tilde{\mathcal{M}}}$  directly, as in Section 5.4.

**Proposition 5.5.** (1) *If the chain is a single edge  $e_x P$ , i.e.  $G = \frac{1}{r}(0, 1, r-1)$ , then*

$$\Psi(\mathcal{O}_0 \otimes \chi) = \mathcal{L}_\chi^{-1} \otimes \mathcal{O}_C$$

*where  $C$  is the toric curve  $E_x \cap P$  corresponding to that edge.*

(2) *If the chain consists of more than one edge, then*

$$\Psi(\mathcal{O}_0 \otimes \chi) = \mathcal{L}_\chi^{-1}(-E_x - P) \otimes \mathcal{O}_Z[1]$$

*where  $Z$  is the union of the divisors which correspond to the internal vertices of  $e_x P$ .*

*Proof.* Claim (1) is proved as in Prop. 5.3. For claim (2) we proceed as in Section 5.4 and compute  $\mathcal{L}_\chi \otimes \mathcal{H}^{-1}(\Psi(\mathcal{O}_0 \otimes \chi))$ . Using Prop. 4.2 and Figure 17(b) we write down explicitly the skew-commutative cube of line bundles corresponding to  $\mathcal{L}_\chi \otimes \text{Hex}(\chi^{-1})_{\tilde{\mathcal{M}}}$ :

$$\begin{array}{ccccc} & & \mathcal{O}_Y(-e_z e_y) & \xrightarrow{\alpha_2^3} & \mathcal{O}_Y(-E_x) \\ & \nearrow \alpha_{23}^1 & & \nearrow \alpha_1^3 & \\ \mathcal{O}_Y(-\Delta) & \xrightarrow{\alpha_{13}^2} & \mathcal{O}_Y(-C y^\bullet) & \xrightarrow{\alpha_2^2} & \mathcal{O}_Y(-T x^\bullet z^\bullet) \\ & \searrow \alpha_{12}^3 & & \searrow \alpha_3^1 & \\ & & \mathcal{O}_Y(-C z^\bullet) & \xrightarrow{\alpha_1^2} & \mathcal{O}_Y(-T x^\bullet y^\bullet) \end{array} \quad (5.9)$$

where maps  $\alpha_i^\bullet$  are given by natural inclusions.

Denote by  $T^\bullet$  the total complex of this cube. Arguing as in the proof of [CL09, Lemma 3.1] we see that  $\text{Ker}(T^{-1} \rightarrow T^0)$  is isomorphic to the cokernel of

$$\mathcal{O}_Y(-E_x - e_y e_z) \xrightarrow{E_x \oplus T x^\bullet z^\bullet \setminus P \oplus T x^\bullet y^\bullet \setminus P} \mathcal{O}_Y(-e_y e_z) \oplus \mathcal{O}_Y(-E_x - T x^\bullet y^\bullet) \oplus \mathcal{O}_Y(-E_x - T x^\bullet z^\bullet)$$

and that  $\text{Im}(T^{-2} \rightarrow T^{-1})$  is then the image in  $\text{Ker}(T^{-1} \rightarrow T^0)$  of the subsheaf

$$\mathcal{O}_Y(-e_y e_z) \oplus \mathcal{O}_Y(-C y^\bullet) \oplus \mathcal{O}_Y(-C z^\bullet).$$

Let  $Z_y$  and  $Z_z$  be the reduced divisors of  $C y^\bullet \setminus (e_x \cup T x^\bullet y^\bullet)$  and  $C z^\bullet \setminus (e_x \cup T x^\bullet z^\bullet)$ , then  $\mathcal{H}^{-1}(T^\bullet)$  is the cokernel of

$$\mathcal{O}_Y(-E_x - e_y e_z) \xrightarrow{T x^\bullet z^\bullet \setminus P \oplus T x^\bullet y^\bullet \setminus P} \mathcal{O}_{Z_y}(-E_x - T x^\bullet y^\bullet) \oplus \mathcal{O}_{Z_z}(-E_x - T x^\bullet z^\bullet). \quad (5.10)$$

Observe that  $Z = Z_x \cap Z_y$ , so we have the natural map

$$\mathcal{O}_{Z_y}(-E_x - T x^\bullet y^\bullet) \oplus \mathcal{O}_{Z_z}(-E_x - T x^\bullet z^\bullet) \xrightarrow{T x^\bullet y^\bullet \setminus P \oplus T x^\bullet z^\bullet \setminus P} \mathcal{O}_Z(-E_x - P). \quad (5.11)$$

It remains to show that the composition of (5.10) and (5.11) is exact in last two terms. We check it on an open cover: on the open piece of  $Y$  which corresponds to triangle  $e_x e_y P$  it is

$$\mathcal{O}_Y(-E_x - Tx^\bullet y^\bullet) \xrightarrow{1 \oplus Tx^\bullet y^\bullet \setminus P} \mathcal{O}_{Z_y}(-E_x - Tx^\bullet y^\bullet) \oplus \mathcal{O}_{Z_y \cap Z_z}(-E_x - P) \xrightarrow{Tx^\bullet y^\bullet \setminus P \oplus 1} \mathcal{O}_{Z_y \cap Z_z}(-E_x - P)$$

and on the open piece of  $Y$  which corresponds to triangle  $e_x e_z P$  it is

$$\mathcal{O}_Y(-E_x - Tx^\bullet z^\bullet) \xrightarrow{Tx^\bullet z^\bullet \setminus P \oplus 1} \mathcal{O}_{Z_y \cap Z_z}(-E_x - P) \oplus \mathcal{O}_{Z_z}(-E_x - Tx^\bullet y^\bullet) \xrightarrow{1 \oplus Tx^\bullet z^\bullet \setminus P} \mathcal{O}_{Z_y \cap Z_z}(-E_x - P).$$

Both sequences are manifestly exact in their last two terms.  $\square$

**5.6. The case of  $\chi = \chi_0$ .** Suppose that  $\chi$  marks nothing in Reid's recipe, i.e.  $\chi = \chi_0$ . Denote by  $F_{23}$ ,  $F_{13}$  and  $F_{12}$  the chains of divisors corresponding to internal vertices of sides  $e_y e_z$ ,  $e_x e_z$  and  $e_x e_y$ , respectively. Recall that  $ZF$  denotes the fibre of  $Y$  over  $0 \in \mathbb{C}^3/G$ , cf. §2.2 and  $ZF_1$  and  $ZF_2$  denote the unions of 1- and 2-dimensional irreducible components of  $ZF$ . For any separated scheme  $S$  of finite type over  $\mathbb{C}$  we denote by  $\omega_S$  the dualizing complex of  $S$  obtained as the twisted inverse image  $f^!(\mathbb{C})$  over the structure morphism  $S \xrightarrow{f} \text{Spec } \mathbb{C}$ . If  $S$  is Cohen-Macaulay, then  $\omega_S = \omega_S[\dim S]$  where  $\omega_S$  is a sheaf on  $S$ . If  $S$  is proper, then  $\omega_S$  is the dualizing sheaf in the sense of [Har77, §III.7]. If  $S$  is regular, then  $\omega_S$  is the canonical bundle [Ver69, Theorem 3].

**Proposition 5.6.** *Let  $\chi$  be the trivial character  $\chi_0$ . Then  $\Psi(\mathcal{O}_0 \otimes \chi) = \omega_{ZF}$  and moreover:*

- (1)  $\mathcal{H}^{-2}(\Psi(\mathcal{O}_0 \otimes \chi)) = \omega_{ZF_2} = \mathcal{O}_Y(ZF_2) \otimes \mathcal{O}_{ZF_2}$ .
- (2)  $\mathcal{H}^{-1}(\Psi(\mathcal{O}_0 \otimes \chi)) = \omega_{ZF_1}(ZF_2)$ .
- (3)  $\mathcal{H}^i(\Psi(\mathcal{O}_0 \otimes \chi)) = 0$  for  $i \neq -1, -2$ .

*Proof.* We use the following trick: instead of writing down the skew-commutative cube of line bundles corresponding to  $\text{Hex}(\chi_0)_{\tilde{\mathcal{M}}}$ , we write down its derived dual. The total complex of this dual cube is the derived dual of the total complex of the original cube, i.e. of  $\Psi(\mathcal{O}_0 \otimes \chi)$ .

Theorem 3.4 tells us the vertex type of  $\chi_0$  for every toric divisor on  $Y$ , using this we write down the cube corresponding to  $\text{Hex}(\chi_0)_{\tilde{\mathcal{M}}}$  as:

$$\begin{array}{ccccc} & \mathcal{O}_Y(-E_y - F_{23} - E_z) & & \mathcal{O}_Y(-E_x) & \\ & \nearrow & \searrow & \nearrow & \searrow \\ \mathcal{O}_Y(-\Delta) & \longrightarrow \mathcal{O}_Y(-E_x - F_{13} - E_z) & & \mathcal{O}_Y(-E_y) & \longrightarrow \underline{\mathcal{O}_Y} \\ & \searrow & \nearrow & \searrow & \nearrow \\ & \mathcal{O}_Y(-E_x - F_{12} - E_y) & & \mathcal{O}_Y(-E_z) & \end{array} \quad (5.12)$$

where we underline the degree 0 term. Its derived dual is:

$$\begin{array}{ccccc} & \mathcal{O}_Y(E_x) & & \mathcal{O}_Y(E_y + F_{23} + E_z) & \\ & \nearrow & \searrow & \nearrow & \searrow \\ \underline{\mathcal{O}_Y} & \longrightarrow \mathcal{O}_Y(E_y) & & \mathcal{O}_Y(E_x + F_{13} + E_z) & \longrightarrow \mathcal{O}_Y(\Delta) \\ & \searrow & \nearrow & \searrow & \nearrow \\ & \mathcal{O}_Y(E_z) & & \mathcal{O}_Y(E_x + F_{12} + E_y) & \end{array} \quad (5.13)$$

Denote by  $T^\bullet$  the total complex of the dual cube and denote by  $\iota_{ZF}$  the inclusion map  $ZF \hookrightarrow Y$ . Lemma 2.1 implies immediately that  $\mathcal{H}^0(T^\bullet) = \iota_{ZF*}\mathcal{O}_{ZF}$  and all the other cohomologies of  $T^\bullet$  vanish. We therefore have

$$\Psi(\mathcal{O}_0 \times \chi_0) \simeq (\iota_{ZF*}\mathcal{O}_{ZF})^\vee[3].$$

The map  $\iota_{ZF}$  is proper, so  $\iota_{ZF}^!$  is right adjoint to  $\iota_{ZF*}$ , and by sheafified Grothendieck duality:

$$(\iota_{ZF*}\mathcal{O}_{ZF})^\vee = \mathbf{R}\mathcal{H}om_Y(\iota_{ZF*}\mathcal{O}_{ZF}, \mathcal{O}_Y) \simeq \iota_{ZF*}\mathbf{R}\mathcal{H}om_{ZF}(\mathcal{O}_{ZF}, \iota_{ZF}^!\mathcal{O}_Y) \simeq \iota_{ZF*}\iota_{ZF}^!\mathcal{O}_Y.$$

Let  $f_Y$  and  $f_{ZF}$  denote the structural morphisms to  $\text{Spec } \mathbb{C}$ . As  $f_{ZF} = f_Y \circ \iota_{ZF}$ , we have

$$\iota_{ZF}^!\mathcal{O}_Y[3] \simeq \iota_{ZF}^!\omega_Y = \iota_{ZF}^!f_Y^!(\mathbb{C}) \simeq f_{ZF}^!(\mathbb{C}) = \omega_{ZF}.$$

Thus we have  $\Psi(\mathcal{O}_0 \times \chi_0) = \iota_{ZF*}\omega_{ZF}$  or, returning to our convention of omitting the pushforward functor where the source scheme is obvious, just  $\Psi(\mathcal{O}_0 \times \chi_0) = \omega_{ZF}$ . This settles the first claim.

There is a short exact sequence of sheaves on  $Y$

$$\mathcal{O}_{ZF_1}(-ZF_2) \rightarrow \mathcal{O}_{ZF} \rightarrow \mathcal{O}_{ZF_2} \quad (5.14)$$

which is an instance of the standard short exact sequence

$$\mathcal{O}_{Z_1} \otimes \mathcal{I}_{Z_2} \rightarrow \mathcal{O}_Z \rightarrow \mathcal{O}_{Z_2}$$

which exists for any reduced scheme  $Z$  which is a union of schemes  $Z_1$  and  $Z_2$ .

Hence (5.14) is an exact triangle in  $D(Y)$ . Taking the derived dual we obtain the triangle

$$\omega_{ZF_2} \rightarrow \omega_{ZF} \rightarrow \omega_{ZF_1}(ZF_2).$$

Whence the claims (1)-(3) follow, since  $ZF_1$  and  $ZF_2$  are Cohen-Macaulay and their dualizing complexes are just the shifts of their dualizing sheaves.  $\square$

## 6. WORKED EXAMPLE

In this section we illustrate our results by explicit computations for  $G = \frac{1}{15}(1, 5, 9)$ .

**6.1. The group  $G = \frac{1}{15}(1, 5, 9)$ , the toric variety  $G\text{-Hilb}(\mathbb{C}^3)$  and classical Reid's recipe.** Let  $G$  be the group  $\frac{1}{15}(1, 5, 9)$ . It is the image in  $\text{SL}_3(\mathbb{C})$  of group  $\mu_{15}$  of 15th roots of unity under the embedding  $\xi \mapsto (\xi^1 \xi^5 \xi^9)$ . We denote by  $\chi_i$  the character of  $G$  induced by  $\xi \mapsto \xi^i$ , then, as explained in Section 2.1,  $\kappa(x_1) = \chi_{14}$ ,  $\kappa(x_2) = \chi_{10}$  and  $\kappa(x_3) = \chi_6$ .

Let  $Y = G\text{-Hilb}(\mathbb{C}^3)$ . We next describe  $Y$  as a toric variety following Section 2.2. First we compute the toric fan of  $Y$  as described in [Cra05, Section 2]. On Fig. 19(a) we depict the triangulation  $\Sigma$  of the junior simplex  $\Delta$  defined by this fan, together with the monomial ratios which carve out each edge of  $\Sigma$ .

The generators  $e_i$  of the one-dimensional cones of the fan have the following coordinates:

$$\begin{array}{lll} e_1 = (1, 0, 0) & e_2 = (0, 1, 0) & e_3 = (0, 0, 1) \\ e_4 = \frac{1}{15}(1, 5, 9) & e_5 = \frac{1}{15}(2, 10, 3) & e_6 = \frac{1}{15}(3, 0, 12) \\ e_7 = \frac{1}{15}(4, 5, 6) & e_8 = \frac{1}{15}(5, 10, 0) & e_9 = \frac{1}{15}(6, 0, 9) \\ e_{10} = \frac{1}{15}(7, 5, 3) & e_{11} = \frac{1}{15}(9, 0, 6) & e_{12} = \frac{1}{15}(10, 5, 0) \\ e_{13} = \frac{1}{15}(12, 0, 3) & & \end{array} \quad (6.1)$$

The corresponding toric divisors are:

- (1) *Strict transforms of coordinate hyperplanes of  $\mathbb{C}^3/G$ :*

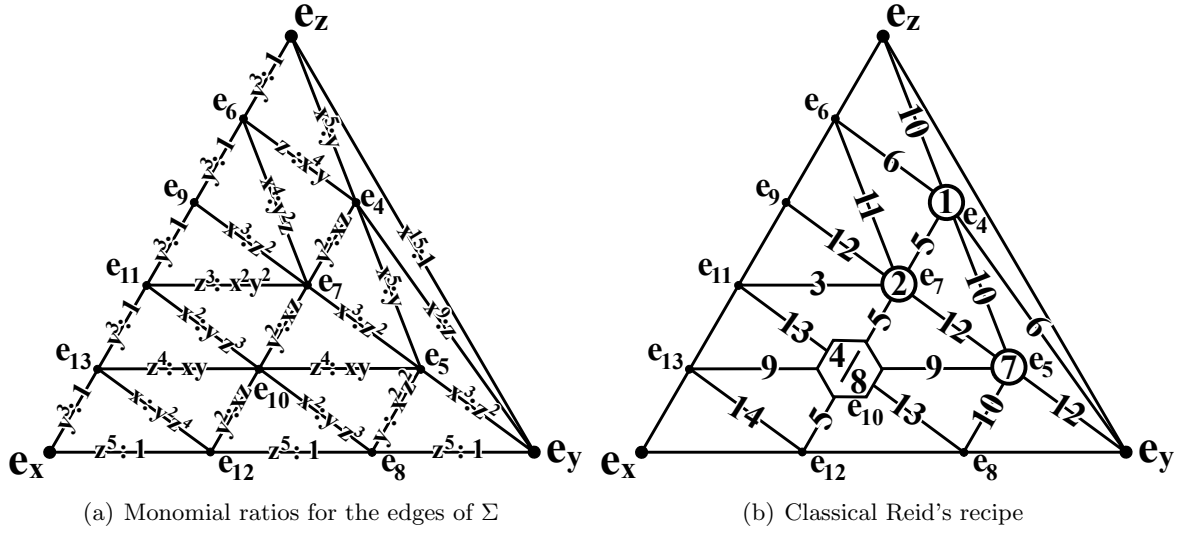


FIGURE 19.  $G\text{-Hilb}(\mathbb{C}^3)$  for  $\frac{1}{15}(1, 5, 9)$

- $E_x, E_y, E_z$ .
- (2) *Non-compact exceptional divisors:*
  - $E_9$ , isomorphic to  $\mathbb{P}^1 \times \mathbb{A}^1$ .
  - $E_6, E_8, E_{11}, E_{12}$  and  $E_{13}$ , each isomorphic to  $\mathbb{P}^1 \times \mathbb{A}^1$  blown up in a point.
- (3) *Compact exceptional divisors:*
  - $E_4$  and  $E_5$ , each isomorphic to a rational scroll blown up in a point.
  - $E_7$ , isomorphic to a rational scroll blown up in two points.
  - $E_8$ , isomorphic to the Del Pezzo surface  $dP_6$ .

The fiber  $ZF$  of  $Y$  over  $0 \in \mathbb{C}^3/G$  is a reducible variety which breaks up into

- *Two-dimensional stratum*  $ZF_2$ : the compact exceptional divisors  $E_4, E_5, E_7$  and  $E_{10}$ .
- *One-dimensional stratum*  $ZF_1$ : a single curve  $E_{12} \cap E_{13} \simeq \mathbb{P}^1$ .

Finally, we compute classical Reid's recipe for  $G = \frac{1}{15}(1, 5, 9)$ , as described in §2.3, and list the result on Fig. 19(b).

**6.2. CT-subdivisions.** We now begin to compute derived Reid's recipe for  $G = \frac{1}{15}(1, 5, 9)$ . The standard way to do this is via explicit computations with  $G$ -Weil divisors, cf. [CL09, §6]. But Prop. 4.2 allows for a new way to do this, which we illustrate below.

The first step is to compute the CT-subdivisions of  $\Delta$  for all the non-trivial characters of  $G$ . These are defined in §4 in terms of the monomials which represent  $\chi$  in the  $G$ -graphs of the basic triangles of  $\Sigma$ . These can be computed as in [Cra05, §5].

On Fig. 20-22 we display the resulting CT-subdivisions together with the above-mentioned monomials. By doing so we are explicitly writing down tautological sheaves  $\mathcal{L}_\chi$ : each  $\mathcal{L}_\chi$  is the subsheaf of constant sheaf  $K(\mathbb{C}^3)$  which is generated on each toric affine piece of  $Y$  by the monomial which represents  $\chi$  in the graph of the corresponding basic triangle of  $\Sigma$ .



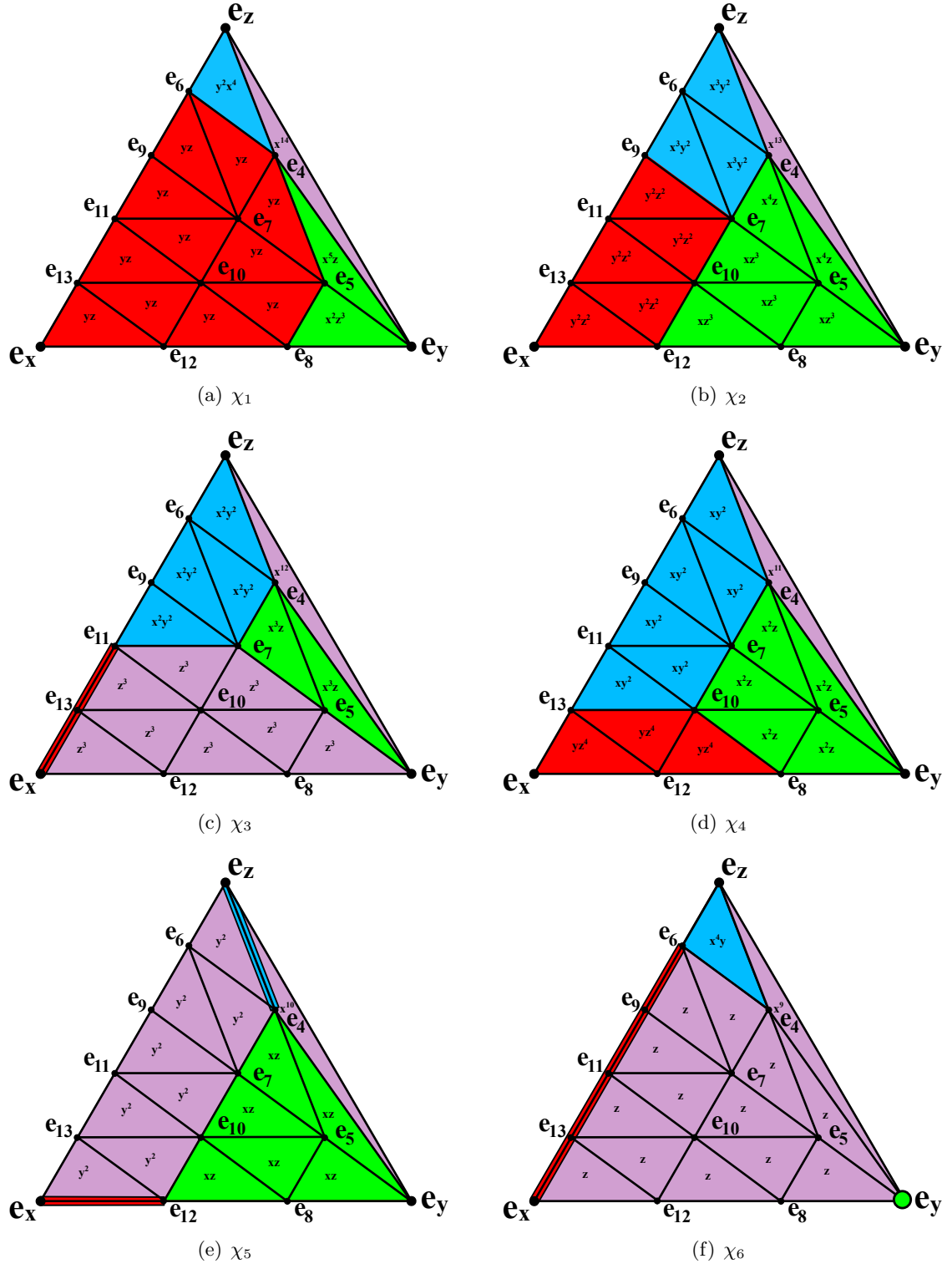
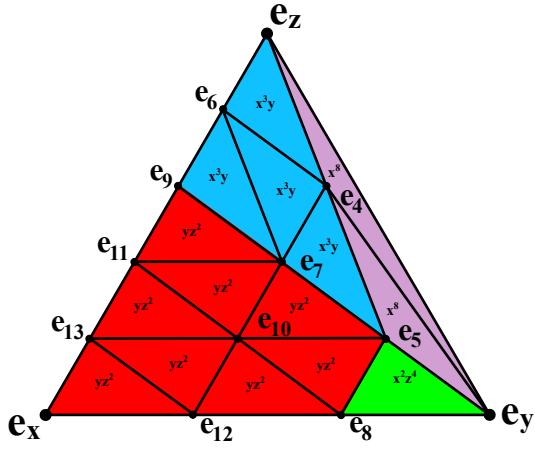
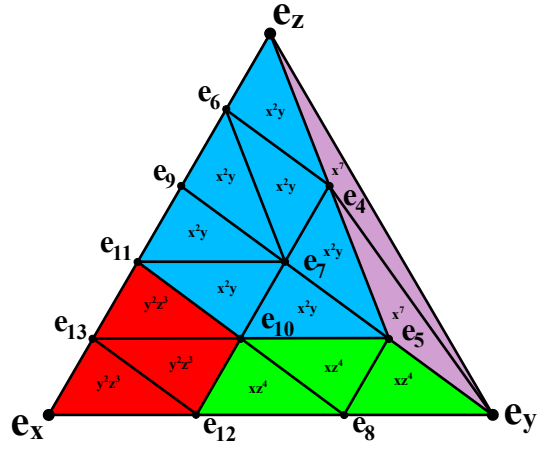


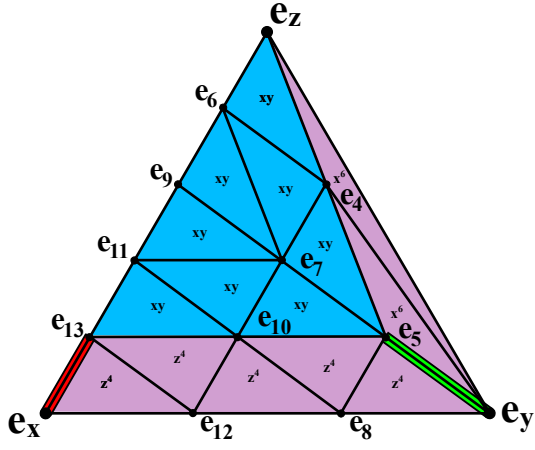
FIGURE 20. CT-subdivisions and monomial generators of  $\mathcal{L}_\chi$  for  $\chi_1$  -  $\chi_6$ .



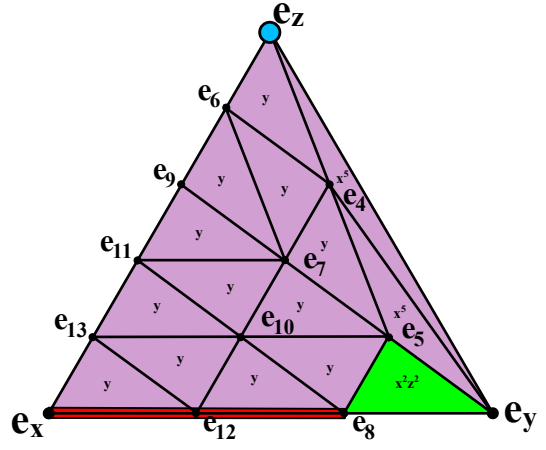
(a)  $\chi_7$



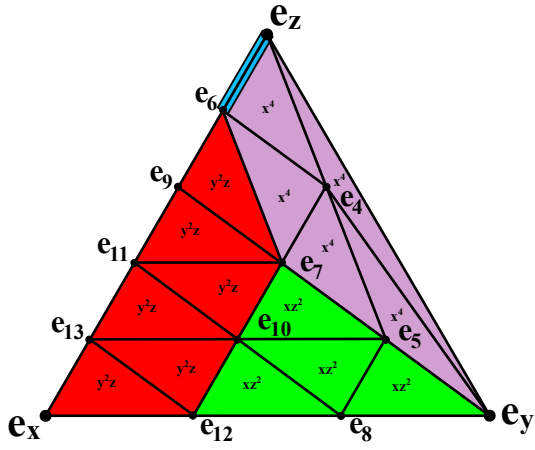
(b)  $\chi_8$



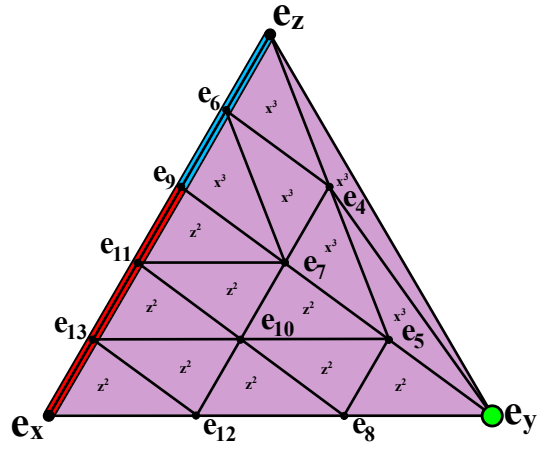
(c)  $\chi_9$



(d)  $\chi_{10}$



(e)  $\chi_{11}$



(f)  $\chi_{12}$

FIGURE 21. CT-subdivisions and monomial generators of  $\mathcal{L}_\chi$  for  $\chi_7 - \chi_{12}$ .

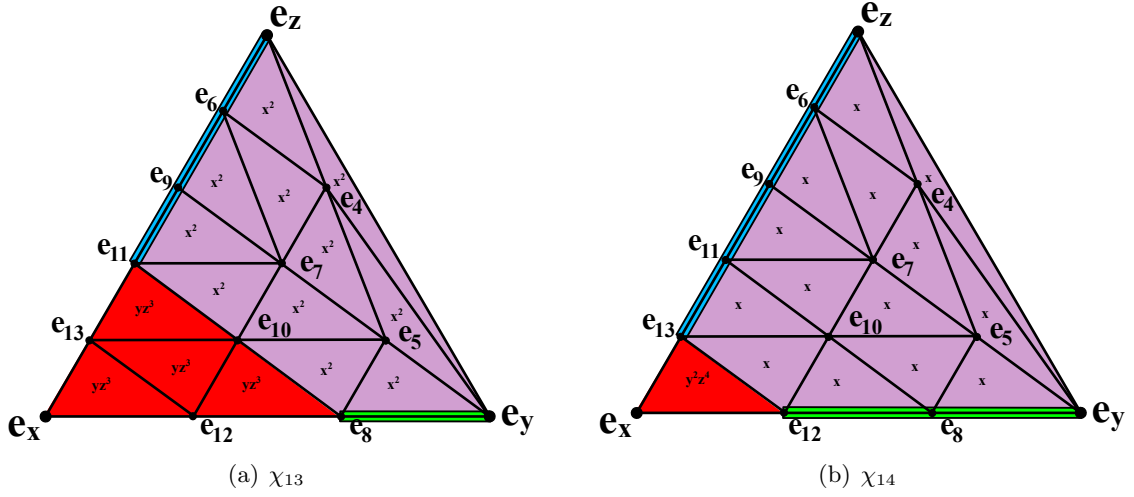
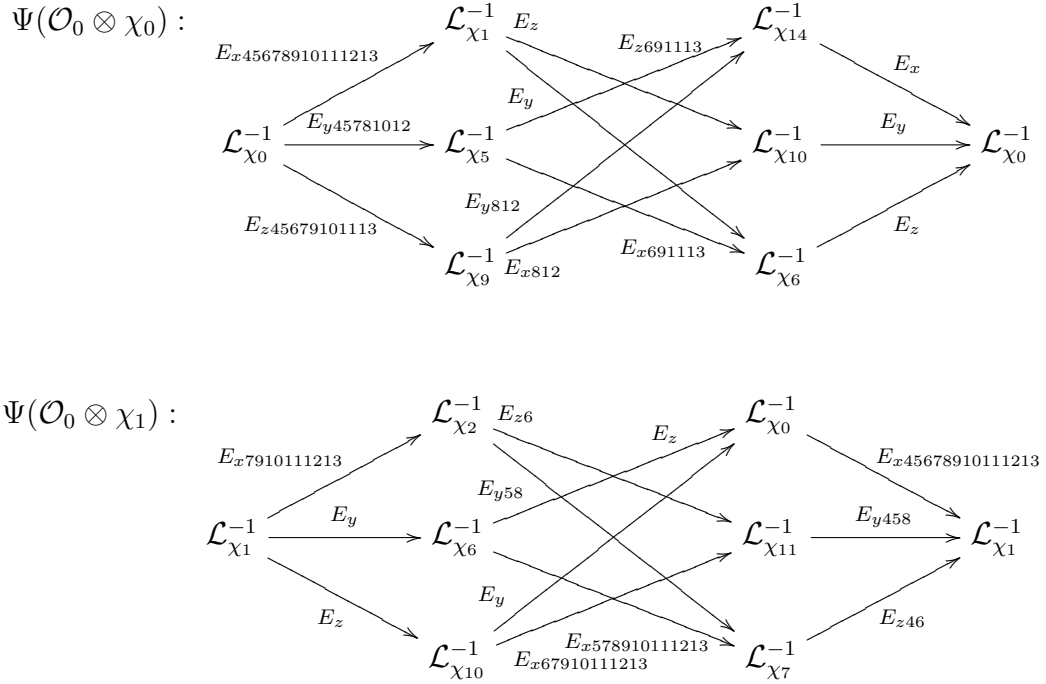
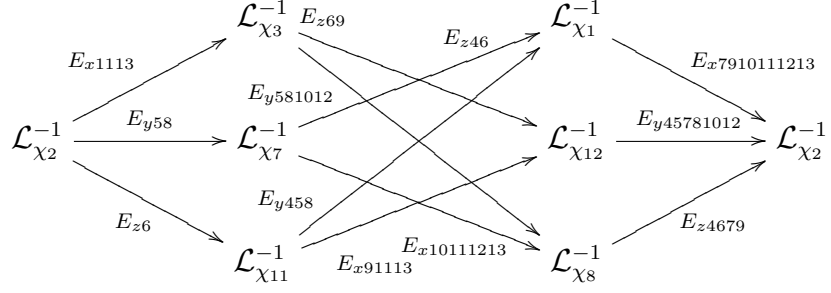


FIGURE 22. CT-subdivisions and monomial generators of  $\mathcal{L}_\chi$  for  $\chi_{13}$  -  $\chi_{14}$ .

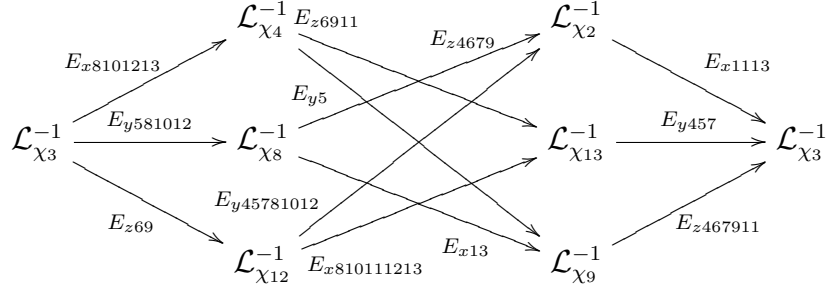
**6.3. Skew-commutative cubes corresponding to  $\Psi(\mathcal{O}_0 \otimes \chi)$ .** Now for each  $\chi \in G^\vee$  we draw the skew-commutative cube of line bundles corresponding to  $\text{Hex}(\chi^{-1})_{\tilde{\mathcal{M}}}$  as per Fig. 2. Next, for each toric divisor  $E$  on  $Y$  we use Prop. 4.2 to determine the arrows of the cube whose corresponding maps in  $\text{Hex}(\chi^{-1})_{\tilde{\mathcal{M}}}$  vanish along  $E$ . We then mark each arrow of the cube by its vanishing divisor in a following shorthand:  $E_{456101213} = E_4 + E_5 + E_6 + E_{10} + E_{12} + E_{13}$  etc. We thus obtain:



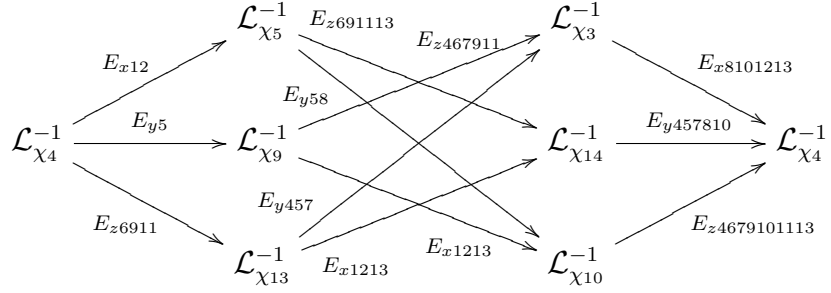
$\Psi(\mathcal{O}_0 \otimes \chi_2) :$



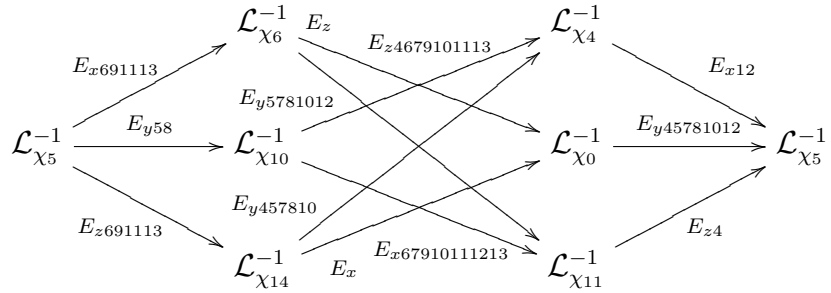
$\Psi(\mathcal{O}_0 \otimes \chi_3) :$



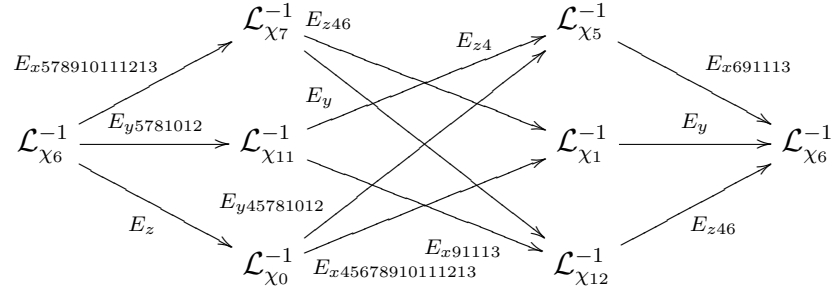
$\Psi(\mathcal{O}_0 \otimes \chi_4) :$



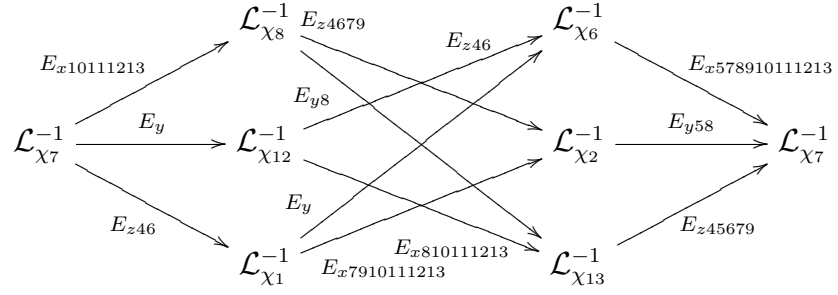
$\Psi(\mathcal{O}_0 \otimes \chi_5) :$



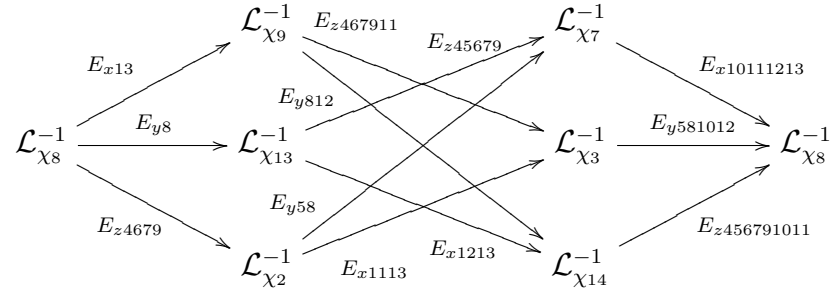
$\Psi(\mathcal{O}_0 \otimes \chi_6) :$



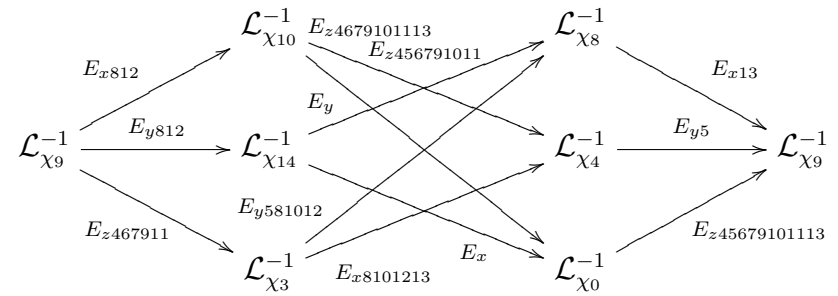
$\Psi(\mathcal{O}_0 \otimes \chi_7) :$



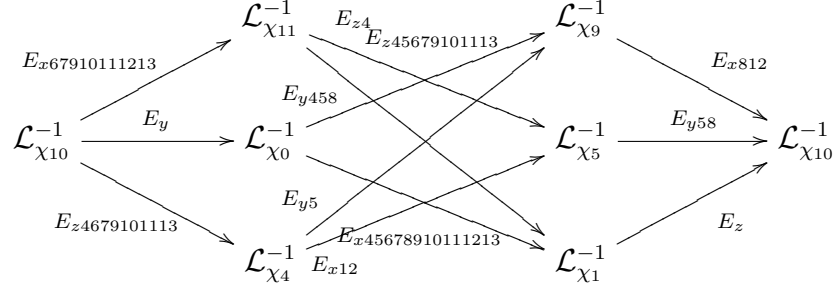
$\Psi(\mathcal{O}_0 \otimes \chi_8) :$



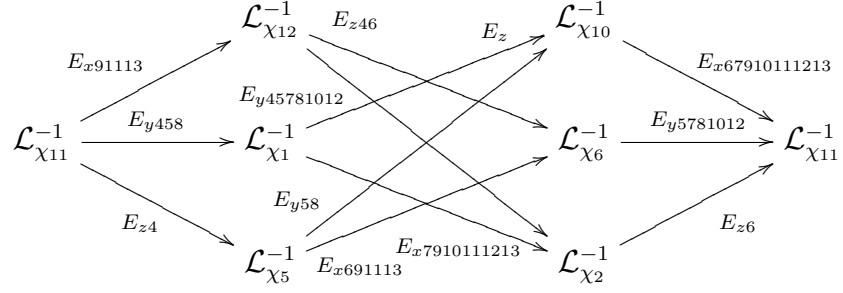
$\Psi(\mathcal{O}_0 \otimes \chi_9) :$



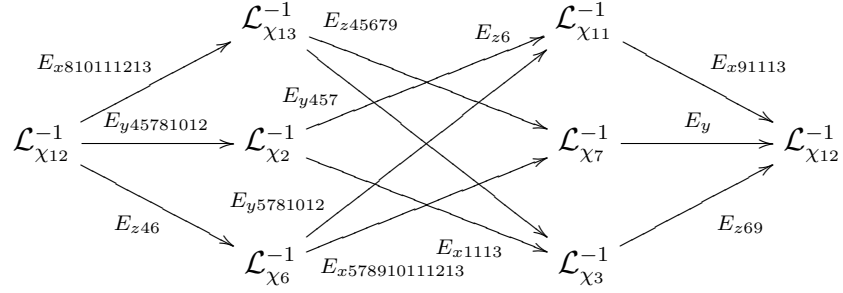
$\Psi(\mathcal{O}_0 \otimes \chi_{10}) :$



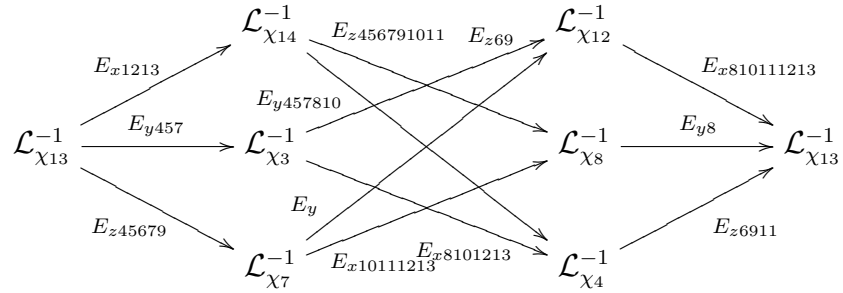
$\Psi(\mathcal{O}_0 \otimes \chi_{11}) :$



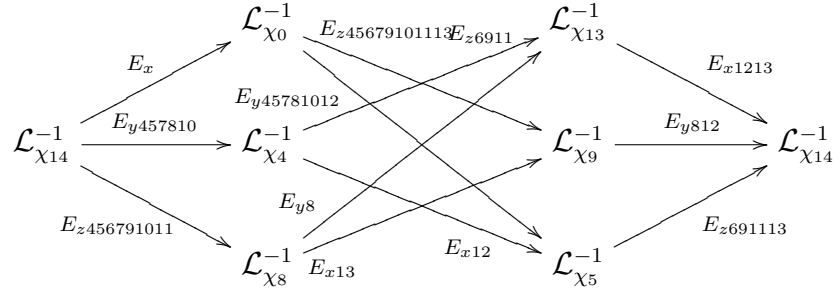
$\Psi(\mathcal{O}_0 \otimes \chi_{12}) :$



$\Psi(\mathcal{O}_0 \otimes \chi_{13}) :$



$\Psi(\mathcal{O}_0 \otimes \chi_{14}) :$



**6.4. Derived Reid's recipe.** We now analyze the skew-commutative cubes computed in the previous section and, using Lemma 2.1 or a more involved analysis where necessary, compute the cohomology sheaves of their total complexes. This completes the derived Reid's recipe computation and we list the results in Fig. 23.

$\chi \setminus \mathcal{H}^\bullet(\Psi(\mathcal{O}_0 \otimes \chi))$	$\mathcal{H}^{-2}$	$\mathcal{H}^{-1}$	$\mathcal{H}^0$
$\chi_0$	$\mathcal{O}_{E_{45710}}(E_{45710})$	$\mathcal{O}_{C_{12 \cap 13}}(-1)$	0
$\chi_1$	0	0	$\mathcal{L}_{\chi_1}^{-1} \otimes \mathcal{O}_{E_4}$
$\chi_2$	0	0	$\mathcal{L}_{\chi_2}^{-1} \otimes \mathcal{O}_{E_7}$
$\chi_3$	0	0	$\mathcal{L}_{\chi_3}^{-1} \otimes \mathcal{O}_{C_{7 \cap 11}}$
$\chi_4$	0	0	$\mathcal{L}_{\chi_4}^{-1} \otimes \mathcal{O}_{E_{10}}$
$\chi_5$	0	$\mathcal{L}_{\chi_5}^{-1}(-E_{412}) \otimes \mathcal{O}_{E_{710}}$	0
$\chi_6$	0	$\mathcal{L}_{\chi_6}^{-1}(-E_{y6}) \otimes \mathcal{O}_{E_4}$	0
$\chi_7$	0	0	$\mathcal{L}_{\chi_7}^{-1} \otimes \mathcal{O}_{E_5}$
$\chi_8$	0	0	$\mathcal{L}_{\chi_8}^{-1} \otimes \mathcal{O}_{E_{10}}$
$\chi_9$	0	$\mathcal{L}_{\chi_9}^{-1}(-E_{513}) \otimes \mathcal{O}_{E_{10}}$	0
$\chi_{10}$	0	$\mathcal{L}_{\chi_{10}}^{-1}(-E_{z8}) \otimes \mathcal{O}_{E_{45}}$	0
$\chi_{11}$	0	0	$\mathcal{L}_{\chi_{11}}^{-1} \otimes \mathcal{O}_{C_{6 \cap 7}}$
$\chi_{12}$	0	$\mathcal{L}_{\chi_{12}}^{-1}(-E_{y9}) \otimes \mathcal{O}_{E_{57}}$	0
$\chi_{13}$	0	$\mathcal{L}_{\chi_{13}}^{-1}(-E_{811}) \otimes \mathcal{O}_{E_{10}}$	0
$\chi_{14}$	0	0	$\mathcal{L}_{\chi_{14}}^{-1} \otimes \mathcal{O}_{C_{12 \cap 13}}$

FIGURE 23. Derived Reid's recipe for  $G = \frac{1}{15}(1, 5, 9)$

**6.5. Sink-source graphs.** Prop. 4.2 determines the vertex type of each  $\chi \in G^\vee$  in the sink-source graph of each toric divisor of  $Y$ . We therefore use the  $CT$ -subdivision data displayed in Fig. 20 - 22 to compute the sink-source graphs of the exceptional divisors of  $Y$ . We list the results on Fig. 24. Though not necessary to compute derived Reid's recipe, it provides both an illustration of the correspondence of Theorem 3.4 and a visual aid for the proof of Prop. 4.2.



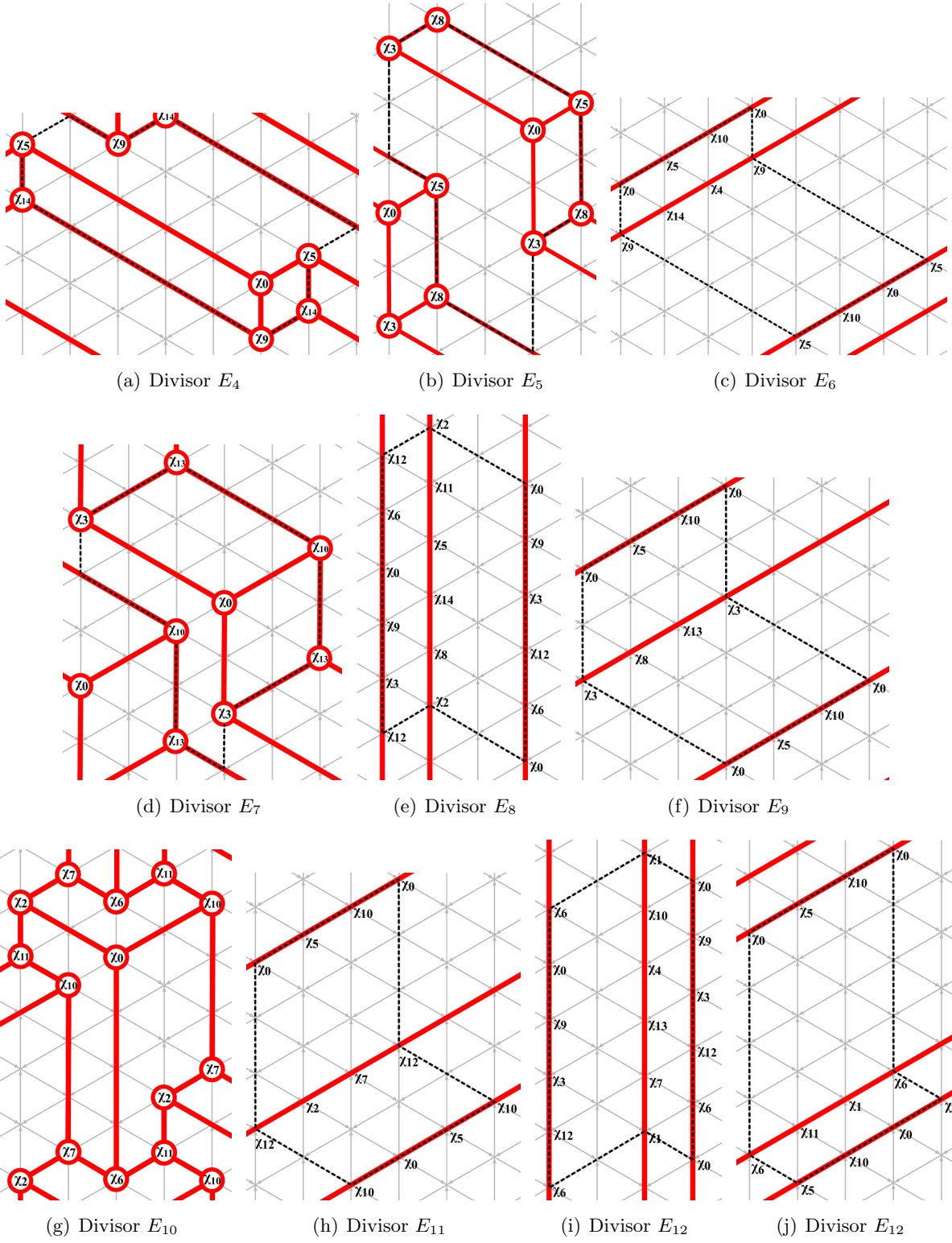


FIGURE 24. Sink-source graphs for  $G = \frac{1}{15}(1, 5, 9)$

## REFERENCES

- [BKR01] Tom Bridgeland, Alastair King, and Miles Reid, *The McKay correspondence as an equivalence of derived categories*, J. Amer. Math. Soc. **14** (2001), 535–554, math.AG/9908027.
- [CI04] Alastair Craw and Akira Ishii, *Flops of  $G$ -Hilb and equivalences of derived category by variation of GIT quotient*, Duke Math J. **124** (2004), no. 2, 259–307, arXiv:math.AG/0211360.
- [CL09] Sabin Cautis and Timothy Logvinenko, *A derived approach to geometric McKay correspondence in dimension three*, J. Reine Angew. Math. **636** (2009), 193–236. MR 2572250 (2011d:14018)
- [CR02] Alastair Craw and Miles Reid, *How to calculate  $A$ -Hilb  $\mathbb{C}^3$* , Geometry of toric varieties, Sémin. Congr., vol. 6, Soc. Math. France, Paris, 2002, pp. 129–154. MR 2075608 (2005d:14004)
- [Cra05] Alastair Craw, *An explicit construction of the McKay correspondence for  $A$ -Hilb  $\mathbb{C}^3$* , J. Algebra **285** (2005), no. 2, 682–705.
- [GSV83] Gérard Gonzalez-Sprinberg and Jean-Louis Verdier, *Construction géométrique de la correspondance de McKay*, Ann. sci. ENS **16** (1983), 409–449.
- [Har77] Robin Hartshorne, *Algebraic geometry*, Springer-Verlag, 1977.
- [KV00] Mikhail Kapranov and Eric Vasserot, *Kleinian singularities, derived categories and hall algebras*, Math. Ann. **316** (2000), no. 3, 565–576, math.AG/9812016.
- [Log03] Timothy Logvinenko, *Families of  $G$ -constellations over resolutions of quotient singularities*, preprint math.AG/0305194, (2003).
- [Log08a] ———, *Derived McKay correspondence via pure-sheaf transforms*, Math. Ann. **341** (2008), no. 1, 137–167, arXiv: math/0606791.
- [Log08b] ———, *Natural  $G$ -constellation families*, Documenta Math. **13** (2008), 803–823, arXiv: math/0601014.
- [Log10] ———, *Reid’s recipe and derived categories*, J. Algebra **324** (2010), no. 8, 2064–2087, arXiv:0812.4503.
- [McK80] John McKay, *Graphs, singularities and finite groups*, Proc. Symp. Pure Math. **37** (1980), 183–186.
- [Nak00] Iku Nakamura, *Hilbert schemes of abelian group orbits*, J. Alg. Geom. **10** (2000), 775–779.
- [Rei97] Miles Reid, *McKay correspondence*, preprint math.AG/9702016, (1997).
- [Tak11] Keisuke Takahashi, *On essential representations in the McKay correspondence for  $SL_3(\mathbb{C})$* , Master’s thesis, Nagoya University, 2011.
- [Ver69] Jean-Louis Verdier, *Base change for twisted inverse image of coherent sheaves*, Algebraic geometry (Bombay Colloquium, 1968), Oxford University Press, 1969, pp. 393–408.

MATHEMATICS DEPARTMENT, COLUMBIA UNIVERSITY, 2990 BROADWAY, NEW YORK, NY 10027, USA  
*E-mail address:* scautis@math.columbia.edu

SCHOOL OF MATHEMATICS AND STATISTICS, UNIVERSITY OF GLASGOW, GLASGOW, G12 8QW, UNITED KINGDOM  
*E-mail address:* Alastair.Craw@glasgow.ac.uk

MATHEMATICS INSTITUTE, UNIVERSITY OF WARWICK, COVENTRY, CV4 7AL, UNITED KINGDOM  
*E-mail address:* T.Logvinenko@warwick.ac.uk